

# **Targeted Proteomics for Exosome Analysis and Its Application to Develop Blood Markers of Liver Drug-Metabolizing Enzymes**

By

**Laura M. Doyle (Drbohlav)**

Submitted to the graduate degree program in Pharmaceutical Chemistry and the Graduate Faculty of the University of Kansas in partial fulfillment of the requirements for the degree of Doctor of Philosophy

---

Chair: Michael Zhuo Wang, PhD

---

Christian Schöneich, PhD

---

John Stobaugh, PhD

---

Jeffrey Krise, PhD

---

Yong Zeng, PhD

Date Defended: 15 April 2019

The Dissertation Committee for Laura M. Doyle (Drbohlav) Certifies  
that this is the approved version of the following dissertation:

**Targeted Proteomics for Exosome Analysis and Its Application to  
Develop Blood Markers of Liver Drug-Metabolizing Enzymes**

---

Chair: Michael Zhuo Wang, PhD

Date Approved: 15 April 2019

## ABSTRACT

Two main routes of drug elimination include renal excretion via the kidney and metabolic degradation via metabolizing enzymes (DMEs) in the liver, followed by renal excretion or biliary elimination of the now more polar molecule. Unlike renal excretion, liver metabolism tends to be highly variable between individuals due to various intrinsic and extrinsic factors such as age, genetics, smoking, and diet. The variability in liver DME activity among individuals creates a challenge in drug development and pharmacotherapy, especially for drugs that are required to be metabolized and have narrow therapeutic windows. If the liver DME activity of an individual could be predicted and each patient dosed according to their unique liver DME activity, the adverse effects or lack of effectiveness associated with these drugs may be prevented. Currently, two methods available for predicting an individual's liver DME activity are genotyping and phenotyping. For genotyping, RT-PCR is used to determine the DNA sequence of the expressed enzyme. This reveals the specific polymorphism of the enzyme and the "typical activity" of the expressed polymorph is used to dose the patient accordingly. The issue with this however, is that it fails to account for other intrinsic or extrinsic factors that can affect the expression level of the given DME polymorph. On the other hand, phenotyping is done by administering a cocktail of drugs to a patient and monitoring the activity of the expressed enzyme(s). Because this reveals the true activity of the liver DMEs, it is more clinically relevant and used more often than genotyping. However, phenotyping is expensive and requires consistent monitoring by medical professionals in the hospital, thus is inconvenient. Accurate prediction of liver DME activity at the individual level in the clinical setting remains challenging, however if a more clinically friendly method were to be developed, it could lead to a broader range of potential drug candidates in drug development and lower risk of adverse drug responses.

In this dissertation, the use of exosomes to act as biomarkers for liver DMEs is investigated. Exosomes are vesicles, typically 50 – 150 nm in diameter, secreted by cells into the extracellular space. In the human body, exosomal vesicles have been found in blood, saliva, urine, breast milk, and other bodily fluids. What makes exosomes unique from other vesicles secreted by cells, is that exosomes are formed by an endosomal route, thus contain cargo that reflecting the cell from which they are being secreted, in the extracellular space. This allows for the development of minimally invasive “liquid biopsies” to probe for markers of different diseases and cancers. While exosomes have been demonstrated as useful tools for diagnosis and monitoring patient response to treatment, they are yet to be used in the clinical setting. This is due to the lack of standardization in exosomal isolation and analysis. These challenges were also addressed in this dissertation.

In summary, this dissertation describes the development of a liquid chromatography multiple-reaction-monitoring mass spectrometry (LC-MRM-MS) method for exosomal analysis and its benefits over more traditional assays. Following the method development, the presence of DMEs in exosomes were explored along with the ability of exosomal DME levels to be altered to reflect a change occurring in the secreting cell. Finally, the ability to isolate liver derived exosomes based on the expression of a liver specific marker protein, ASGR1, is explored. Further efforts of this project could lead to the development of a blood-based biopsy to evaluate the DME content of liver derived exosomes, which may correlate to liver DME activity, providing a new-found basis of personalized medicine.

## ACKNOWLEDGEMENTS

First and foremost, my thanks go to my graduate advisor, Dr. Michael Zhuo Wang. Your mentorship and advice over the last three and a half years have been invaluable. While working in your lab, I learned that science is not simply performing experiments and producing data but rather an opportunity to think critically and solve problems. This is something I will use throughout my career. I am grateful for the patience, encouragement, and constructive criticism you have given me during my time in your lab as it has helped me get to where I am today. I am extremely privileged to have been guided by your expertise. I value the many lessons you have taught me and hope to follow your example in my career moving forward.

If there is one aspect I could change about my graduate school experience, it would have been to have had more discussions with Dr. Judy Wu. I was only able to talk with you about my research on 2 or 3 brief occasions; however, these were arguably the most enlightening, motivating, and truly enriching discussions of my graduate school years. You inspired me and demonstrated how women in science can balance both their personal and professional lives. You set a fantastic example that will remember and treasure.

Additionally, I express my gratitude to Dr. George Chumanov and Dr. Steve Harley. You both had a significant influence in my undergraduate and high school careers. Your mentorship during those critical years assured that I would attain my goal. Frequently, you encouraged and nudged me out of my comfort zone. Without your mentorship, I would not have been able to manage the rigors of graduate school, as I was outside my comfort zone 90 % of the time. Thank you.

Also I extend my appreciation to my graduate committee members: Dr. Schöneich, Dr. Stobaugh, Dr. Krise, and Dr. Zeng. I value the time you have taken to meet with me and share

your ideas and insights about the direction of my research project. Our meetings were not only helpful, but challenging, which helped me to become a more independent and confident scientist.

In addition to my advisors and mentors, I want to acknowledge the University of Kansas Department of Pharmaceutical Chemistry. During my recruitment weekend, I vividly remember mentally begging for the opportunity to study in this department. To be a student here and be instructed by, work for and with, and be advised by some of the most influential people in the field of Pharmaceutical Chemistry has been a privilege. I am eternally grateful for the opportunity to be a part of the KU Pharm Chem family. In addition, I would like to acknowledge the administrative staff including Nancy Helm, Nicole Brooks, Karen Hall, and Michelle Huslig, as you all have done so much to benefit me.

While in graduate school, I had the privilege of connecting with others in the pharmaceutical field on an international level through the Globalization of Pharmaceutical Education Network (GPEN). The GPEN2016 conference was held in Lawrence, KS, and I was fortunate enough to have helped organize the conference. This opportunity was critical in the development of some leadership, organizational, and communication skills that I simply never would have learned in the laboratory. I am thankful to Dr. Ron Borchardt for making this conference possible and for allowing me to be a part of the organizing committee. I am also thankful to GPEN2018 for providing me the chance to present my research in Singapore. Through these conferences, I have connected with other students around the world, specifically in Australia, Finland, and Japan, and created long-lasting relationships. Thank you Dr. Borchardt and GPEN for allowing me to be a part of this organization.

The undergraduates, Sarah Schaefer, Rebecca Clark, Joan Cheng, and Monica Saha, whom I mentored during graduate school, have also influenced me. I appreciate your interest in science and your desire to learn. Mentoring each of you was definitely one of the most

rewarding components of my graduate school career. Although mentoring was a challenge for me, I developed a useful and important skillset. Determining how each of you learned and discovering how to communicate with each of you the research project, the goals, the ideas, and the technical skills necessary to get good, reliable, reproducible data was something I truly enjoyed. Watching each of you learn and grow in the lab was sincerely rewarding.

During my time at KU, I completed an internship at Eli Lilly and Company. I am grateful to the scientists I worked with while I was there: Lihua Huang, Scott Bradley, Ganapathy Gopalrathnam, and most especially Anant Sharma. Each of you taught me about working in big pharma and about bioproduct pharma design and formulations. Starting the project at Lilly involved a big learning curve for me since I came from a drug metabolism/proteomics lab. Your patience and guidance made being at Lilly a great experience. I am very grateful for the impact each of you made on me during my time there.

Much of my success in graduate school is attributed to those acknowledged above. However, I could not have completed the journey without the love and support of my friends and family. To my in-laws, Jan, Trey, Zack, Luke and Sydney Doyle, thank you for your support over the last several years. Although I will not be able to celebrate this moment with three of my grandparents, I know they would be proud. I am thankful for the support of my grandfather and my husband's grandparents. Your love over the last few years has inspired me, even during difficult times. To my brothers, Joey and Paul, sister-in-law Madyson, and niece Adales, thank you for your encouragement. Last, but certainly not least, my parents, Carol and Joe Drbohlav. The road has been long and tough, but the two of you were always available. Whenever I needed reassurance or advice, you were there. I have no words to describe the appreciation I have for all you have sacrificed and done for me. While I may never find the words, I hope you both know

you are and always have been wonderful parents, and I am extremely fortunate call you mom and dad.

Finally, to my husband, Jacob Doyle, none of this would have been possible without you. You have been by my side even before the thought of graduate school, and for that I am thankful. Your friendship, love, encouragement, and support are invaluable to me. Whether the days were good or bad, you were there. I knew I could count on you for anything - even when we were 1,000 miles apart. There were many times I felt you wanted this degree for me more than I wanted it for myself. These moments are what got me through some of the most difficult moments of graduate school. Thank you for never letting me quit, for your unconditional love, for all the laughs, for the shoulder to cry on, and for being my partner in life.

I thank God for blessing my life with these people and for the opportunities I have had. I hope to use this degree to honor Him, to bring Him glory, and to share these blessings with others by making a difference.

Laura M. Doyle (Drbohlav)

15 April 2019



## TABLE OF CONTENTS

<b>Chapter I:</b> Overview of Extracellular Vesicles, Their Origin, Composition, Purpose, and Methods for Exosome Isolation and Analysis .....	1
<b>Chapter II:</b> Development of Liquid Chromatography – Multiple Reaction Monitoring – Mass Spectrometry (LC-MRM-MS)-Based Targeted Proteomic Method for Analysis of Exosome Marker Proteins and Its Application in Evaluating Different Exosome Preparations .....	48
<b>Chapter III:</b> Treatment of Hepatoma Cell Line, HepG2, with $\beta$ -naphthoflavone Simultaneously Increased Intracellular and Exosomal Expression of CYP1A1 .....	77
<b>Chapter IV:</b> Isolation and Characterization of Liver-derived Exosomes by Liver Marker Protein Asialoglycoprotein-1 (ASGR1) and Proteomic Analysis.....	105
<b>Chapter V:</b> Major Conclusions and Future Directions.....	132

## APPENDICIES

<b>Appendix I:</b> A Mechanistic Understanding of Polysorbate 80 Oxidation in Histidine and Citrate Buffer Systems.....	146
<b>Appendix II:</b> Development of an In Vitro Model to Screen CYP1B1-Targeted Anticancer Prodrugs .....	149
<b>Appendix III:</b> Quantification of Human Hepatic Drug-metabolizing Enzymes by Quantitative Filter-aided Sample Preparation (qFASP) .....	151
<b>Appendix IV:</b> Lack of Miltefosine for Amebic Encephalitis Despite Higher-Than-Recommended Dosing .....	154
<b>Appendix V:</b> Development of Liquid Chromatography – Multiple Reaction Monitoring – Mass Spectrometry (LC-MRM-MS)-Based Targeted Proteomics Method for Analysis of Exosome Marker Proteins and Its Application in Evaluating Different Exosome Preparations .....	156

**Chapter I: Overview of Extracellular Vesicles, Their Origin, Composition,  
Purpose, and Methods for Exosome Isolation and Analysis**

## TABLE OF CONTENTS

<b>1.1 Introduction.....</b>	<b>5</b>
1.1.1 Exosomes .....	5
1.1.1.1 Origin and Size .....	6
1.1.1.2 Composition.....	6
1.1.1.3 Biological Purpose.....	7
1.1.1.4 Applications and Uses.....	8
1.1.2 Microvesicles .....	9
1.1.2.1 Origin and Size .....	9
1.1.2.2 Composition.....	9
1.1.2.3 Biological Purpose.....	10
1.1.2.4 Applications and Uses.....	11
1.1.3 Apoptotic Bodies .....	11
1.1.3.1 Origin and Size .....	11
1.1.3.2 Composition.....	11
<b>1.2. Isolation Methods.....</b>	<b>12</b>
1.2.1 Ultracentrifugation Techniques .....	13
1.2.1.1 Differential Ultracentrifugation .....	13
1.2.1.2 Density Gradient Centrifugation.....	14
1.2.1.2.1 Rate-Zonal Centrifugation .....	15
1.2.1.2.2 Isopycnic Centrifugation.....	15
1.2.2 Size Based Techniques .....	16
1.2.2.1 Ultrafiltration .....	16
1.2.2.2 Exosome Isolation Kit.....	16
1.2.2.3 Sequential Filtration.....	17
1.2.2.4 Size Exclusion Chromatography (SEC).....	17
1.2.2.5 Flow Field-Fractionation (FFFF).....	18
1.2.2.6 Hydrostatic Filtration Dialysis (HFD) .....	18

1.2.3 Immunoaffinity Capture-Based Techniques .....	19
1.2.3.1 Enzyme-Linked Immunosorbent Assay (ELISA).....	20
1.2.3.2 Magneto-immunoprecipitation .....	20
1.2.4 Exosome Precipitation .....	21
1.2.4.1 PEG Precipitation.....	21
1.2.4.2 Lectin Induced Agglutination .....	22
1.2.5 Microfluidic Based Isolation Techniques .....	22
1.2.5.1 Acoustic Nanofilter .....	23
1.2.5.2 Immuno-based Microfluidic Isolation .....	23
<b>1.3. Analysis of Exosomes.....</b>	<b>24</b>
1.3.1 Physical Analysis .....	25
1.3.1.1 Nanoparticle Tracking Analysis (NTA).....	25
1.3.1.2 Dynamic Light Scattering (DLS).....	25
1.3.1.3 Electron Microscopy .....	26
1.3.1.4 Tunable Resistive Pulse Sensing (tRPS).....	26
1.3.2 Chemical, Biochemical, and Compositional Analysis.....	27
1.3.2.1 Immunodetection Methods .....	27
1.3.2.1.1 Flow Cytometry .....	27
1.3.2.1.2 Western Blotting .....	28
1.3.2.1.3 Integrated Immuno-isolation and Protein Analysis of Exosomes.....	29
1.3.2.2 Thermophoretic Profiling.....	30
1.3.2.3 Mass Spectrometry (MS)-Based Proteomic Analysis.....	30
1.3.2.3.1 Global Proteomic Approaches .....	30
1.3.2.3.2 Targeted Proteomic Approaches.....	33
<b>1.4. Conclusions.....</b>	<b>34</b>
<b>1.5. References.....</b>	<b>36</b>

## LIST OF TABLES

<b>Table 1.</b> Comparison of exosomal isolation techniques based on recovery, purity, required sample volume and time required for isolation.....	12
--	----

## LIST OF FIGURES

<b>Figure 1.</b> Workflow of Differential Ultracentrifugation for Exosome Isolation.....	13
<b>Figure 2.</b> Overview of Isolation and Analysis Methods Covered in This Review .....	35

## 1.1 Introduction

Extracellular vesicles (EVs) are lipid bound vesicles secreted by cells into the extracellular space [1, 2]. The three main subtypes of EVs are microvesicles (MVs), exosomes, and apoptotic bodies and are differentiated based upon their biogenesis, release pathways, size, content, and function [1-3]. The content, or cargo, of EVs consists of lipids, nucleic acids, and proteins, specifically proteins associated with the plasma membrane, cytosol, and those involved in lipid metabolism [1, 4]. The primary focus of this review will be on the protein content of EVs, however, the nucleic acid and lipid composition of EVs is well described in [1, 2, 5] and [6-8], respectively. While no specific protein markers have been identified to distinguish between the different types of EVs, MVs, exosomes, and apoptotic bodies have different protein profiles due to their different routes of formations [9-11]. However, substantial overlap of protein profiles is often observed, due in part to the lack of standardized isolation and analysis methods of EVs [2, 12]. Further, it has been demonstrated that the proteomic profiles of EVs from the same source are dependent on their isolation method [2]. The field of EVs has led to much understanding in the area of cell-cell communication and cancer metastasis and their use in the clinical setting as carriers of biomarkers for diagnostic purposes has been demonstrated [13-28], however, standardized methods for EV isolation and analysis must be developed in order for them to become tools that can truly be used in the clinical setting.

### 1.1.1 Exosomes

Exosomes, also referred to as intraluminal vesicles (ILVs), are enclosed within a single outer membrane and are secreted by all cell types and have been found in plasma, urine, semen, saliva, bronchial fluid, cerebral spinal fluid (CSF), breast milk, serum, amniotic fluid, synovial fluid, tears, lymph, bile, and gastric acid [18, 22-24, 29-40].

#### *1.1.1.1 Origin and Size*

Exosomes are a subtype of EVs formed by an endosomal route and are typically 30 – 150 nm in diameter [1, 3-5]. Specifically, exosomal vesicles form by inward budding of the endosome membrane of multivesicular bodies (MVBs) [2, 4, 5]. MVBs form upon maturation of early endosomes [3]. Early endosomes form by inward budding of the cell's plasma membrane and interact with the Golgi apparatus and endoplasmic reticulum to “pick up” proteins produced by the cell [3]. Early endosomes, and eventually the mature MVBs are involved in the endocytic and trafficking functions of the cell's material [3]. Specifically, they are involved in protein sorting, recycling, storage, transport, and release [3]. Exosomes form from inward budding of either the early endosome or MVB membrane. MVBs are eventually either sent to the lysosome to be degraded along with all of its components or fused with the cell's plasma membrane to release its content, including exosomes, into the extracellular space [4, 41-43]. The factors that determine the fate of a specific MVB are not well understood [5]. However, studies have been done to demonstrate that the fate of a particular MVB depends on the level of cholesterol in the MVB. Specifically, a cholesterol rich vesicle was secreted while a morphologically identical vesicle that lacked cholesterol was sent to the lysosome for degradation [44]. The regulation of MVB and exosome formation and release is through the ESCRT pathway [45, 46]. While the exact mechanism is still not fully understood, it appears the formation of MVBs can be stimulated by growth factors and the cell adjusts its exosome production according to its needs [29, 47].

#### *1.1.1.2 Composition*

The biogenesis of exosomes can be used to understand the proteome of the vesicles. Because exosomal formation and MVB transportation is regulated by ESCRT proteins, these proteins and its accessory proteins (Alix, TSG101, HSC70, and HSP90 $\beta$ ) are expected to be found in



exosomes regardless of the type of cell from which they originate [11, 48-51]. Thus, this set of proteins are often termed “exosomal marker proteins.” Some studies indicate there is another mechanism, an ESCRT independent mechanism, by which some cells release exosomes into the extracellular space [52]. In such cases, exosome release is thought to depend on sphingomyelinase enzyme instead of ESCRT, since cells depleted of the ESCRT machinery still produced CD63 positive exosomes [53-56]. The CD63, along with CD9 and CD81, are proteins in the tetraspanin family. These transmembrane proteins and other proteins associated with the plasma membrane are commonly found in exosomes and are often enriched in the vesicles compared to the cell lysate [57, 58]. Originally, it was thought that tetraspanin proteins were specific markers of exosomes, however these proteins have since been identified in MVs and apoptotic bodies [59, 60]. Exosomes tend to be enriched in glycoproteins compared to the secreting cells, however MVs (discussed in 1.2) are thought to contain proteins with higher levels of posttranslational modifications (PTMs), such as glycosylation and phosphorylation, compared to exosomes, which is a potential way to distinguish the vesicles based on content rather than size [58, 61, 62]. Finally, proteins associated with organelles such as the nucleus and mitochondria are not expected to be observed in the exosomal vesicles. Proteins associated with the Golgi apparatus and endoplasmic reticulum, however, may be present at low levels since early endosomes can interact with these organelles. However, such proteins are typically still considered to be non-exosomal marker proteins since they are at lower levels in the exosomes compared to the lysate.

#### *1.1.1.3 Biological Purpose*

Exosomes were originally thought to be a source of cellular dumping, or a way for cells to get rid of unneeded or wanted materials, however it has since been found that exosomes participate in cell-cell communication, cell maintenance, and tumor progression, as discussed in section 1.2.3.

In addition, exosomes have been found to stimulate immune responses by acting as antigen presenting vesicles [63, 64]. In the nervous system, exosomes are found to help promote myelin formation, neurite growth, and neuronal survival, thus playing a role in tissue repair and regeneration [65-69]. At the same time, exosomes in the central nervous system (CNS) have been found to contain pathogenic proteins, such as beta amyloid peptide, superoxide dismutase, and alpha synuclein that may aid in disease progression [70-73].

#### *1.1.1.4 Applications and Uses*

A common interest in exosomal research is in studying their ability to act carriers of biomarkers for diseases. For example, exosomes in both plasma and CSF have been found to contain alpha synuclein, a protein associated with Parkinson's disease [74-76]. Exosomes isolated from urine have been demonstrated to reflect acute kidney injury [77]. There has also been success in finding markers for pancreatic cancer and lung cancer in exosomes as well [28, 78]. The use of exosomes as carries of biomarkers is ideal because these vesicles are found in bodily fluids, such as blood and urine, which allows for minimally to non-invasive "liquid biopsy" type methods to diagnose and even monitor a patient's response to treatment. The ability of exosomes to monitor a patient's response is yet another potential application of these vesicles in the clinical setting [79]. If the disease marker directly correlates to disease state, and if the patient's treatment is working, one should observe a change in the presence of the biomarker as the patient undergoes treatment. Others have suggested that exosomes can be used in vaccine development and for other immunological purposes [64, 80]. Because exosomes act inherently as antigen presenting vesicles, it may be possible to capitalize on this inherent property. Further, exosomes have a long circulating half-life, are well tolerated by the human body, and capable of not only penetrating cellular membranes but also potentially targeting specific cell types, which makes them an even better candidate for such immunological applications [81]. Also, because of these

inherent advantages of exosomes, they are also ideal for the development of drug delivery systems [82]. While methods are still being developed for introduction of RNA and protein to exosomes and to target these exosomes to a specific region of the body, the ability to load both protein and genetic material into exosomes is yet another advantage making exosomes an attractive drug delivery system [81]. Finally, it has been demonstrated the mesenchymal stem cell exosomes themselves can act a therapeutic entity to help reduce tissue injury [83-87]. While there is a broad potential application and use of exosomes in the clinical setting, more standardized methods for exosome isolation and analysis are needed in order to meet regulatory requirements the FDA and other regulatory agencies to use exosomes as biomarkers, vaccines, drug delivery devices, and therapeutic tools [5].

## 1.1.2 Microvesicles

### *1.1.2.1 Origin and Size*

MVs are EVs that form by direct outward budding, or pinching, of the cell's plasma membrane. The size of MVs typically range from 100 nm up to 1  $\mu\text{m}$  in diameter [1-5]. The route of MV formation is not well understood, however it is thought to require cytoskeleton components, such as actin and microtubules, along with molecular motors (kinesins and myosins) and fusion machinery (SNAREs and tethering factors) [88]. The number of MVs produced depends on the donor cells physiological state and microenvironment [1]. Likewise, it has been previously demonstrated that the number of MVs consumed depends on the recipient cells physiological state and microenvironment [1]. Further, the uptake of MVs is likely an energy dependent process, as uptake is suppressed at lower temperatures [62, 89, 90].

### *1.1.2.2 Composition*

While the proteomic profiles of MVs heavily depend on the isolation method, there are a category of proteins termed “marker proteins,” which are proteins found in MVs, regardless of

cell origin, as a result of their biogenesis process [62, 91-93]. Because MVs form by an outward budding of the cell's plasma membrane, it is easily understood that MVs contain mainly cytosolic and plasma membrane associated proteins, especially proteins known to cluster at the plasma membrane surface, such as tetraspanins [94, 95]. It has been reported that such proteins can have 100-fold higher concentration in MVs compared to the cell lysate [94, 95]. Other proteins commonly identified in MVs include cytoskeletal proteins, heat shock proteins, integrins, and proteins containing post translational modifications, such as glycosylation and phosphorylation [96-98]. Interestingly, the glycan binding proteins on the surface of MVs maybe a key factor in understanding how MVs are targeted to and interact with other cells. The focus of this review will remain on the proteome of MVs, however, the glycome of MVs is thoroughly discussed in [2]. The presence of cytosolic and plasma membrane proteins can be understood based on the biogenesis of MVs, similarly, it can be understood that proteins associated with different organelles such as the mitochondria, Golgi apparatus, nucleus, and endoplasmic reticulum should be depleted in MVs, especially compared to the cell's lysate, as these organelles are not involved in the biogenesis of MVs [58, 90].

#### *1.1.2.3 Biological Purpose*

Originally, it was thought that, like exosomes, MVs were a cellular dumping or maintenance mechanism, by which the cell would get rid of unwanted material [2]. However, it has since been understood that MVs (and exosomes) are involved in cell-cell communication between local and distant cells. The ability of these EVs to alter the recipient cell has been well demonstrated [99, 100]. These new discoveries in biological purpose of EVs have spurred a global interest in fully understanding EVs and the diagnostic and therapeutic potential. Other forms of cell-cell communication, such as hormones, growth factors, cytokines, and direct interaction are better understood and play an important role as to how multi-cellular organisms

are able to function as a single system [2]. The uniqueness of EVs is that they have the ability to package active cargo (proteins, nucleic acids, and lipids) and deliver it to another cell, neighboring or distant, and alter the recipient cells functions with its delivery [1]. While such forms of communication occur between physiologically healthy cells, one could understand that diseased cells, such as cancer cells, release their active machinery in EVs, transport it to otherwise healthy cells, thus playing a role in cancer metastasis [101, 102]. Perhaps a better understanding of MV and exosomal formation and regulation could lead to new options for cancer therapies, since they appear to play a critical role in cancer development and progression.

#### *1.1.2.4 Applications and Uses*

The applications of and uses of MVs in the clinical setting are similar to those of exosomes (1.1.4)

### 1.1.3 Apoptotic Bodies

#### *1.1.3.1 Origin and Size*

Apoptotic bodies are released by dying cells into the extracellular space. They are reported to range in size from 50 nm up to 5000 nm in diameter, with the size of most apoptotic bodies tending to be on the larger side [3]. These bodies form by a separation of the cell's plasma membrane from the cytoskeleton as a result of increase hydrostatic pressure after the cell contracts [103].

#### *1.1.3.2 Composition*

The composition of apoptotic bodies is in direct contrast with exosomes and MVs. Unlike exosomes and MVs, apoptotic bodies contain intact organelles, chromatin, and small amounts of glycosylated proteins [3, 49, 62, 104]. Thus, one would expect to observe higher levels of proteins associated with the nucleus (i.e. histones), mitochondria (i.e. HSP60), Golgi apparatus, and endoplasmic reticulum (i.e. GRP78). Further, the proteomic profiles of apoptotic bodies and

cell lysate are quite similar whereas there are stark differences in the proteomic profiles between exosomes and cell lysate.

## 1.2. Isolation Methods

The potential benefits and uses of exosomes and EVs in the clinical setting has been described above, however a major hindrance in bringing exosomes into the clinical setting is the lack of standardization in isolation methods. Exosomes were originally isolated by ultracentrifugation-based methods, and while these methods remain the gold standard, other methods have been developed to address the challenges associated with ultracentrifugation [105, 106]. These alternative methods have been developed based on isolation by size, immunoaffinity capture, and precipitation of exosomes, however even these methods fail to exclusively isolate exosomes, and typically result in complex mixtures of EVs and other components of the extracellular space [1, 2]. This is due to the complexity of biological fluids from which exosomes are being isolated from, the drastic overlap in the physiochemical and biochemical properties between exosomes and different EVs, and the heterogeneity among exosomes themselves [107, 108]. Thus, the challenge remains to develop isolation techniques that can differentiate the different types of EVs in the extracellular matrix and do so rapidly, efficiently, reproducibly, and in a clinically friendly manner [5]. Further, the use of multiple isolation methods consecutively has been used to further enrich the exosomal content of a particular isolation, however this also leads to increased cost, time, and technical training making it less clinically friendly [109]. An overview of some methods described in this review can be seen in **Table 1**.

**Table 1.** Comparison of exosomal isolation techniques based on recovery, purity, required sample volume and time required for isolation.

Isolation Technique	Recovery	Purity	Sample Volume	Time Required	Reference
Ultracentrifugation	5-25%	Low	100s of mLs	8 hours	[11]
Density Gradient	Higher than UC	Similar to UC	up to 1 mL	20 hours	[161]

Precipitation Kits	N/A	Low	> 100 $\mu$ L	Overnight	[114]
ExoChip	N/A	N/A	< 400 $\mu$ L	< 2 hours	[142]
Immunoprecipitation	> 99% bead recovery	Higher than UC	up to 1 mL	Overnight	[11]
ExoSearch Chip	42-97%	Higher than UC	20 $\mu$ L	40 minutes	[140]
Acoustic Nanofilter	>80%	High	50 $\mu$ L	< 30 minutes	[138]

## 1.2.1 Ultracentrifugation Techniques

### 1.2.1.1 Differential Ultracentrifugation

Differential ultracentrifugation was the first method used for exosome isolation and remains the gold standard for exosome isolation to date [105, 110, 111]. As is the case with all centrifugation methods, the separation of exosomes and EVs from the extracellular matrix depends on density, size, and shape, with larger and more dense particles sedimenting out first [112]. A sample protocol for exosome isolation by differential ultracentrifugation is represented in the diagram in **Figure 1**.

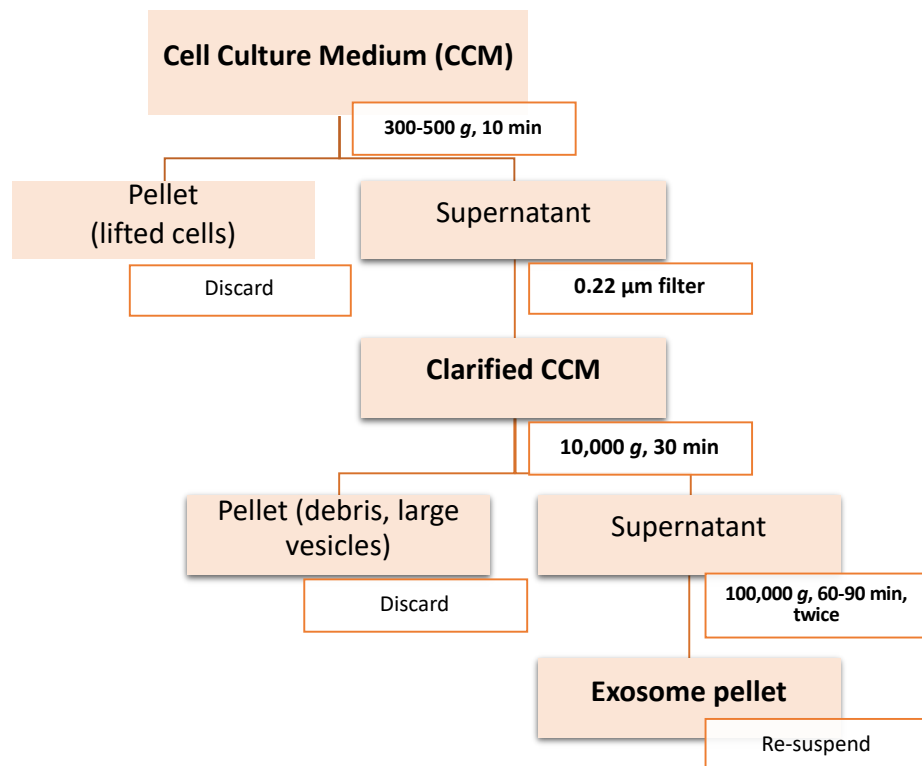


**Figure 1.** Workflow of Differential Ultracentrifugation for Exosome Isolation

The 500 x g step helps to pellet-out cellular debris and larger particles from the matrix. The 0.22 µm filtration and 10,000 x g steps further purify the matrix, removing larger EVs and apoptotic bodies. Finally, the exosomes are pelleted out and washed in the 100,000 x g centrifugation steps. The exosomal yield can be increased by using longer centrifugation times during the 100,000 x g spins, however it has been demonstrated that if > 4 hours is used, there is significant mechanical damage to the exosomes and higher levels of soluble protein contamination in the final preparation [113, 114]. Even when less than 4 hours is used during the 100,000 x g spins, differential centrifugation only results in an enrichment of exosomes, not a complete separation of exosomes from other components in the extracellular space [1]. In addition, differential ultracentrifugation is time consuming and requires large starting volumes (100s of mLs) of sample, making it difficult to process several biological samples in a short amount of time [1]. At the same time, however, differential ultracentrifugation requires little technical expertise, little to no sample pre-treatment, and affordability over time since only one ultracentrifuge is needed for long term use [106].

#### *1.2.1.2 Density Gradient Centrifugation*

Density gradient centrifugation is another ultracentrifugation method that is commonly employed in research setting. Like differential ultracentrifugation, separation is still based on size and density, however in density gradient centrifugation this occurs in the presence of a preconstructed density gradient, typically made of sucrose or iodixanol, in the centrifuge tube [106, 109]. The sample is placed at the top of the gradient, and when centrifugal force is applied, the particles in the sample pass through the gradient, which increases in density from top to bottom, at unique rates to allow for separation. The exosomes can then be collected by fractionation collection, typically in the density range of 1.1 and 1.2 g/mL [106, 109]. Density gradient ultracentrifugation is very effective in separating EVs and exosomes from protein



aggregates and non-membranous particles and is particularly useful for separating exosomes and EVs from bodily fluids. However, like differential ultracentrifugation, it suffers from low exosome recovery [11, 41, 94, 115]. Previous studies have demonstrated the coupling of differential ultracentrifugation with either Rate-Zonal Centrifugation or Isopycnic Centrifugation (2 types of density gradient ultracentrifugation) can drastically improve the purity and quality of the isolated exosomes, however it requires additional time for gradient preparation and extra care during the acceleration and deceleration to prevent damage to the gradient [116].

#### *1.2.1.2.1 Rate-Zonal Centrifugation*

Rate-Zonal centrifugation allows for separation of particles based primarily on their sedimentation rate [116]. The sample containing EVs is placed on top of a gradient and upon centrifugation the sample particles will separate into different zones based on their sedimentation rate as they move through a gradient with increasing density towards the bottom of the ultracentrifuge tube. The more dense particles will travel more quickly to the bottom of the tube as they can pass through the more dense layers easier than the smaller particles [116]. It is important to control the duration of centrifugation because eventually, since the particles are denser than the gradient, they will eventually pellet at the bottom of the ultracentrifugation tube.

#### *1.2.1.2.2 Isopycnic Centrifugation*

In isopycnic centrifugation, particles sediment into the fraction of the density gradient with the same density, also known as the isopycnic position [116]. At this position, the gradient density is equal to the buoyant density of the particles, and the particles therefore remain in the given portion of the gradient [116]. In this method, the exosomes will remain at their unique isopycnic position and will not pellet out, no matter how long the centrifugation time lasts [116]. Since apoptotic bodies, microvesicles, exosomes, and soluble proteins have different densities,

their isopycnic positions will be at different levels of the gradient, providing a separation between the extracellular components.

## 1.2.2 Size Based Techniques

### *1.2.2.1 Ultrafiltration*

Ultrafiltration is one of the most common size-based techniques used for exosome isolation; the idea behind this method is the same as with conventional membrane filtration, where the separation of particles is based on the size and molecular weight cut off (MWCO) of the membrane being used [109]. That is, particles larger than the MWCO of the particular filter are retained by the filter and particles smaller than the MWCO of the filter are passed through the filter into the filtrate [106, 109]. One challenge with ultrafiltration is the clogging and trapping of vesicles (and therefore loss of exosomes) on the filter unit [117]. While this can be minimized by starting with larger MWCO filters and moving to smaller ones, it leads to low isolation efficiency and the exosomes lost on the membrane cannot be used in downstream analysis [106]. While ultrafiltration is less time consuming than ultracentrifugation and requires no special instrumentation, it can still lead to particle deformation and lysis of exosomes due to the shear force, though this can be reduced by monitoring and regulating transmembrane pressure [114].

### *1.2.2.2 Exosome Isolation Kit*

A commercially available isolation kit, the ExoMir Kit has been developed to isolate exosomes based on size [118]. Essentially, two membranes (200 nm and 20 nm) are placed into a syringe with the 200 nm filter at the top and the 20 nm filter at the bottom [118]. The sample is typically pre-treated with a low speed centrifugation, to pellet cells and cellular debris, and proteinase K, to help breakdown larger particles and prevent the membrane from clogging [118]. After pre-treatment, the sample is passed through the syringe where the larger vesicles (>200 nm) remain above the first filter, the smaller vesicles (<200 nm and >20 nm) remain between the two filters

in the syringe, and the smallest vesicles (<20 nm) are passed through the syringe and discarded [118]. Other methods relying on the same general principle have also been developed, such as the ExoTIC technology, in order to make the isolation of exosomes a more clinically friendly procedure [119].

#### *1.2.2.3 Sequential Filtration*

The idea behind sequential filtration for exosome isolation is similar to the ExoMir Kit or ExoTIC methods discussed in 2.2.2, in that it relies on a series of filtration steps for exosome enrichment. In sequential filtration, the initial steps involves filtration with a 100 nm filter to eliminate cells, cellular debris, and large rigid particles [120]. Particles that are larger than 100 nm in diameter, such as exosomes and macrovesicles, are able to pass through the 100 nm filter as long as they are soft and flexible [120]. However, the more rigid components associated with cellular debris are filtered away [120]. The filtrate then undergoes tangential flow filtration with a 500 kDa MWCO membrane to remove soluble proteins and other contaminants [120]. Finally, concentrated retentate is filtered with a 100 nm track-etch filter for exosome enrichment [120]. The primary advantages of this methodology is that it can isolate exosomes from 150 mL of media within a day, is automatable, and produces intact and biologically active exosome material, some of which have been used in clinical trials [120-122].

#### *1.2.2.4 Size Exclusion Chromatography (SEC)*

The use of size exclusion chromatography (SEC) to isolate exosomes from other EVs based on size is performed the same way as if one wanted to separate proteins of different sizes. That is, a column is packed with a porous stationary phase in which small particles can penetrate. This penetration slows down the movement of the smaller particles through the tube, causing them to elute later in the gradient, after the larger particles. Typically, size exclusion is used in parallel to ultracentrifugation methods, where the exosome pellet is re-suspended after enrichment by

ultracentrifugation and then further purified using SEC [123, 124]. While SEC methods preserve vesicle structure, integrity, and biological activity, they require run times of several hours, are, not easily scalable, and cannot be used for high throughput applications [124]. However, iZON science has produced qEV Exosome Isolation Kit that allows for rapid, cost effective, high precision exosome isolation within 15 minutes based on the SEC methodology [125]. Their products allow for exosome isolation from < 150  $\mu$ L up to 10 mL volume of starting material with porous resins of 35 nm or 75 nm for optimal exosome isolation [125]. Development of such methodologies may bring about standardization in the area of exosome isolation, making the use of exosomes in the clinical setting more realistic.

#### *1.2.2.5 Flow Field-Fractionation (FFFF)*

Flow Field-Flow Fractionation (FFFF) is a new technique used to isolate exosomes based on size. In this method, the sample is injected into a chamber and subjected to parabolic flow as it is pushed down the length of the chamber [126]. At the same time a crossflow (a flow perpendicular to the parabolic flow) is used to create the separation of the particles in the sample [126]. Larger particles are more affected by the crossflow, so they are pushed closer to the walls of the chamber, where the parabolic flow is slower [126]. Thus, the larger particles elute after the smaller particles, which are less affected by the crossflow, remain in the center of the parabolic flow, and elute earlier [126].

#### *1.2.2.6 Hydrostatic Filtration Dialysis (HFD)*

In traditional dialysis, separation of particles in the sample is achieved by diffusion of particles across a porous membrane. The selectivity of the separation is dependent on the MWCO of the given membrane; particles smaller than the MWCO of the membrane will diffuse across the membrane and particles larger than the MWCO of the membrane will remain on the starting side of the membrane. In HFD, the sample is forced through a dialysis tube with a MWCO of 1,000

kDa by hydrostatic pressure. The solvent and small solutes pass easily through the tube and the larger particles, such as exosomes and other EVs remain in the tube, where they can be collected [127]. Typically, ultracentrifugation methods are used after HFD isolation to further separate exosomes from other EVs retained in the dialysis tube [127].

### 1.2.3 Immunoaffinity Capture-Based Techniques

Immunoaffinity capture-based techniques rely on the use of an antibody to capture exosomes based on the expression of the antigen on the surface of the exosome. Antibodies for a specific antigen of interest can be attached to plate (ex. ELISA, see section 2.3.1 below), magnetic beads (see section 2.3.2 below), resins, and microfluidic devices (see section 2.5.3 below) [106]. A major benefit of these techniques over others is that it allows for isolation of exosomes derived from a specific source [11, 128, 129]. For example, a well-established hepatocellular protein marker is Asialoglycoprotein receptor 1 (ASGR1). The presence of this protein has been established in hepatocyte derived exosomes [130] and therefore has the ability to be used as a marker to isolate liver derived exosomes. Not only do immunoaffinity methods have the potential to aid in the isolation of a specific sub-set of exosomes from a complex mixture, it also has the potential to separate exosomes from other types of EVs, should a specific marker for exosomes be identified and agreed upon [114]. The main limitation in developing this method is that the protein/antigen used to capture the exosomes must be expressed on the surface of exosomes, since the antibody will not be able to capture an antigen enclosed within the vesicle [109]. In addition, the specificity of the assay is limited to the specificity of the antibody used, however it has been well demonstrated that immunoaffinity methods result in lower yield of isolated exosomes with higher purity than for methods that isolate exosomes based on other properties [131]. Due to the complexity of biological fluids, such as plasma, immunoaffinity

capture-based techniques are often used after exosomal enrichment by ultracentrifugation or ultrafiltration [128].

#### *1.2.3.1 Enzyme-Linked Immunosorbent Assay (ELISA)*

An ELISA based assay, in which an antibody against an antigen of interest is immobilized on the surface of a microplate, is one type of immunoaffinity capture-based technique that is used to isolate exosomes from a sample. The exosome sample is exposed to the well containing the immobilized antibody and the exosomes expressing the antigen are now immobilized onto the plate due to the antibody-antigen interaction. The un-captured exosomes and sample contents are washed away and the immobilized exosomes can be detected using another antibody containing an absorbent tag. In the EV field, ELISA has been used to isolate exosomes from urine, plasma, and serum, and can even be quantitative when standards (of known exosome amounts) are used to create a calibration curve. This method has been around for many years and is currently used in the clinical setting to test a patient's blood for different antibodies against different infectious diseases, such as HIV, Zika, Lyme Disease, and others [132]. However, it is yet to be used in the clinical setting for exosome applications due to the required sample pre-treatment by ultracentrifugation or ultrafiltration.

#### *1.2.3.2 Magneto-immunoprecipitation*

In the case of magneto-immunocapture, a biotinylated antibody against the antigen of interest is attached to the surface of streptavidin coated magnetic beads. The antibody coated beads are then incubated with the sample from which exosomes are to be isolated from. The major benefits of this method over ELISA is that the beads provide a larger surface area for capturing exosomes, leading to higher isolation efficiency. Additionally, there is no upper limit of sample starting volume when using the magnetic beads, whereas the microplate-based ELISA assay has a maximum sample volume of 100  $\mu$ L that can be held within the well of a typical 96-well

microplate. Not only does magneto-immunocapture provide better isolation efficiency and capable of handling large sample volumes, the exosomes captured on the beads can be eluted and used for downstream analysis. When comparing magneto-immunocapture to the gold standard exosome isolation method, ultracentrifugation, magneto-immunocapture leads to a more pure exosome preparation, is quicker, and requires no advanced or expensive instrumentation [109]. Additionally, the magneto-immunocapture methodology is better for preserving the activity of exosomal proteins than other isolation methods, such as ultracentrifugation or ultrafiltration [133].

#### 1.2.4 Exosome Precipitation

##### *1.2.4.1 PEG Precipitation*

Precipitation of exosomal vesicles is typically done by introducing a water excluding polymer, such as PEG into the sample. The PEG polymer then “ties-up” the water molecules, causing other particles, such as exosomes to precipitate out of solution [114]. The precipitated vesicles can then be pelleted by centrifugation and used for different downstream analysis [114]. This isolation method is quick, simple, requiring little technical expertise or expensive equipment [106, 109]. Additionally, it can be used for a variety of starting volumes (from 100  $\mu$ L up to several mLs) and therefore is suitable for use in various research and clinical settings [106, 109]. However, the major drawback with this methodology, and the reason it cannot be immediately employed in the clinical setting is due to the lack of selectivity [114, 131]. Not only do the PEG polymers cause precipitation of exosomal vesicles, it also causes precipitation of other extracellular vesicles, extracellular proteins and protein aggregates [105]. Therefore, it is important to include some sample pretreatment, such as filtration and/or centrifugation, before using such methods in order to reduce contamination of final exosomal preparation [109].

Several commercially available kits have been produced based on exosome precipitation for isolation of exosomes from cell culture medium and a variety of bodily fluids [134-136].

#### *1.2.4.2 Lectin Induced Agglutination*

An alternative to PEG precipitation is lectin precipitation. Lectins are a family of proteins that bind carbohydrate moieties of other particles at a very high specificity. This is able to aid in exosome isolation when lectins bind to carbohydrates on the surface of exosomes. When lectins bind to the carbohydrates on the surface of exosomes, it alters their solubility, causing them to precipitate out of solution. Typically, the sample is pre-treated by ultracentrifugation to remove any cellular debris or other components that may also contain carbohydrates. The sample is then incubated overnight with the lectin, for example Concanavalin A or Phytohemagglutinin at 1 mg/L, and the precipitated exosomes can then be pelleted using centrifugation [137]. Like PEG precipitation methods, the lectin precipitation methods are straightforward requiring little time and expertise, however the co-precipitation of other soluble components is negligible unless they are highly glycosylated.

#### *1.2.5 Microfluidic Based Isolation Techniques*

Microfluidic based exosome isolation methods have been developed in order to address issues with more traditional methods and make the use of exosomes in the clinical setting more feasible. The primary advantage of microfluidic techniques is that they have the ability to isolate exosomes based on their physical and biochemical properties simultaneously [109].

Additionally, microfluidic isolation methods typically are rapid, efficient, require small starting volumes (10s – 100s of  $\mu\text{L}$ ), and allow for the development of innovative separation mechanisms such as acoustic, electrophoretic, and electromagnetic properties of the exosomal vesicles [138, 139].



#### *1.2.5.1 Acoustic Nanofilter*

Acoustic nanofilter is a microfluidic isolation technique in which exosomes and EVs are separated from the matrix based on size. The matrix, containing exosomes, EVs, and other extracellular components is injected into a chamber where it is exposed to ultrasound waves. These waves exert radiation forces onto the particles and the particles response to these forces are dependent upon their size and density [138]. Specifically, larger particles experience stronger radiation forces and therefore migrate faster towards the pressure nodes [138]. The ultrasonic waves can be tuned in such a way to separate particles above and below any desired size [138]. While this specific methodology is still in development stages, its simplicity, quickness, tunability, and low starting volume (50  $\mu$ L) of material make it a promising tool for potential use in the clinical setting.

#### *1.2.5.2 Immuno-based Microfluidic Isolation*

The principles behind immuno-based microfluidic isolation techniques is very similar to those of ELISA (section 2.3.1). The isolation of exosomes is based on an interaction between a membrane bound protein on the exosomal vesicle and an antibody against the protein which is immobilized on a microfluidic chip. The primary advantage of this technique over ELISA is that exosomes have been isolated from as little 10s – 100s of  $\mu$ L of serum in 60 minutes, whereas ELISA assays require prior isolation of exosomes (via ultracentrifugation, ultrafiltration etc..) from the plasma or serum [140, 141]. Much like ELISA, the specificity of the assay is dependent on the specificity of the antibody used. A commercially available product, ExoChip, has been developed for isolation of exosomes using the microfluidic technology. This product has an anti-CD63 antibody immobilized on the surface of the chip. The CD63 protein is considered an exosomal marker protein and found to be expressed in exosomes from many cell types, and thus allows for isolation of exosomes from a sample matrix regardless of the cell source [142]. Other

microfluidic based isolation methodologies have been developed, for example the ExoSearch Chip which has demonstrated the ability to isolate exosomes from as little as 20  $\mu$ L of plasma in 40 minutes [140]. Unlike the ExoChip, the ExoSearch Chip allows for isolation of specific subpopulations of exosomes of interest, assuming that the antigen used to differentiate the subpopulation of exosomes is expressed on the surface of the exosomes and can be recognized by the immobilized antibody on the beads [140]. The development of the microfluidic based technologies is essential to bringing the diagnostic, therapeutic, and prognostic capabilities of exosomes to the clinical setting because in comparison to all other isolation methods, these methods require the smallest amounts of plasma/serum, least amount of time, and are most cost efficient and require minimal expertise and training.

### **1.3. Analysis of Exosomes**

Initially, isolated extracellular vesicles were characterized primarily by their protein concentration [1]. However, the protein concentration of isolated EVs is typically overestimated due to contamination and does not take into consideration the different protein profiles that can vary between different subtypes of EVs [1]. Thus, as the uses of EVs became more prevalent and of interest, they were studied by more sophisticated methods. Today, there are typically two different types of analysis performed on the isolated vesicles, that is physical and chemical/biochemical/compositional analysis. Physical analysis, which gives insight to particle size and/or concentration, is done using nanoparticle tracking analysis (NTA), dynamic light scattering (DLS), electron microscopy, and tunable resistive pulse sensing (tRPS). The chemical/biochemical/compositional analysis is typically done via staining, immunoblotting, or proteomic analysis and gives information regarding the content of the isolated vesicles. A major challenge in the area is developing methodologies that can differentiate the different types of extracellular vesicles, are easily standardized, and well multiplexed. What makes this the most

difficult is the fact that the proteomic profiles of exosomes are changed when different isolation methods are used to isolate exosomes from the same cell line [2]. In this dissertation, the development of a liquid-chromatography multiple reaction monitoring mass spectrometry is described in order to address some of the challenges associated with current analysis methods. This section is an overview of the current methods used for exosomal protein analysis and unless otherwise noted, required some sort of isolation or enrichment of exosomal vesicles (see section 2 of this paper) prior to analysis.

### 1.3.1 Physical Analysis

#### *1.3.1.1 Nanoparticle Tracking Analysis (NTA)*

Nanoparticle Tracking Analysis, or NTA, allows for the determination of both particle size and concentration. The size of the particles is estimated using the Stokes-Einstein equation, where diffusion coefficient is based on the Brownian motion of particles within the chamber. The laser light is scattered as it interacts with the particles (under Brownian motion) within the chamber, and the scattered light is collected by a microscope that has a camera mounted to it [143]. The camera on top of the microscope captures the movement of particles in a video and then the NTA software uses the movement of the particles in the video to estimate the particle size and concentration [143]. NTA is capable of determining particle size between 10 and 1,000 nm in diameter, which is within the size of exosomes which are known to be between 50 – 150 nm [5, 144]. The challenge with NTA, however, is that it requires sample volumes of ~0.5 mL and optimization of data collection and analysis parameters [145, 146].

#### *1.3.1.2 Dynamic Light Scattering (DLS)*

Like NTA, dynamic light scattering, or DLS, uses the scattered light due to Brownian motion of particles to estimate particle size and concentration. However, instead of using the scattered light to determine the particles diffusion coefficient, DLS uses the fluctuations in the intensity of

the scattered light to estimate the particles size [145-147]. Unlike NTA, DLS requires very little sample volume (70  $\mu$ L) and is easy to use, with few parameters needed for optimization [145, 146]. While DLS has its benefits over NTA, its major drawback is in the analysis of heterogenous mixtures. Specifically, the intensity of scattered light is proportional to the sixth power of particle diameter, making the scattered light due to smaller particles harder to detect, thus often produces data that is skewed towards larger particle sizes when there is a mixture of particle sizes present in the suspension [145, 146]. Therefore, NTA is best for differentiation of heterogenous populations of particles [146].

#### *1.3.1.3 Electron Microscopy*

The two common types of electron microscopy used to assess the morphology of exosomal vesicles are transmission electron microscopy (TEM) and scanning electron microscopy (SEM). Both SEM and TEM produce high resolution images of submicron particles using a beam of electrons. The difference between the two is what electrons are detected. Simply put, in SEM, the scattered electrons are detected and in TEM, the electrons that pass through the sample are detected [148]. More specifically, in SEM, the electrons are scattered when they interact with the particles in the sample. The scattered electrons are then captured and detected, which produces this image of particles. In TEM, however, the electrons that do not interact with the particles pass through the sample and are detected using a fluorescent screen. The particles of the sample create dark areas, or shadows, on the fluorescent screen thus producing an image [148]. In the case of exosomes, both TEM and SEM demonstrate similar size distribution of particles but slightly different morphologies [149]. That is, in TEM, the exosomal vesicles typically have a divot in their center. This is likely due to the drying process associated with the sample preparation required for TEM [149].

#### *1.3.1.4 Tunable Resistive Pulse Sensing (tRPS)*

Tunable resistive pulse sensing, or tRPS, is another technique that can be used in order to get the size distribution and concentration of particles in a sample. Essentially, a fluid cell is divided in half by a non-conductive nano-membrane [150]. One half of the cell contains the suspension and the other half contains a particle free electrolyte [150]. A potential is applied across the 2 cells and the particles then flow from their half, through the nano-membrane, and to the other half. As the particles cross the membrane, however, it causes a disruption, or resistive pulse, in the current across the 2 different cells [150]. The length of the resistive pulse can be correlated to the size of the particle producing that particular resistive pulse, if a series of standards with known diameters is used to build the calibration curve [150]. In addition, the number of resistive pulses can be measured over a given time (the rate of resistive pulses) which reveals information regarding particle concentration within a sample [150].

### 1.3.2 Chemical, Biochemical, and Compositional Analysis

#### *1.3.2.1 Immunodetection Methods*

Immunodetection methods are analysis methods that rely on the recognition of a polyclonal or monoclonal antibody to its antigen in the sample. Such methods are commonly employed in biomedical research laboratories and are often used to establish the purity of isolated EVs by observing the presence or absence of marker proteins, as well as detect target proteins of interest.

#### *1.3.2.1.1 Flow Cytometry*

Flow cytometry is often considered a physical form of analysis since it allows for visual observation of exosomes, however it requires some knowledge regarding the protein composition of the exosomal vesicles in order for the vesicles to be detected, thus is also considered a form of compositional analysis. While the flow cytometry technology is quickly advancing, with newer instruments having detection limits as low as 100-200 nm, most instruments have a 300 - 500 nm limit of detection, which is much larger than the size of exosomal vesicles [151, 152]. The

challenge of flow cytometry in the field of EVs is that, despite the recent advances, it requires a single particle suspension which can be very challenging to achieve when the exosomal concentration is high or if aggregation of exosomal vesicles occurs during the isolation process [152]. Aggregation of vesicles results in the observation of multiple particles at a single time which results in inaccurate data [152]. Thus, it requires the immobilization of exosomes on the surface of beads (either by immunocapture or covalent conjugation) in order to be observed by the flow cytometer. Once exosomes are immobilized on the surface of the beads, the exosomal vesicles are exposed to a fluorescently conjugated antibody against an antigen that is known/expected to be expressed on the exosomal surface [152]. The exosomal vesicles conjugated to the beads and the fluorescent antibody can be viewed under an epifluorescent microscope (EPI) prior to flow cytometry. Then, as the sample passes through the laser of the flow cytometer, it emits a fluorescent signal which is detected [151, 152]. Not only does this allow for high throughput analysis of exosomes, it also allows for quantification or classification of exosomes based on the antigen expression [152].

#### *1.3.2.1.2 Western Blotting*

The principles behind immunoblotting, or Western blotting, are similar to that of EPI and flow cytometry, except that it occurs on the surface of a membrane rather than in solution on the surface of beads. Unlike flow cytometry and EPI, Western blotting does not allow for observation of intact vesicles, rather, the vesicles are lysed and the proteins are denatured and reduced during the sample preparation [153]. After denaturation, the proteins are separated by SDS-PAGE and then transferred to a nitrocellulose or polyvinylidene fluoride (PVDF) membrane. The remaining open pores on the membrane are filled with protein (from non-fat milk) and/or detergent and then exposed to an antibody against an antigen of interest. The antibody ideally specifically recognizes the antigen on the surface of the membrane. The

membrane is then exposed to a secondary antibody, which is an antibody against the species of the initial (primary) antibody used to recognize the antigen. The secondary antibody is detected due to its fluorescent tag, or by the horseradish peroxidase/alkaline phosphatase group coupled to the secondary antibody. The Western blotting methodology is among the most commonly-used analysis methods for analysis of exosomes due to its ease of use, wide accessibility, and the ability to detect exosomal surface proteins and internal proteins. The primary pitfall, however, is that it is not well-multiplexed, and specificity and reproducibility are limited by the quality of the antibody used. The lack of multiplicity results in the use of a large amount of exosomal protein used to gain minimal amount of information. Since the collection and isolation of exosomes is often a time-consuming process with low yield, more multiplexed analysis methods would be highly beneficial. This issue was addressed in chapter 2 of this dissertation with the development of a liquid-chromatography multiple reaction monitoring mass spectrometry-based method.

#### *1.3.2.1.3 Integrated Immuno-isolation and Protein Analysis of Exosomes*

A novel microfluidic assay has been developed that allows for not only isolation, but also for protein analysis of exosomal vesicles. As discussed above in section 2.5.3 (Immuno-based Microfluidic Isolation) microfluidic devices are a developing technology that may be key to bringing exosomes to use in the clinical setting. Many of the existing microfluidic techniques allow for detection of exosomes using fluorescent antibodies against an antigen of interest on the surface of exosomes, this time taking place on the surface of a chip rather than a membrane or magnetic bead. However, the novel device described in [141] allows for isolation of the exosomal vesicles, on a microfluidic chip, but then introduces a lysis buffer to lyse the captured exosomal vesicles. The lysate is then eluted from the microfluidic chip, and the biomarkers of interest can be probed for, independent of whether or not the biomarker is contained within the

vesicles or on the surface of the exosomal vesicle. This allows for a more broad spectrum of antigens to be detected and allows for the development of biomarkers within exosomes to be used rather than those only on the exosome surface.

#### *1.3.2.2 Thermophoretic Profiling*

This methodology is similar to the integrated immune-isolation discussed above (3.2.1.3) in that it isolates, or enriches, the vesicles while giving some compositional information at the same time. The difference in thermophoretic profiling compared to the integrated immune-isolation, is that it does not rely on the use of antibodies. Instead, < 1  $\mu$ L of serum is diluted 10x into PBS and incubated with 7 different fluorescently conjugated nucleotide aptamers, which specifically target different proteins on the surface of exosomes in the serum [154]. The aptamer-exosome incubation takes place for 2 hours at room temperature, at which point the chamber is exposed to a 1,480 nm laser for 10 minutes. This process drives the exosomal vesicles to the center of the laser point, leading to accumulation of the vesicles, which can then be investigated for presence/absence of specific proteins based on the fluorescent detection of the EV conjugated aptamers. The authors demonstrated lack of fluorescent signal without the laser heating and also that free aptamers and small serum proteins could not be enriched when exposed to the laser [154]. Such methodologies, which use very little serum, do not require any sample pre-treatment or time-consuming exosome isolation, are reliable, reproducible, specific, do not require high technical expertise or training, and give information regarding the presence of cancer biomarkers in the EVs within hours, are methods that could make the use of exosomes in the clinical setting a reality.

#### *1.3.2.3 Mass Spectrometry (MS)-Based Proteomic Analysis*

##### *1.3.2.3.1 Global Proteomic Approaches*



Global proteomics is a method used to identify as many proteins as possible within a sample. This can be done two different ways, via data dependent acquisition (DDA) or data independent acquisition (DIA), with DDA being used more commonly than DIA [155]. In DDA experiments, a survey MS spectrum is collected, and the most abundant ions are then selected for fragmentation and MS/MS analysis. Thus, the data depends on the abundance of the ion in the survey MS spectrum relative to other ions eluting at the same retention time in the same MS spectrum. The tandem MS data is processed using software (for example Mascot) to get information on the amino acid sequence which can then be used to identify the proteins present in a sample. In DIA experiments, ions are not selected based on abundance for fragmentation, but rather it is an attempt to fragment and get MS/MS data on all ions within a given mass range. In these experiments, fragmentation libraries are used to sort the mixed MS/MS data and identify the proteins present within the sample. Both DDA and DIA experiments can be done with top-down sample preparation and bottom up sample preparation. The top down approach, which is when no proteolysis of the proteins takes place prior to MS analysis, remains challenging from a technological perspective [156]. While advances have been made in the ability to separate and fragment intact proteins, the bottom up approach remains the most commonly used sample preparation method. In bottom up approach, the sample is digested with a protease, such as trypsin or pepsin, prior to MS analysis. The smaller protein fragments (peptides) produced by the enzymes are easier to separate, ionize, and fragment for high quality MS/MS data. However, the versatility of this technique is limited because the MS/MS data collected occurs after fragmentation by collision induced dissociation (CID). During CID, the weakest bonds are broken first, and these bonds are typically bonds associated with PTMs, thus making the PTM analysis of these peptides difficult. The use of top down approaches, however, would reveal information regarding a protein's PTMs as the MS/MS data is collected after electron-transfer

dissociation (ETD), which causes fragmentation of the peptide/protein backbone while leaving PTMs intact. Additionally, top down approaches would reveal sequence variations in proteins between the exosomes and parent cell, which may be useful in further understanding the role of specific proteins within exosomal vesicles. Typically, global proteomic experiments on exosomes results in several hundred to several thousand of proteins identified, dependent upon the amount of starting material used, the sample preparation method, and the algorithm used for data analysis. The use of global proteomics in the field of exosomes is often for identification novel biomarkers for different cancers or diseases, but sometimes the presence of the protein (or biomarker) is also present in exosomes from healthy tissues. Thus, it is not only important to identify the proteins present in the exosomal vesicles, but also be able to quantify the proteins present within the exosomal vesicles. Protein quantification in global proteomics can be done with labeled techniques, such as SILAC or iTRAQ, which involve the incorporation of a stable heavy isotope labeled amino acid into the peptide of interest [157]. However, not only is this an expensive process, but the peptide of interest may not always be known. Thus, label free techniques have been developed in order to quantify the proteins identified in DDA or DIA experiments. The techniques rely either on the peak area of the parent ion or the spectral count, which is the number of times a specific peptide is selected for fragmentation in a data dependent LC-MS/MS [158]. While both of these methods require some sort of normalization, they are now used more frequently than the labeling techniques. The use of global proteomics in the field of EVs, and specifically exosomes, has aided and continues to aid in the development of biomarkers for different diseases and cancers. Further, there is potential for this technique to reveal the purpose and activity of different proteins in the exosomal vesicles and how they are similar and different to those in the parent cells as the technology around the top down methodology continues to develop.

#### *1.3.2.3.2 Targeted Proteomic Approaches*

As opposed to global proteomics, where the goal is to identify as many proteins as possible in a sample, targeted proteomic analysis is used to identify and quantify a predefined set of proteins in a given sample [155]. The most common targeted proteomic approach is multiple reaction monitoring, or MRM. Due to upper mass limitations of triple quadrupole instruments, used for MRM methods, the bottom up approach must be used and specific peptides for each protein of interest must be selected prior to analysis. That is, a peptide generated by the trypsin or pepsin digestion must be selected and be unique for the protein that is to be monitored [159, 160]. Once the peptide is selected, transitions, or fragments, of the peptide can be established and detected by the instrument. Essentially, in the first quadrupole (Q1) of a triple quadrupole instrument, the parent ion, which is the intact peptide selected to represent the protein of interest, is selected to pass through into the second quadrupole (q2). All other ions are filtered out in Q1 quadrupole and do not pass into q2 [155]. Once in q2, the parent ion will be fragmented and then passed into the third quadrupole, Q3. In Q3, a specific fragment ion is selected to reach the detector and all other fragment ions are filtered out and do not reach the detector. By monitoring multiple unique peptides for a single protein, and then multiple fragments for each peptide, the specificity and accuracy of the method can be greatly enhanced. Typically, it is recommended that at least 2 unique peptides are used to monitor a specific protein and at least three transitions are used to monitor each peptide, thus a total of 6 signals are used to monitor a single protein of interest. Additionally, the MRM method is extremely well multiplexed, as long as the chromatography allows for good separation of the peptides. By monitoring different peptides at different retention times, the MRM method can give highly sensitive, specific, and quantitative information on hundreds of peptides in a single experiment. Absolute quantification for proteins (via peptides) in a sample can be assessed using the MRM methodology by spiking stable

isotope labeled peptides into the sample prior to analysis. Relative quantification can be done using simple normalization techniques, similar to the normalization done in the label free global proteomic approaches. However, because MRM methods have lower limits of detection, greater dynamic ranges, and increased specificity, it is the mass spectrometry proteomic approach of choice for the rapid identification and quantification of a predetermined set of proteins in a sample [155]. In the realm of EVs, specifically exosomes, the development of MRM methods to characterize isolated exosomes would be beneficial not only due to its multiplicity and specificity over the traditional Western blot methodology, but also because a predefined set of proteins (exosomal marker proteins and non exosomal marker proteins) have been described.

#### **1.4. Conclusions**

The uses of EVs in the clinical setting for diagnostic, prognostic, therapeutic, and drug delivery tools has well been demonstrated and continues to be a subject of intense study simply based on the ever-growing literature on the topic. However, the lack of standardization in isolation and analysis methods is heavily impacting the advancement of exosomes and EVs into the clinical setting. Each isolation and analysis method (see **Figure 2** for review) has its own set of benefits and drawbacks, and it has been demonstrated that different isolation methods used to isolate exosomes from the same cell type results in different proteomic profiles, further complicating the situation. Therefore, instead of focusing on establishing a set of exosomal/non exosomal marker proteins secreted by all cell types independent of the isolation method, it may be more beneficial to focus on the development exosomal/non exosomal marker proteins for a given cell type, independent of isolation method, or a set of exosomal/non exosomal marker proteins for all exosomes, regardless of their origin, when isolated by a specific method.

## **Starting Material**

### **Cell Culture Medium**

### **Biological Samples**

Blood/Plasma/Serum  
Urine  
Saliva  
Others

## **Isolation Methods**

### **Ultracentrifugation**

Differential  
Density Gradient  
Moving Zone  
Isopycnic

### **Size Based Techniques**

Hydrostatic Filtration  
Dialysis  
Flow Field Fractionation  
Exosome Isolation Kit  
Sequential Filtration  
Ultrafiltration  
SEC

### **Immunoaffinity**

Immunocapture  
ELISA

### **Precipitation**

PEG Induced  
Lectin Induced

### **Microfluidic**

Acoustic Nanofilter  
Immuno-based

## **Analysis Methods**

### **Physical Analysis**

Tunable Resistive Pulse Sensing  
Nanoparticle Tracking Analysis  
Dynamic Light Scattering  
Electron Microscopy

### **Compositional Analysis**

Immunodetection  
Western Blotting  
Flow Cytometry  
Mass Spectrometry  
Global  
Targeted  
Microfluidic  
Acoustic Nanofilter  
Immuno-based

**Figure 2.** Overview of Isolation and Analysis Methods Covered in This Review

## 1.5. References

1. Zaborowski, M.P., et al., *Extracellular Vesicles: Composition, Biological Relevance, and Methods of Study*. BioScience, 2015. **65**(8): p. 783-797.
2. Yáñez-Mó, M., et al., *Biological properties of extracellular vesicles and their physiological functions*. Journal of Extracellular Vesicles, 2015. **4**(1).
3. Borges, F.T., L.A. Reis, and N. Schor, *Extracellular vesicles: structure, function, and potential clinical uses in renal diseases*. Braz J Med Biol Res, 2013. **46**(10): p. 824-30.
4. Bebelman, M.P., et al., *Biogenesis and function of extracellular vesicles in cancer*. Pharmacol Ther, 2018. **188**: p. 1-11.
5. Raposo, G. and W. Stoorvogel, *Extracellular vesicles: exosomes, microvesicles, and friends*. J Cell Biol, 2013. **200**(4): p. 373-83.
6. Haraszti, R.A., et al., *High-resolution proteomic and lipidomic analysis of exosomes and microvesicles from different cell sources*. Journal of Extracellular Vesicles, 2016. **5**(1).
7. Skotland, T., K. Sandvig, and A. Llorente, *Lipids in exosomes: Current knowledge and the way forward*. Progress in Lipid Research, 2017. **66**: p. 30-41.
8. Dang, V.D., et al., *Lipidomic and proteomic analysis of exosomes from mouse cortical collecting duct cells*. FASEB J, 2017. **31**(12): p. 5399-5408.
9. <Comparative proteomics evaluation of plasma exosome isolation techniques and assessment of the stabi.pdf>.
10. Kalra, H., et al., *Comparative proteomics evaluation of plasma exosome isolation techniques and assessment of the stability of exosomes in normal human blood plasma*. Proteomics, 2013. **13**(22): p. 3354-64.
11. Tauro, B.J., et al., *Comparison of ultracentrifugation, density gradient separation, and immunoaffinity capture methods for isolating human colon cancer cell line LIM1863-derived exosomes*. Methods, 2012. **56**(2): p. 293-304.
12. Giuseppe Palmisano, S.S.J., Marie-Catherine Le Bihan, and J.N.M. Jeanne Laine', Flemming Pociot, and Martin Røssel Larsen, *Characterization of Membrane-shed Microvesicles from Cytokine-stimulated -Cells Using Proteomics Strategies*. Molecular & Cellular Proteomics, 2012. **11** (8) **230-243**.
13. Sonoda, H., et al., *Decreased abundance of urinary exosomal aquaporin-1 in renal ischemia-reperfusion injury*. Am J Physiol Renal Physiol, 2009. **297**(4): p. F1006-16.
14. Hua Zhou, T.P., Angel Aponte, Peter S.T. Yuen, Jason D. Hoffert, Hideo, X.H. Yasuda, Lakhmir Chawla, Rong-Fong Shen, Mark A. Knepper, and Robert, and A. Star,

- Exosomal Fetuin-A identified by proteomics: a novel urinary biomarker for detecting acute kidney injury.* *Kidney Int*, 2006. **70**(10): p. 1847-1857.
15. Miranda, K.C., et al., *Nucleic acids within urinary exosomes/microvesicles are potential biomarkers for renal disease.* *Kidney Int*, 2010. **78**(2): p. 191-9.
  16. Neal, C.S., et al., *Circulating microRNA expression is reduced in chronic kidney disease.* *Nephrology Dialysis Transplantation*, 2011. **26**(11): p. 3794-3802.
  17. Stephanie N. Hurwitz<sup>1</sup>, M.A.R., Joseph L. Bundy, Xia Liu, Rakesh K. Singh, David G. Meckes, Jr., *Proteomic profiling of NCI-60 extracellular vesicles uncovers common protein cargo and cancer type-specific biomarkers.* *Oncotarget*, 2016. **7**(52): p. 86999-87015.
  18. Hornick, N.I., et al., *Serum Exosome MicroRNA as a Minimally-Invasive Early Biomarker of AML.* *Scientific Reports*, 2015. **5**(1).
  19. Wang, J.L., Yuanyuana; Sun, Wangweia; Zhang, Qinghua; Gu, Taoa; Li, Guangxinb, *Plasma exosomes as novel biomarker for the early diagnosis of gastric cancer.* *Cancer Biomarkers*, 2018. **21**(4): p. 805-812.
  20. Rabinowits, G., et al., *Exosomal microRNA: a diagnostic marker for lung cancer.* *Clin Lung Cancer*, 2009. **10**(1): p. 42-6.
  21. Chen, I.H., et al., *Phosphoproteins in extracellular vesicles as candidate markers for breast cancer.* *Proceedings of the National Academy of Sciences*, 2017. **114**(12): p. 3175-3180.
  22. Akers, J.C., et al., *MiR-21 in the extracellular vesicles (EVs) of cerebrospinal fluid (CSF): a platform for glioblastoma biomarker development.* *PLoS One*, 2013. **8**(10): p. e78115.
  23. Rui Shi, P.-Y.W., Xin-Yi Li, Jian-Xin Chen, Yan Li, Xin-Zhong Zhang, Chen-Guang Zhang, Tao Jiang, Wen-Bin Li<sup>1</sup>, Wei Ding, Shu-Jun Cheng, *Exosomal levels of miRNA-21 from cerebrospinal fluids associated with poor prognosis and tumor recurrence of glioma patients.* *Oncotarget*, 2015. **6**(29).
  24. Goto, T., et al., *An elevated expression of serum exosomal microRNA-191, -21, -451a of pancreatic neoplasm is considered to be efficient diagnostic marker.* *BMC Cancer*, 2018. **18**(1): p. 116.
  25. Fu, F., et al., *Circulating Exosomal miR-17-5p and miR-92a-3p Predict Pathologic Stage and Grade of Colorectal Cancer.* *Transl Oncol*, 2018. **11**(2): p. 221-232.
  26. Qingyun Liu, Z.Y., Shuai Yuan, Weijia Xie, Chengying Li, Zeyao Hu, Ying Xiang, Na Wu, Long Wu, Li Bai, Yafei Li, *Circulating exosomal microRNAs as prognostic biomarkers for non-small-cell lung cancer.* *Oncotarget*, 2017. **8**(8): p. 13048-13058.

27. Whiteside, T.L., *The potential of tumor-derived exosomes for noninvasive cancer monitoring*. Expert Review of Molecular Diagnostics, 2015. **15**(10): p. 1293-1310.
28. Melo, S.A., et al., *Glypican-1 identifies cancer exosomes and detects early pancreatic cancer*. Nature, 2015. **523**(7559): p. 177-82.
29. Trairak Pisitkun, R.-F.S., and Mark A. Knepper, *Identification and proteomic profiling of exosomes in human urine*. 2004.
30. Caby, M.P., et al., *Exosomal-like vesicles are present in human blood plasma*. Int Immunol, 2005. **17**(7): p. 879-87.
31. Vojtech, L., et al., *Exosomes in human semen carry a distinctive repertoire of small non-coding RNAs with potential regulatory functions*. Nucleic Acids Res, 2014. **42**(11): p. 7290-304.
32. Zlotogorski-Hurvitz, A., et al., *Human saliva-derived exosomes: comparing methods of isolation*. J Histochem Cytochem, 2015. **63**(3): p. 181-9.
33. Yuan, Z., Bedi, B., Sadikot, R. T., *Bronchoalveolar Lavage Exosomes in Lipopolysaccharide-induced Septic Lung Injury*. J. Vis. Exp., 2018. **135**.
34. Edward R. Sauter, D.R., *Bronchoalveolar Lavage Exosomes in Lipopolysaccharide-induced Septic Lung Injury*. Translational Cancer Research, 2017. **6**.
35. Dixon, C.L., et al., *Amniotic Fluid Exosome Proteomic Profile Exhibits Unique Pathways of Term and Preterm Labor*. Endocrinology, 2018. **159**(5): p. 2229-2240.
36. Li, Z., et al., *Emerging Role of Exosomes in the Joint Diseases*. Cell Physiol Biochem, 2018. **47**(5): p. 2008-2017.
37. Grigor'eva, A.E., et al., *Exosomes in tears of healthy individuals: Isolation, identification, and characterization*. Biochemistry (Moscow) Supplement Series B: Biomedical Chemistry, 2016. **10**(2): p. 165-172.
38. Milasan, A., et al., *Extracellular vesicles are present in mouse lymph and their level differs in atherosclerosis*. J Extracell Vesicles, 2016. **5**: p. 31427.
39. Yoon, S.B. and J.H. Chang, *Extracellular vesicles in bile: a game changer in the diagnosis of indeterminate biliary stenoses?* Hepatobiliary Surg Nutr, 2017. **6**(6): p. 408-410.
40. Yoshida Y, et al., *Detection of DNA methylation of gastric juice-derived exosomes in gastric cancer*. Integr Mol Med, 2014.
41. Simons, M. and G. Raposo, *Exosomes--vesicular carriers for intercellular communication*. Curr Opin Cell Biol, 2009. **21**(4): p. 575-81.



42. Thery, C., M. Ostrowski, and E. Segura, *Membrane vesicles as conveyors of immune responses*. Nat Rev Immunol, 2009. **9**(8): p. 581-93.
43. Simpson, S.M.a.R.J., *ExoCarta: A compendium of exosomal proteins and RNA*. Proteomics, 2009.
44. Wiebke Möbius, Y.O.I., Elly G. van Donselaar, Viola M.J. Oorschot, Yukiko Shimada, Toyoshi Fujimoto, Harry F.G. Heijnen, Hans J. Geuze, and Jan W. Slot, *Immunoelectron Microscopic Localization of Cholesterol Using Biotinylated and Non-cytolytic Perfringolysin O*. 2002.
45. Markus Babst, D.J.K., T.M. Eden J. Estepa-Sabal, and a.S.D. Emr, *ESCRT-III: An Endosome-Associated Heterooligomeric Protein Complex Required for MVB Sorting*. 2002.
46. Wollert, T. and J.H. Hurley, *Molecular mechanism of multivesicular body biogenesis by ESCRT complexes*. Nature, 2010. **464**(7290): p. 864-9.
47. Borges, F.T., et al., *TGF-beta1-containing exosomes from injured epithelial cells activate fibroblasts to initiate tissue regenerative responses and fibrosis*. J Am Soc Nephrol, 2013. **24**(3): p. 385-92.
48. Morita, E., et al., *Human ESCRT and ALIX proteins interact with proteins of the midbody and function in cytokinesis*. EMBO J, 2007. **26**(19): p. 4215-27.
49. Thery, C., et al., *Proteomic Analysis of Dendritic Cell-Derived Exosomes: A Secreted Subcellular Compartment Distinct from Apoptotic Vesicles*. The Journal of Immunology, 2001. **166**(12): p. 7309-7318.
50. van Niel, G., et al., *Exosomes: a common pathway for a specialized function*. J Biochem, 2006. **140**(1): p. 13-21.
51. Charles Ge' minard, A.d.G., LionelBlanc and Michel Vidal, *Degradation of AP2 During Reticulocyte MaturationEnhances Binding of Hsc70 and Alix to a Common Siteon TfR for Sorting into Exosomes*. 2004.
52. Katarina Trajkovic, C.H., Salvatore Chiantia, Lawrence Rajendran, Dirk Wenzel, Felix Wieland, Petra Schwille, Britta Brügger, Mikael Simons, *Ceramide Triggers Budding of Exosome Vesicles into Multivesicular Endosomes*. 2008.
53. Stuffers, S., et al., *Multivesicular endosome biogenesis in the absence of ESCRTs*. Traffic, 2009. **10**(7): p. 925-37.
54. Buschow, S.I., et al., *MHC class II-associated proteins in B-cell exosomes and potential functional implications for exosome biogenesis*. Immunol Cell Biol, 2010. **88**(8): p. 851-6.

55. Theos, A.C., et al., *A luminal domain-dependent pathway for sorting to intraluminal vesicles of multivesicular endosomes involved in organelle morphogenesis*. Dev Cell, 2006. **10**(3): p. 343-54.
56. van Niel, G., et al., *The tetraspanin CD63 regulates ESCRT-independent and -dependent endosomal sorting during melanogenesis*. Dev Cell, 2011. **21**(4): p. 708-21.
57. Witwer, K.W., et al., *Standardization of sample collection, isolation and analysis methods in extracellular vesicle research*. J Extracell Vesicles, 2013. **2**.
58. Sinha, A., et al., *In-depth proteomic analyses of ovarian cancer cell line exosomes reveals differential enrichment of functional categories compared to the NCI 60 proteome*. Biochem Biophys Res Commun, 2014. **445**(4): p. 694-701.
59. Tauro, B.J., et al., *Two distinct populations of exosomes are released from LIM1863 colon carcinoma cell-derived organoids*. Mol Cell Proteomics, 2013. **12**(3): p. 587-98.
60. Crescitelli, R., et al., *Distinct RNA profiles in subpopulations of extracellular vesicles: apoptotic bodies, microvesicles and exosomes*. J Extracell Vesicles, 2013. **2**.
61. Palmisano, G., et al., *Characterization of membrane-shed microvesicles from cytokine-stimulated beta-cells using proteomics strategies*. Mol Cell Proteomics, 2012. **11**(8): p. 230-43.
62. Escrevente, C., et al., *Interaction and uptake of exosomes by ovarian cancer cells*. BMC Cancer, 2011. **11**: p. 108.
63. Ang'elique Bobrie, M.C., Grac,a Raposo, and Clotilde Th'ery, *Exosome Secretion: Molecular Mechanisms and Roles in Immune Responses*. 2011.
64. Nathalie Chaput, C.T., *Exosomes: immune properties and potential clinical implementations*. 2011.
65. Faure, J., et al., *Exosomes are released by cultured cortical neurones*. Mol Cell Neurosci, 2006. **31**(4): p. 642-8.
66. Kramer-Albers, E.M., et al., *Oligodendrocytes secrete exosomes containing major myelin and stress-protective proteins: Trophic support for axons?* Proteomics Clin Appl, 2007. **1**(11): p. 1446-61.
67. Lachenal, G., et al., *Release of exosomes from differentiated neurons and its regulation by synaptic glutamatergic activity*. Mol Cell Neurosci, 2011. **46**(2): p. 409-18.
68. Bakhti, M., C. Winter, and M. Simons, *Inhibition of myelin membrane sheath formation by oligodendrocyte-derived exosome-like vesicles*. J Biol Chem, 2011. **286**(1): p. 787-96.

69. Wang, S., et al., *Synapsin I is an oligomannose-carrying glycoprotein, acts as an oligomannose-binding lectin, and promotes neurite outgrowth and neuronal survival when released via glia-derived exosomes*. J Neurosci, 2011. **31**(20): p. 7275-90.
70. Benoit Fevrier, D.V., Fabienne Archer, Damarys Loew, Wolfgang Faigle, Michel Vidal, Hubert Laude, and Grac a Raposo, *Cells release prions in association with exosomes*. 2004.
71. Lawrence Rajendran, et al., *Alzheimer's disease -amyloid peptides are released in association with exosomes*. 2006.
72. Gomes, C., et al., *Evidence for secretion of Cu,Zn superoxide dismutase via exosomes from a cell model of amyotrophic lateral sclerosis*. Neurosci Lett, 2007. **428**(1): p. 43-6.
73. Emmanouilidou, E., et al., *Cell-produced alpha-synuclein is secreted in a calcium-dependent manner by exosomes and impacts neuronal survival*. J Neurosci, 2010. **30**(20): p. 6838-51.
74. Alvarez-Llamas, G., et al., *Recent advances in atherosclerosis-based proteomics: new biomarkers and a future perspective*. Expert Rev Proteomics, 2008. **5**(5): p. 679-91.
75. Al-Nedawi, K., B. Meehan, and J. Rak, *Microvesicles: messengers and mediators of tumor progression*. Cell Cycle, 2009. **8**(13): p. 2014-8.
76. Simpson, R.J., et al., *Exosomes: proteomic insights and diagnostic potential*. Expert Rev Proteomics, 2009. **6**(3): p. 267-83.
77. Zhou, H., et al., *Exosomal Fetuin-A identified by proteomics: a novel urinary biomarker for detecting acute kidney injury*. Kidney Int, 2006. **70**(10): p. 1847-57.
78. Sandfeld-Paulsen, B., et al., *Exosomal proteins as prognostic biomarkers in non-small cell lung cancer*. Mol Oncol, 2016. **10**(10): p. 1595-1602.
79. Sonoda, H., et al., *Decreased abundance of urinary exosomal aquaporin-1 in renal ischemia-reperfusion injury*. American Journal of Physiology-Renal Physiology, 2009. **297**(4): p. F1006-F1016.
80. Bobrie, A., et al., *Exosome secretion: molecular mechanisms and roles in immune responses*. Traffic, 2011. **12**(12): p. 1659-68.
81. Lai, R.C., et al., *Exosomes for drug delivery - a novel application for the mesenchymal stem cell*. Biotechnol Adv, 2013. **31**(5): p. 543-51.
82. Lydia Alvarez-Erviti, et al., *Delivery of siRNA to the mouse brain by systemic injection of targeted exosomes*. 2011.

83. Gatti, S., et al., *Microvesicles derived from human adult mesenchymal stem cells protect against ischaemia-reperfusion-induced acute and chronic kidney injury*. *Nephrol Dial Transplant*, 2011. **26**(5): p. 1474-83.
84. Reis, L.A., et al., *Bone Marrow-Derived Mesenchymal Stem Cells Repaired but Did Not Prevent Gentamicin-Induced Acute Kidney Injury through Paracrine Effects in Rats*. *PLoS ONE*, 2012. **7**(9).
85. Bruno, S., et al., *Microvesicles Derived from Mesenchymal Stem Cells Enhance Survival in a Lethal Model of Acute Kidney Injury*. *PLoS ONE*, 2012. **7**(3).
86. Akao, Y., et al., *Microvesicle-mediated RNA molecule delivery system using monocytes/macrophages*. *Mol Ther*, 2011. **19**(2): p. 395-9.
87. Bruno, S., et al., *Mesenchymal stem cell-derived microvesicles protect against acute tubular injury*. *J Am Soc Nephrol*, 2009. **20**(5): p. 1053-67.
88. Cai, H., K. Reinisch, and S. Ferro-Novick, *Coats, tethers, Rabs, and SNAREs work together to mediate the intracellular destination of a transport vesicle*. *Dev Cell*, 2007. **12**(5): p. 671-82.
89. Morelli, A.E., et al., *Endocytosis, intracellular sorting, and processing of exosomes by dendritic cells*. *Blood*, 2004. **104**(10): p. 3257-66.
90. Christianson, H.C., et al., *Cancer cell exosomes depend on cell-surface heparan sulfate proteoglycans for their internalization and functional activity*. *Proc Natl Acad Sci U S A*, 2013. **110**(43): p. 17380-5.
91. Gonzales, P.A., et al., *Large-scale proteomics and phosphoproteomics of urinary exosomes*. *J Am Soc Nephrol*, 2009. **20**(2): p. 363-79.
92. Jeppesen, D.K., et al., *Quantitative proteomics of fractionated membrane and lumen exosome proteins from isogenic metastatic and nonmetastatic bladder cancer cells reveal differential expression of EMT factors*. *Proteomics*, 2014. **14**(6): p. 699-712.
93. Ostergaard, O., et al., *Quantitative proteome profiling of normal human circulating microparticles*. *J Proteome Res*, 2012. **11**(4): p. 2154-63.
94. Escola, J.-M., et al., *Selective Enrichment of Tetraspan Proteins on the Internal Vesicles of Multivesicular Endosomes and on Exosomes Secreted by Human B-lymphocytes*. *Journal of Biological Chemistry*, 1998. **273**(32): p. 20121-20127.
95. Zoller, M., *Tetraspanins: push and pull in suppressing and promoting metastasis*. *Nat Rev Cancer*, 2009. **9**(1): p. 40-55.
96. Harry F.G. Heijnen, A.E.S., Rob Fijnheer, Hans J. Geuze, and Jan J. Sixma, *Activated Platelets Release Two Types of Membrane Vesicles: Microvesicles by Surface Shedding and Exosomes Derived From Exocytosis of Multivesicular Bodies and -Granules*. 1999.

97. Di Vizio, D., et al., *Large oncosomes in human prostate cancer tissues and in the circulation of mice with metastatic disease*. Am J Pathol, 2012. **181**(5): p. 1573-84.
98. Morello, M., et al., *Large oncosomes mediate intercellular transfer of functional microRNA*. Cell Cycle, 2013. **12**(22): p. 3526-36.
99. Harding, C.V., J.E. Heuser, and P.D. Stahl, *Exosomes: looking back three decades and into the future*. J Cell Biol, 2013. **200**(4): p. 367-71.
100. Ian J White, L.M.B. and S.E.M.a.C.E.F. Minoo Razi Aghakhani, *EGF stimulates annexin I-dependent inward vesiculation in a multivesicular endosome subpopulation*. The EMBO Journal, 2006.
101. Rak, J., *Microparticles in Cancer*. Semin Thromb Hemos, 2010.
102. Joshua L. Hood, S.S.R., and Samuel A. Wickline, *Exosomes Released by Melanoma Cells Prepare Sentinel Lymph Nodes for Tumor Metastasis*. Cancer Research, 2011.
103. Wickman, G., L. Julian, and M.F. Olson, *How apoptotic cells aid in the removal of their own cold dead bodies*. Cell Death & Differentiation, 2012. **19**(5): p. 735-742.
104. Kerr, J.F.R., A.H. Wyllie, and A.R. Currie, *Apoptosis: A Basic Biological Phenomenon with Wideranging Implications in Tissue Kinetics*. 1972.
105. Zarovni, N., et al., *Integrated isolation and quantitative analysis of exosome shuttled proteins and nucleic acids using immunocapture approaches*. Methods, 2015. **87**: p. 46-58.
106. Zhang, M., et al., *Methods and Technologies for Exosome Isolation and Characterization*. Small Methods, 2018. **2**(9).
107. Laulagnier, K., et al., *Characterization of exosome subpopulations from RBL-2H3 cells using fluorescent lipids*. Blood Cells, Molecules, and Diseases, 2005. **35**(2): p. 116-121.
108. Smith, Z.J., et al., *Single exosome study reveals subpopulations distributed among cell lines with variability related to membrane content*. J Extracell Vesicles, 2015. **4**: p. 28533.
109. Li, P., et al., *Progress in Exosome Isolation Techniques*. Theranostics, 2017. **7**(3): p. 789-804.
110. Muller, L., et al., *Isolation of biologically-active exosomes from human plasma*. J Immunol Methods, 2014. **411**: p. 55-65.
111. Hiemstra, T.F., et al., *Human urinary exosomes as innate immune effectors*. J Am Soc Nephrol, 2014. **25**(9): p. 2017-27.

112. Livshits, M.A., et al., *Isolation of exosomes by differential centrifugation: Theoretical analysis of a commonly used protocol*. Sci Rep, 2015. **5**: p. 17319.
113. Cvjetkovic, A., J. Lotvall, and C. Lasser, *The influence of rotor type and centrifugation time on the yield and purity of extracellular vesicles*. J Extracell Vesicles, 2014. **3**.
114. Zeringer, E., et al., *Strategies for isolation of exosomes*. Cold Spring Harb Protoc, 2015. **2015**(4): p. 319-23.
115. Runz, S., et al., *Malignant ascites-derived exosomes of ovarian carcinoma patients contain CD24 and EpCAM*. Gynecol Oncol, 2007. **107**(3): p. 563-71.
116. ANDERSON, N.G., *An Introduction to Particle Separations in Zonal Centrifuges*. National Cancer Institute Monograph, 1966.
117. Liga, A., et al., *Exosome isolation: a microfluidic road-map*. Lab Chip, 2015. **15**(11): p. 2388-94.
118. Scientific, B., *ExoMir™ Kit Manual*. 2010.
119. Liu, F., et al., *The Exosome Total Isolation Chip*. ACS Nano, 2017. **11**(11): p. 10712-10723.
120. Heinemann, M.L., et al., *Benchtop isolation and characterization of functional exosomes by sequential filtration*. J Chromatogr A, 2014. **1371**: p. 125-35.
121. Escudier, B., et al., *Vaccination of metastatic melanoma patients with autologous dendritic cell (DC) derived-exosomes: results of the first phase I clinical trial*. J Transl Med, 2005. **3**(1): p. 10.
122. Lamparski HG, M.-D.A., Yao JY, Patel S, Hsu DH, Ruegg C, Le Pecq JB, *Production and characterization of clinical grade exosomes derived from dendritic cells*. Journal of Immunological Methods, 2002.
123. Gheinani, A.H., et al., *Improved isolation strategies to increase the yield and purity of human urinary exosomes for biomarker discovery*. Sci Rep, 2018. **8**(1): p. 3945.
124. Gamez-Valero, A., et al., *Size-Exclusion Chromatography-based isolation minimally alters Extracellular Vesicles' characteristics compared to precipitating agents*. Sci Rep, 2016. **6**: p. 33641.
125. Vogel, R., et al., *A standardized method to determine the concentration of extracellular vesicles using tunable resistive pulse sensing*. J Extracell Vesicles, 2016. **5**: p. 31242.
126. Dukjin Kang, S.O., Sung-Min Ahn, Bong-Hee Lee, and Myeong Hee Moon, *Proteomic Analysis of Exosomes from Human Neural Stem Cells by Flow Field-Flow Fractionation and Nanoflow Liquid Chromatography-Tandem Mass Spectrometry*. 2008.

127. Musante, L., et al., *A simplified method to recover urinary vesicles for clinical applications, and sample banking*. Sci Rep, 2014. **4**: p. 7532.
128. Suresh Mathivanan, J.W.E.L., Bow J. Tauro, Hong Ji, Robert L. Moritz, and Richard J. Simpson, *roteomics Analysis of A33 Immunoaffinity- purified Exosomes Released from the Human Colon Tumor Cell Line LIM1215 Reveals a Tissue-specific Protein Signature*. 2010.
129. Taylor, D.D. and C. Gercel-Taylor, *MicroRNA signatures of tumor-derived exosomes as diagnostic biomarkers of ovarian cancer*. Gynecol Oncol, 2008. **110**(1): p. 13-21.
130. Javier Conde-Vancells, E.R.-S., Nieves Embade, David Gil, Rune Matthiesen, Mikel Valle, Felix Elortza, Shelly C. Lu, Jose M. Mato, and Juan M. Falcon- Perez, *Characterization and Comprehensive Proteome Profiling of Exosomes Secreted by Hepatocytes*. 2008.
131. Batrakova, E.V. and M.S. Kim, *Using exosomes, naturally-equipped nanocarriers, for drug delivery*. J Control Release, 2015. **219**: p. 396-405.
132. Hosseini, S., et al., *General Overviews on Applications of ELISA*, in *Enzyme-linked Immunosorbent Assay (ELISA)*. 2018. p. 19-29.
133. Hong, C.S., et al., *Isolation and characterization of CD34+ blast-derived exosomes in acute myeloid leukemia*. PLoS One, 2014. **9**(8): p. e103310.
134. Inc, E.O.S.B., <1.pdf>.
135. Inc., T.E.I.T.F.S., <2.pdf>.
136. Amarnath, S., et al., *Bone marrow-derived mesenchymal stromal cells harness purinergic signaling to tolerize human Th1 cells in vivo*. Stem Cells, 2015. **33**(4): p. 1200-12.
137. Malek, R.S.T.S.V.B.A.G.E.T.L.B.A.N.V.E.M.F.A., *Lectin-induced agglutination method of urinary exosomes isolation followed by mi-RNA analysis: Application for prostate cancer diagnostic*. 2016.
138. Kyunghoon Lee, et al., *Acoustic Purification of Extracellular Microvesicles*. 2015.
139. Davies, R.T., et al., *Microfluidic filtration system to isolate extracellular vesicles from blood*. Lab Chip, 2012. **12**(24): p. 5202-10.
140. Zheng Zhao, Y.Y., Yong Zeng, and Mei He, *A microfluidic ExoSearch chip for multiplexed exosome detection towards blood-based ovarian cancer diagnosis*. 2016.
141. He, M., et al., *Integrated immunoisolation and protein analysis of circulating exosomes using microfluidic technology*. Lab Chip, 2014. **14**(19): p. 3773-80.

142. Kanwar, S.S., et al., *Microfluidic device (ExoChip) for on-chip isolation, quantification and characterization of circulating exosomes*. Lab Chip, 2014. **14**(11): p. 1891-900.
143. Dragovic, R.A., et al., *Sizing and phenotyping of cellular vesicles using Nanoparticle Tracking Analysis*. Nanomedicine, 2011. **7**(6): p. 780-8.
144. Soo, C.Y., et al., *Nanoparticle tracking analysis monitors microvesicle and exosome secretion from immune cells*. Immunology, 2012. **136**(2): p. 192-197.
145. Palmieri, V., et al., *Dynamic light scattering for the characterization and counting of extracellular vesicles: a powerful noninvasive tool*. Journal of Nanoparticle Research, 2014. **16**(9).
146. Filipe, V., A. Hawe, and W. Jiskoot, *Critical evaluation of Nanoparticle Tracking Analysis (NTA) by NanoSight for the measurement of nanoparticles and protein aggregates*. Pharm Res, 2010. **27**(5): p. 796-810.
147. Frisken, B.J., *Revisiting the method of cumulants for the analysis of dynamic light-scattering data*. 2001.
148. Douglas A. Skoog, F.J.H., Stanley R. Crouch, *Principles of Instrumental Analysis*. 6th ed. 1998, Philadelphia: Saunders College Pub.
149. Wu, Y., W. Deng, and D.J. Klinke, 2nd, *Exosomes: improved methods to characterize their morphology, RNA content, and surface protein biomarkers*. Analyst, 2015. **140**(19): p. 6631-42.
150. Maas, S.L.N., J. De Vrij, and M.L.D. Broekman, *Quantification and Size-profiling of Extracellular Vesicles Using Tunable Resistive Pulse Sensing*. Journal of Visualized Experiments, 2014(92).
151. Ko, J., E. Carpenter, and D. Issadore, *Detection and isolation of circulating exosomes and microvesicles for cancer monitoring and diagnostics using micro-/nano-based devices*. Analyst, 2016. **141**(2): p. 450-460.
152. Szatanek, R., et al., *The Methods of Choice for Extracellular Vesicles (EVs) Characterization*. Int J Mol Sci, 2017. **18**(6).
153. Gallagher, S., et al., *Immunoblotting and immunodetection*. Curr Protoc Mol Biol, 2004. **Chapter 10**: p. Unit 10 8.
154. Liu, C., et al., *Low-cost thermophoretic profiling of extracellular-vesicle surface proteins for the early detection and classification of cancers*. Nature Biomedical Engineering, 2019.
155. Schey, K.L., J.M. Luther, and K.L. Rose, *Proteomics characterization of exosome cargo*. Methods, 2015. **87**: p. 75-82.



156. Rosa-Fernandes, L., et al., *A Perspective on Extracellular Vesicles Proteomics*. *Frontiers in Chemistry*, 2017. **5**.
157. Schmidt, C., et al., *Mass spectrometry-based relative quantification of proteins in precatalytic and catalytically active spliceosomes by metabolic labeling (SILAC), chemical labeling (iTRAQ), and label-free spectral count*. *RNA*, 2014. **20**(3): p. 406-20.
158. Lai, X., L. Wang, and F.A. Witzmann, *Issues and applications in label-free quantitative mass spectrometry*. *Int J Proteomics*, 2013. **2013**: p. 756039.
159. Chen, Y., et al., *Quantification of Flavin-containing Monooxygenases 1, 3, and 5 in Human Liver Microsomes by UPLC-MRM-Based Targeted Quantitative Proteomics and Its Application to the Study of Ontogeny*. *Drug Metab Dispos*, 2016. **44**(7): p. 975-83.
160. Michaels, S. and M.Z. Wang, *The revised human liver cytochrome P450 "Pie": absolute protein quantification of CYP4F and CYP3A enzymes using targeted quantitative proteomics*. *Drug Metab Dispos*, 2014. **42**(8): p. 1241-51
161. Zhang, Z., et al., *Comparison of ultracentrifugation and density gradient separation methods for isolating Tca8113 human tongue cancer cell line-derived exosomes*. *Oncol Lett*, 2014. **8**(4): p. 1701-1706.

**Chapter II: Development of Liquid Chromatography – Multiple Reaction  
Monitoring – Mass Spectrometry (LC-MRM-MS)-Based Targeted Proteomic  
Method for Analysis of Exosome Marker Proteins and Its Application in  
Evaluating Different Exosome Preparations**

## TABLE OF CONTENTS

<b>2.1 INTRODUCTION .....</b>	<b>52</b>
<b>2.2 MATERIALS AND METHODS .....</b>	<b>55</b>
2.2.1 Chemicals and Reagents .....	55
2.2.2 Identification of Signature Peptides for Marker Proteins .....	56
2.2.3 LC-MRM-MS Method Development .....	56
2.2.4 Collection and Isolation of HepG2 and HeLa Exosomes by Differential Ultracentrifugation .....	57
2.2.5 Isolation of HepG2 and HeLa Exosomes by TEIK .....	57
2.2.6 NTA of Exosomes.....	58
2.2.7 Western Blot Analysis .....	58
2.2.8 Sample Preparation for LC-MRM-MS Analysis .....	59
2.2.9 LC-MRM-MS Analysis .....	59
<b>2.3 RESULTS .....</b>	<b>61</b>
2.3.1 LC-MRM-MS Method Development .....	61
2.3.2 NTA of HepG2 and HeLa Exosomes Isolated by Differential Ultracentrifugation and TEIK .....	62
2.3.3 Comparison of Isolation Efficiency Between Differential Ultracentrifugation and TEIK .....	63
2.3.4. Western Blot Analysis of HepG2 and HeLa Cell Lysate and Exosomes .....	65
2.3.5 LC-MRM-MS Analysis of Isolated HepG2 and HeLa Exosomes.....	66
<b>2.4 DISCUSSION .....</b>	<b>69</b>
<b>2.5 CONCLUSION .....</b>	<b>72</b>
<b>2.6 REFERENCES.....</b>	<b>73</b>

## LIST OF TABLES

<b>Table 1.</b> Selected peptides, mass transitions, and retention times for LC-MRM-MS method development. The bolded mass transitions are the transitions with the highest intensity whose peaks are present on the chromatogram in Figure 1. ....	61
<b>Table 2.</b> Summary of NTA results for exosomes isolated from HepG2 and HeLa cell culture medium by differential ultracentrifugation and TEIK. ....	62
<b>Table 3.</b> Amount ( $\mu\text{g}$ ) of exosomal protein isolated, starting volume (mL) of cell culture medium, and $\mu\text{g}/\text{mL}$ of exosomal protein for 4 biological replicates. ....	64

## LIST OF FIGURES

<b>Figure 1.</b> Chromatogram of Selected Peptides for LC-MRM-MS Method Development. ....	62
<b>Figure 2.</b> NTA Analyses of HepG2 and HeLa Exosomes Isolated by Differential Ultracentrifugation and TEIK. Exosomes were isolated from HeLa cell culture media by differential ultracentrifugation (A) and by TEIK (B). Exosomes were also isolated from HepG2 cell culture medium by differential ultracentrifugation (C) and TEIK (D). ....	63
<b>Figure 3.</b> Comparing Isolation Efficiency of Differential Ultracentrifugation and TEIK Exosomes Isolation Methods. The amount ( $\mu\text{g}$ ) of exosomal protein isolated was quantified by BCA and then normalized to the amount (mL) of starting material for 4 biological replicates (n=4). ....	64

**Figure 4.** Western Blot Analysis of HepG2 and HeLa Exosomes Isolated by Differential Ultracentrifugation and TEIK and Corresponding HepG2 and HeLa Cell Lysate. HepG2 cell lysate and exosomes (A) and HeLa cell lysate and exosomes (B) isolated by differential ultracentrifugation and TIEK were assessed for exosomal marker proteins CD9, HSP90, and HSC70 and non-exosomal marker proteins GRP78 and HSP60. .... 65

**Figure 5.** LC-MRM-MS Analysis of HepG2 and HeLa Exosomes Isolated by Differential Ultracentrifugation and TEIK and Corresponding HepG2 and HeLa Cell Lysate. A total of 30  $\mu$ g of cellular and exosomal proteins from HeLa (A) and HepG2 (B) were trypsin digested and assessed for the presence of exosomal marker proteins (HSC70, HSP90 $\beta$ , CD9, TSG101, and ALIX) and non-exosomal marker proteins (PHB1, HSP60, and GRP78) by LC-MRM-MS for 4 biological replicates (n=4). Exosomal marker proteins in exosome preparations whose fold change value was significantly different from the lysate level are marked by (\*). Exosomal marker protein levels which were significantly different between the 2 different isolation methods are marked by (\*\*). .... 68

## 2.1 INTRODUCTION

The use of exosomes as biomarkers for diagnosis, prognosis, and monitoring patient response to treatment is one of increasing interest. The proteins, lipids, and other exosomal cargo reflect the cells from which they originate, be it diseased or healthy. While some exosomal proteins are unique due to its cell of origin, there have been several proteins identified in exosomes from various cell types. These are termed exosomal marker proteins and are typically associated with the cytosol or cell membrane including Heat Shock Cognate 70 kDa (HSC70), Cluster of Differentiation 9 (CD9), Heat Shock Protein 90 kDa beta (HSP90 $\beta$ ), Programmed Cell Death 6-Interacting Protein (ALIX), and Tumour Suppression Gene 101 (TSG101) [1, 2]. Often, these marker proteins are found to be enriched in exosome preparations compared to the cell lysate. Additionally, there are a set of proteins reported in literature, termed non-exosomal marker proteins, and are typically organelle-associated proteins such as endoplasmic reticulum (ER) luminal protein Glucose Regulated Protein 78 kDa (GRP78) and mitochondrial proteins Prohibitin - 1 (PHB1) and Heat Shock Protein 60 kDa (HSP60) [1, 2]. In the field of exosomal research, the presence of the exosomal marker proteins and absence the non-exosomal marker proteins often is how the purity and quality of the exosomal preparation is determined, usually by Western blot analysis using antibodies specific to these marker proteins.

Western blot has been the considered the gold-standard technique for protein identification due to its low cost, simplicity and wide accessibility [3]. As is the case with all immuno-based assays, Western blot relies on the use of a single antibody for identification of the antigen of interest. Therefore, the specificity and reproducibility of the Western blot assay are limited to the antibody being used, which can be largely variable between different vendors and lots within the same vendor [4-7]. The band observed on a Western blot is considered to be specific if the

molecular weight of the band matches the expected molecular weight of the antigen of interest. The presence of bands at different molecular weights, due to potential non-specific binding, lowers the confidence in the identification of the antigen of interest [3]. In addition, the Western blot assay is meant to detect one protein at a time, meaning it is not well multiplexed and therefore requires an abundance of sample in order to monitor several proteins of interest [6-8]. This poses a major challenge in using Western blot to monitor the presence or absence of the exosomal/non-exosomal marker proteins in an exosomal preparation, as the exosomal protein yield is very low [1, 2, 9].

Targeted proteomic methods, such as liquid chromatography – multiple reaction monitoring – mass spectrometry (LC-MRM-MS), can be developed to address the challenges associated with traditional Western blot methodologies. LC-MRM-MS detection relies on both retention time and mass to charge ratios ( $m/z$ ) of precursor and product ion(s) of signature peptides (also referred to as surrogate, proteotypic, or ACQUA peptides) for the target protein using a triple-quadrupole MS [5]. The selection of both precursor and product ions results in a high signal to noise (S/N) ratio, low limit of detection (fmol), and allows for detection of both high and low abundant proteins within the same starting mixture [3-5, 8]. LC-MRM-MS methods can be developed such that multiple signature peptides for a single protein, and multiple product ions for a single peptide, are detected to further increase the confidence that the protein of interest is being detected [3, 8]. Due to the nature of the LC-MRM-MS methodology, it is more well multiplexed than Western blot with up to 10 proteins detected in a single 20 minute LC run [3, 8]. Finally, because protein digestions are reproducible and many steps of sample preparation can be automated, several studies have demonstrated that MS based methods are more reproducible, robust, and accurate than immuno-based methods, such as Western blot [3, 4, 8].

The major downfall of LC-MRM-MS methods compared to Western blot is that it requires sophisticated instrumentation with expertise to be operated correctly [8]. However, because of the increase in sensitivity, selectivity, specificity, reproducibility, and ability to be multiplexed, this technique is arguably an important technique that needs to be implemented in the field of exosomal research and development.

Here, a LC-MRM-MS method was developed for detection of exosomal marker proteins (HSC70, HSP90 $\beta$ , CD9, ALIX and TSG101) and non-exosomal marker proteins (GRP78, HSP60, and PHB1) and used to assess the purity and quality of exosomal preparations from a hepatoma cell line, HepG2, and a cervical cancer cell line, HeLa, isolated by differential ultracentrifugation and a Total Exosome Isolation Kit (TEIK).



## 2.2 MATERIALS AND METHODS

### 2.2.1 Chemicals and Reagents

Optima LC-MS/MS grade acetonitrile, water and formic acid were purchased from Fisher Chemical (Fair Lawn NJ). HepG2 and HeLa cells were purchased from American Type Culture Collection (Manassas, VA). Dulbecco's modified Eagle's medium (DMEM), cell culture grade sodium bicarbonate, dithiothreitol (DTT), ammonium bicarbonate (ABC), iodoacetamide (IAM), tris-base (Tris), and tween-20 were purchased from Sigma-Aldrich Co. (St. Louis). Fetal bovine serum (FBS) was purchased from Life Technologies (Carlsbad, CA). Sterile cell culture flasks and 0.22-micron filters were purchased from Corning (Corning, NY). A Beckman Optima™ L-90K class S preparative ultracentrifuge, type 35 rotor, swinging 28 (SW28) rotor, and ultracentrifuge tubes were purchased from Beckman Coulter (Brea, CA). Phosphate buffered saline (PBS) 10 x was purchased from Cellgro (Manassas, VA). A bicinchoninic acid (BCA) protein assay kit was purchased from Pierce Biotechnology (Rockford, IL). The TEIK and sterile 15 mL conical tubes were purchased from Invitrogen by Thermo Fisher Scientific (Carlsbad, CA). Micron centrifugal filters ultracel regenerated cellulose 10,000 molecular weight cut off (MWCO) columns were purchased from Millipore (Billerica, MA). Sequencing grade modified trypsin was purchased from Promega (Madison, WI). Laemmli sample buffer, Mini-PROTEAN® TGX™ gels, and Immun-Blot® PVDF membranes for protein blotting were purchased from Bio-Rad (Hercules, CA). Protein low bind tubes were purchased from eppendorff (Westbury, NY). Non-fat dry milk was purchased from Associated Wholesale Groceries Inc (Kansas City, KS). Antibodies against CD9 ( $\alpha$ -CD9), HSP90 ( $\alpha$ -HSP90), HSC70 ( $\alpha$ -HSC70), GRP78 ( $\alpha$ -GRP78), HSP60 ( $\alpha$ -HSP60), and horseradish peroxidase (HRP) conjugated antibodies against rabbit ( $\alpha$ -rabbit-HRP) and mouse ( $\alpha$ -mouse-HRP) were purchased from Abcam (Cambridge, MA).

### 2.2.2 Identification of Signature Peptides for Marker Proteins

Signature peptides for proteins of interest were selected based on a set of criteria [10, 11] to ensure specificity towards target protein, optimal retention on analytical LC column, chemical stability, digestion efficiency, and lack of posttranslational modifications and mutations. The amino acid sequence of the different isoforms for each of the proteins of interest were found using PubMed Protein BLAST and the sequences of each isoform were then aligned using EMBL Protein Align. Using these results, the region that had the best alignment for all isoforms was chosen for *in-silico* digestion, resulting in a list of potential peptides with masses between 500 – 2000 Da, a minimum length of 5 amino acids, no missed cleavages, and included an alkylation modification of cysteine by IAM. Any peptides containing methionine, N-terminal glutamine, or the sequence asparagine glycine (NG) were then discarded from the list of potential peptides. Additionally, any peptides that were too hydrophobic (HPLC index >50; predicted by MS-Digest of ProteinProspector), contained consecutive lysine or arginine, or lysine/arginine followed by aspartic acid or glutamic acid were also considered not ideal. Lastly, peptides containing cysteine or either C or N terminus were also discarded. Once the list of peptides was narrowed down to those that are most stable and lead to reproducible, quantitative, trypsin digestion, PubMed Protein BLAST was then used to determine peptide specificity against all other proteins in *homo sapiens*.

### 2.2.3 LC-MRM-MS Method Development

Arginine and lysine stable isotope-labelled crude peptides were purchased from Thermo Fisher Scientific (Carlsbad, CA). Upon arrival, an aliquot of each peptide was diluted 10 x in 50/50 v/v acetonitrile/water and designated as the working stock and was stored at -20 °C. Immediately before LC-MS method development, an aliquot of the working stock was diluted 100 x into 50/50 v/v acetonitrile/water and labelled infusion stock. The infusion stock was then infused at 5

$\mu\text{L}/\text{minute}$  into a Waters Xevo TQ-S triple-quadrupole MS (Waters, Millford, MA) combined with an LC flow of 15 % acetonitrile with 0.1 % v/v formic acid and 85 % water with 0.1 % v/v formic acid at 0.4 mL/minute and an MS1 scan was collected to select the precursor ion of the peptide. The intellistart software was then used for tuning the peptide which produced a list of identified mass transitions (product ions) with optimal cone voltage and collision energy. Using this information, an MRM method could then be developed, using at least three mass transitions to identify each peptide.

## **2.2.4 Collection and Isolation of HepG2 and HeLa Exosomes by Differential**

### **Ultracentrifugation**

HepG2 and HeLa cells were cultured to 100 % confluency in 4 x T-150 flasks in DMEM containing 10% v/v FBS at 37 °C and 5 % CO<sub>2</sub>. Each flask was then incubated for 48 hours at 37 °C and 5 % CO<sub>2</sub> with 25 mL of exosome collection media (DMEM with no FBS). This resulted in 100 mL of media collected from the 4 x T-150 flasks for each cell line, which was centrifuged at 500 x g for 10 minutes at 4 °C, filtered with a 0.22- $\mu\text{m}$  filter, and stored at -80 °C. The 48-hour incubation in exosome collection media was repeated two more times to collect a total of 300 mL of media for both cell lines. Once 300 mL of media was collected and filtered, the frozen media was thawed on ice and centrifuged at 10,000 x g for 30 minutes to pellet larger vesicles. The pellets were discarded, and the supernatant was centrifuged at 100,000 x g for 1 hour. The supernatant was then discarded, and each pellet was re-suspended in 10 mL of 1 x PBS and centrifuged once more at 100,000 x g for 1 hour. Each pellet was re-suspended in 50  $\mu\text{L}$  of 1 x PBS and quantified using the BCA protein assay kit.

## **2.2.5 Isolation of HepG2 and HeLa Exosomes by TEIK**

A 3 mL aliquot of the 300 mL of collected media (above) was set aside for isolation by the TEIK according to the manufacturer's instructions. Briefly, the 3 mL aliquot of media was put into a 15 mL conical tube and 1.5 mL of the TEIK reagent was added. The mixture was vortexed briefly and incubated at 4 °C overnight (~16 hours). The sample was then centrifuged at 10,000 x g for 1 hour at 4 °C and the supernatant discarded. The exosome pellet was then re-suspended in 300 µL of ice cold 1 x PBS and quantified using the BCA protein assay kit.

### **2.2.6 NTA of Exosomes**

A Malvern NanoSight LM10 Nanoparticle Analysis System (Malvern Panalytical Inc.; Westborough, MS) equipped with a charged coupled device (CCD) camera and a 638 nm class 3B laser source was used to determine the size and particle concentration of the isolated exosomal vesicles. Prior to analysis, the position of the visual reference (the thumbprint-like shape) was checked to ensure and the optimal imaging location was located. The chamber was then flushed with 1 x PBS and the exosomal sample was injected into the chamber. The camera settings were then adjusted so that the particles appeared as single bright points in the imaging field and then 3 x 30 second videos of the exosomal vesicles were collected, with a fresh volume of sample introduced into the chamber between each video. The videos were then analysed with NanoSight software version 3.2, with auto function selected for the detection threshold, blur, minimum tracking length, and minimum particle size analysis parameters.

### **2.2.7 Western Blot Analysis**

Fifteen (15) µg of exosomal or cellular protein were mixed with 4 x Laemmli sample buffer and diluted to 1 x with water. The protein-buffer mixture was incubated at 95 °C for 5 minutes prior to electrophoretic separation on Mini-PROTEAN TGX precast gels for 60 minutes at 150 V on

ice. The proteins were transferred onto PVDF membranes using Trans-Blot® Turbo™ Transfer System and the membranes were blocked with 5 % fat-free milk in tris-buffered saline containing 0.05 % tween 20 (TBS – T20 (0.05%)) for 1 hour at room temperature. The membranes were exposed to  $\alpha$ -CD9,  $\alpha$ -HSP90,  $\alpha$ -HSC70,  $\alpha$ -GRP78,  $\alpha$ -HSP60 antibodies (previously validated with either total cell lysate or HLMs for activity and specificity) overnight (~16 hours) at 4 °C. Following primary antibody exposure, the membranes were washed and exposed to the appropriate secondary antibodies, either  $\alpha$ -rabbit-HRP or  $\alpha$ -mouse-HRP, prior to imaging was with a Kodak Image Station 400<sub>CF</sub>.

### **2.2.8 Sample Preparation for LC-MRM-MS Analysis**

Thirty (30)  $\mu$ g exosomal and total cellular proteins were digested by trypsin and prepared for LC-MRM-MS analysis using the qFASP protocol. Briefly, the proteins were reduced with 10 mM DTT in 20 mM ABC and denatured at 95 °C for 3 minutes. The solution was then cooled to room temperature and loaded onto a 10 kDa MWCO centrifugal filter unit. The proteins were washed with 50 mM ABC and centrifuged at 14,000 x g at 20 °C for 20 minutes followed by alkylation with 10 mM IAM. The excess IAM was removed by centrifugation at 14,000 x g for 20 minutes at 20 °C, and the proteins were trypsin-digested at 37°C for 4 hours with 1  $\mu$ g trypsin. The peptides were eluted from the filter unit by centrifugation into a protein low binding tube prior to being spiked with arginine and lysine stable isotope-labelled crude peptides, which served as internal standards.

### **2.2.9 LC-MRM-MS Analysis**

A total of 3  $\mu$ g of digested cellular and exosomal protein, spiked with internal standard, were injected on to an analytical column (ACQUITY UPLC, C18, 1.7  $\mu$ m, 2.1 x 100 mm) and

separated with a gradient of water with 0.1 % v/v formic acid (A) and acetonitrile with 0.1 % v/v formic acid (B) at a flow rate of 0.4 mL/minute. The gradient started at 2 % B and increased to 30 % B over the course of 9 minutes. The gradient increased from 30 % B to 95 % B in 1.5 minutes before re-equilibrating to the initial conditions (2 % B) for 2 minutes. Signature peptides for exosomal marker proteins (HSC70, HSP90 $\beta$ , CD9, ALIX, and TSG101) and non-exosomal marker proteins (GRP78, HSP60, and PHB1) were detected using the specific mass transitions on a Waters Xevo TQ-S triple-quadrupole MS operating in electrospray ionization positive (ESI+) mode.

The Waters Xevo TQ-S triple-quadrupole MS was operated using the Waters MassLynx 4.1 software (Waters, Millford, MA). The data were analysed with the TargetLynx Application Manager within the MassLynx software. The chromatographic peaks of each peptide and its internal standard were integrated by the TargetLynx software to determine the area under the curve (AUC). The response ratio was then calculated by dividing the AUC of the peptide from the digest (light peptide) by the AUC of the internal standard (heavy peptide). The “Fold Change” value, normalized to the cell lysate, on the y-axis was calculated by Equation 1.

*Equation 1:*

$$\frac{\text{Response Ratio in the Cell Lysate (or Exosome) Digest}}{\text{Response Ratio in the Cell Lysate Digest}}$$

Two-way ANOVA statistical analysis, in Graph Pad Prism (version 7; San Diego, CA) was used to compare the fold change in the lysate to each different exosome preparation, noted with \* in the graphs, and to compare the different preparations to each other, noted with \*\* in the graphs.

## 2.3 RESULTS

### 2.3.1 LC-MRM-MS Method Development

The signature peptides selected for each protein of interest along with the 3 mass transitions used to monitor each peptide in the MRM method are summarized in **Table 1**. The bolded mass transitions in **Table 1** are the mass transitions of highest intensity, and the peaks associated with these mass transitions can be seen in the chromatogram of **Figure 1**. For most proteins, at least 2 different signature peptides were monitored. However, for CD9, Alix, and TSG101, only 1 peptide was selected as the other peptide candidates produced by the *in-silico* digestions were discarded based on the criteria previously established [10, 11].

**Table 1.** Selected peptides, mass transitions, and retention times for LC-MRM-MS method development. The bolded mass transitions are the transitions with the highest intensity whose peaks are present on the chromatogram in Figure 1.

	Protein	Signature Peptide	Average Mass MH+ (Da)	MRM Precursor Ion (m/z)	MRM Product Ions (m/z)			Retention Time (Minutes)
					1	2	3	
Non-Exosomal Markers	PHB1	VFESIG(K)	780.8	390.22	680.36	<b>533.29</b>	404.25	3.79
		VLPSITTEIL(K)	1214.46	607.37	904.61	817.5	<b>704.42</b>	7.21
	HSP60	LSDGVAVL(K)	902.05	451.27	<b>701.42</b>	430.3	260.2	4.37
		VTDALNAT(R)	961.04	480.76	<b>760.39</b>	645.37	461.25	3.34
	GRP78	LTPEEIE(R)	987.07	493.76	<b>772.38</b>	675.33	546.29	3.73
		ITITNDQN(R)	1075.14	537.78	860.42	<b>747.34</b>	646.29	3.25
Exosomal Markers	HSC70	ITITND(K)	804.89	402.73	691.4	<b>590.3</b>	477.2	3.24
		FEELNADLF(R)	1254.36	627.3	848.5	735.4	<b>435.3</b>	7.21
	CD9	DVLETFIV(K)	1052.19	526.29	<b>724.39</b>	595.35	494.3	6.28
	ALIX	FTDLFE(K)	899.99	450.23	752.38	<b>651.33</b>	536.31	5.50
	TSG101	GVIDLDVFL(K)	1119.32	559.83	<b>849.47</b>	734.44	506.33	9.82
	HSP90B	HFSVEGQLEF(R)	1349.46	450.22	<b>749.39</b>	692.37	564.31	5.28
		HLEINPDHPIVETL(R)	1783.99	594.98	827.5	740.5	<b>617.36</b>	5.20

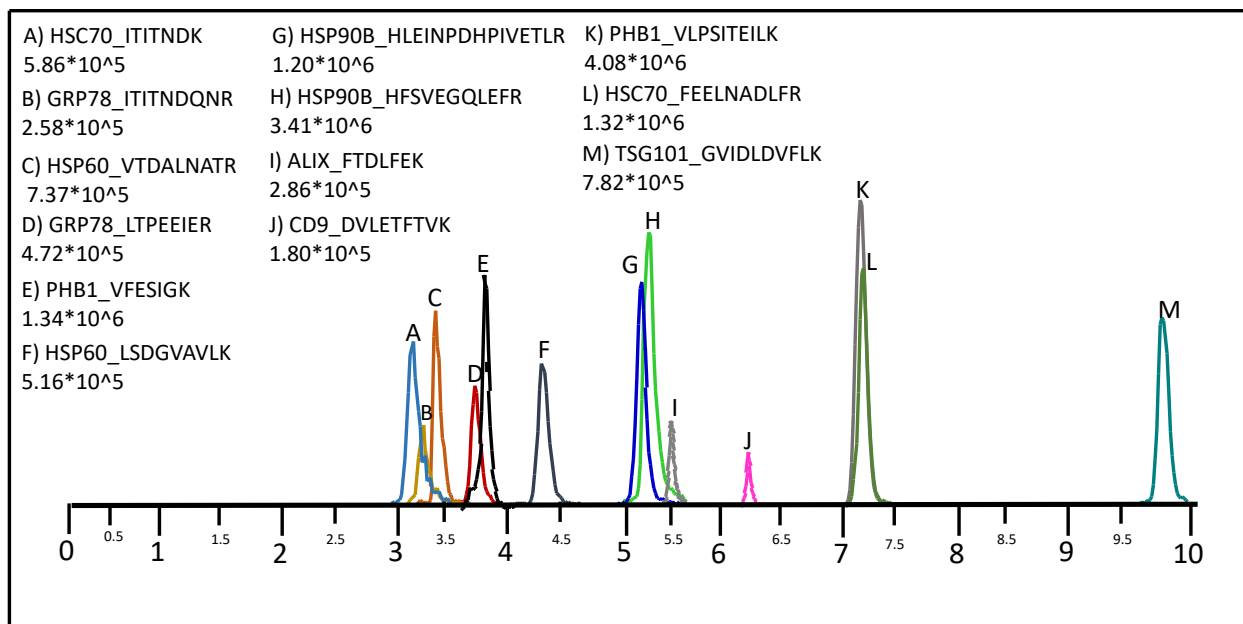


**Figure 1.** Chromatogram of Selected Peptides for LC-MRM-MS Method Development.

### 2.3.2 NTA of HepG2 and HeLa Exosomes Isolated by Differential Ultracentrifugation and TEIK

The size distribution of the HepG2 and HeLa exosomes isolated by differential ultracentrifugation and the TEIK was assessed by NTA and can be seen in **Figure 2A – D**. The average size (mean +/- SD) of the isolated exosomes from the HepG2 and HeLa cell culture medium by differential ultracentrifugation and TEIK are summarized in **Table 2**, and were within the expected 30 -150 nm size for exosomes [12-15]. However, larger particles ( $>0.22 \mu\text{m}$ , pore size of the filter used in during exosome isolation) could also be seen in ultracentrifuge samples, which may be due to particle clumping when resuspending lipidic particles in aqueous PBS.

**Table 2.** Summary of NTA results for exosomes isolated from HepG2 and HeLa cell culture medium by differential ultracentrifugation and TEIK.

Cell Type	Isolation Method	Particle Size (nm) mean +/- SD
HeLa	Ultracentrifugation	132 +/- 5



	TEIK	127 +/- 8
HepG2	Ultracentrifugation	140 +/- 3
	TEIK	126 +/- 4

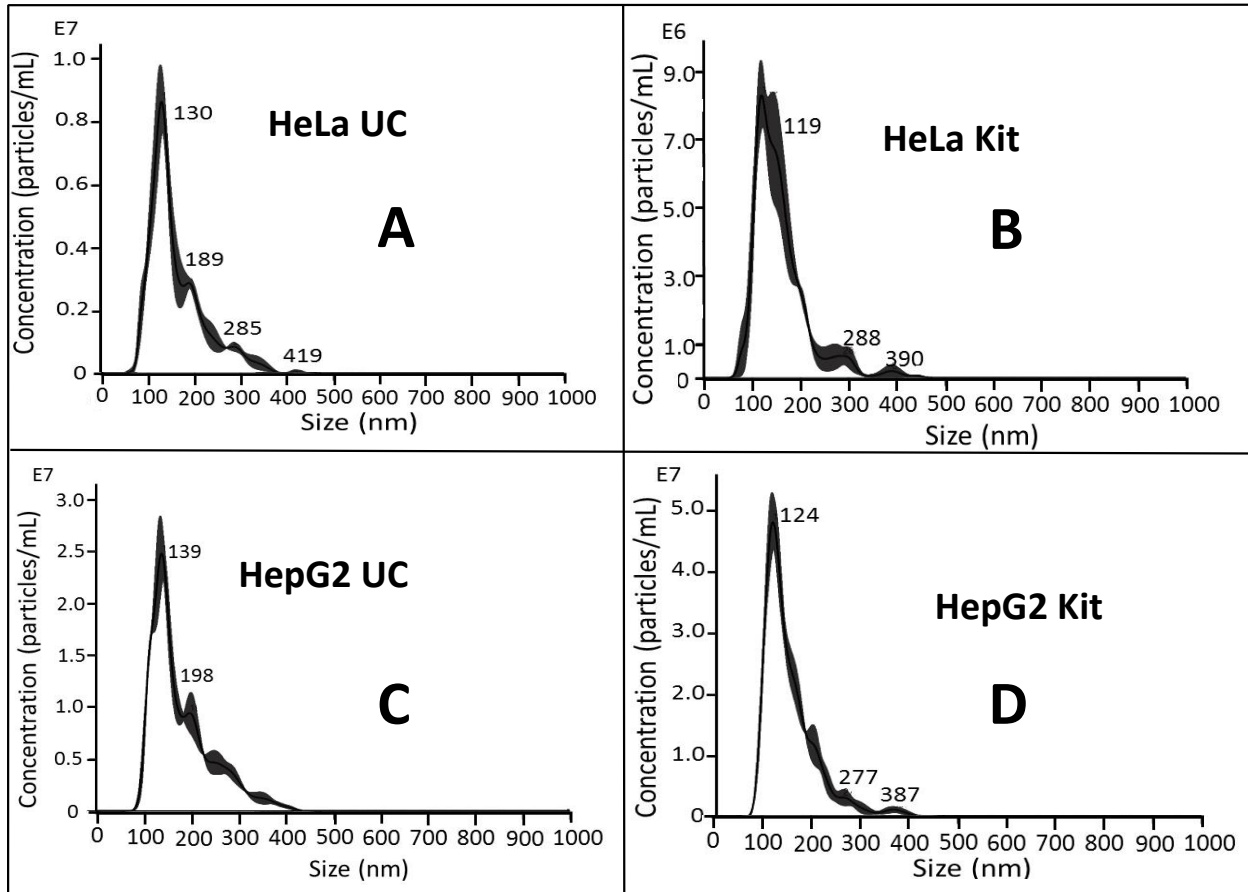


**Figure 2.** NTA Analyses of HepG2 and HeLa Exosomes Isolated by Differential Ultracentrifugation and TEIK. Exosomes were isolated from HeLa cell culture media by differential ultracentrifugation (A) and by TEIK (B). Exosomes were also isolated from HepG2 cell culture medium by differential ultracentrifugation (C) and TEIK (D).

### 2.3.3 Comparison of Isolation Efficiency Between Differential Ultracentrifugation and TEIK

**Figure 3** shows the amount ( $\mu\text{g}$ ) of isolated protein per volume (mL) of cell culture medium averaged together for the 4 biological replicates ( $n=4$ ). For the HepG2 and HeLa exosomes isolated by differential ultracentrifugation, approximately 3 and 1  $\mu\text{g}$  of protein was isolated per

mL of starting material, respectively. For HepG2 and HeLa exosomes isolated by the TEIK, approximately 70 and 23  $\mu\text{g}$  of protein was isolated per mL of starting material, respectively.

**Table 3** shows the amount of protein isolated, the starting volume, and amount of protein isolated per mL of starting material for the 4 biological replicates individually. The average of the values reported in **Table 3** were used to plot the data in **Figure 3**.

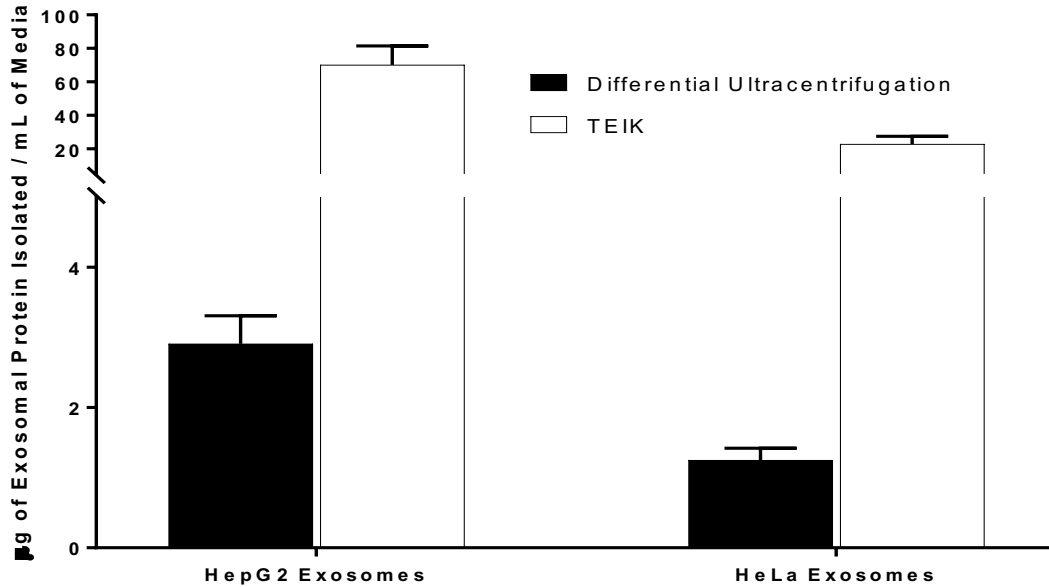


**Figure 3.** Comparing Isolation Efficiency of Differential Ultracentrifugation and TEIK Exosomes Isolation Methods. The amount ( $\mu\text{g}$ ) of exosomal protein isolated was quantified by BCA and then normalized to the amount (mL) of starting material for 4 biological replicates (n=4).

**Table 3.** Amount ( $\mu\text{g}$ ) of exosomal protein isolated, starting volume (mL) of cell culture medium, and  $\mu\text{g}/\text{mL}$  of exosomal protein for 4 biological replicates.

HepG2 Exosome Isolation						
Biological Replicate	Differential Ultracentrifugation			TEIK		
	Amount ( $\mu\text{g}$ ) Isolated	Starting Volume (mL)	Amount ( $\mu\text{g}/\text{mL}$ )	Amount ( $\mu\text{g}$ ) Isolated	Starting Volume (mL)	Amount ( $\mu\text{g}/\text{mL}$ )
1	942.9	297	3.2	285.6	3	95.2
2	1147.5	297	3.9	237.3	3	79.1
3	589.7	297	2.0	125.0	3	41.7
4	778.0	297	2.6	194.0	3	64.7
HeLa Exosome Isolation						
Biological Replicate	Differential Ultracentrifugation			TEIK		
	Amount ( $\mu\text{g}$ ) Isolated	Starting Volume (mL)	Amount ( $\mu\text{g}/\text{mL}$ )	Amount ( $\mu\text{g}$ ) Isolated	Starting Volume (mL)	Amount ( $\mu\text{g}/\text{mL}$ )
1	259.8	297	0.9	97.2	3	32.4
2	351.0	297	1	32.1	3	10.7
3	503.7	297	2	83.1	3	27.7
4	369.6	297	1	60.0	3	20.0

### 2.3.4. Western Blot Analysis of HepG2 and HeLa Cell Lysate and Exosomes

HeLa and HepG2 total cell lysate and exosomal protein isolated by differential ultracentrifugation and TEIK were assessed by Western blot for expression of exosomal marker proteins (HSC70, HSP90, and CD9) and non-exosomal marker proteins (HSP60, and GRP78).

The blots can be seen in **Figure 4A** and **4B** respectively for HepG2 and HeLa cell lines.

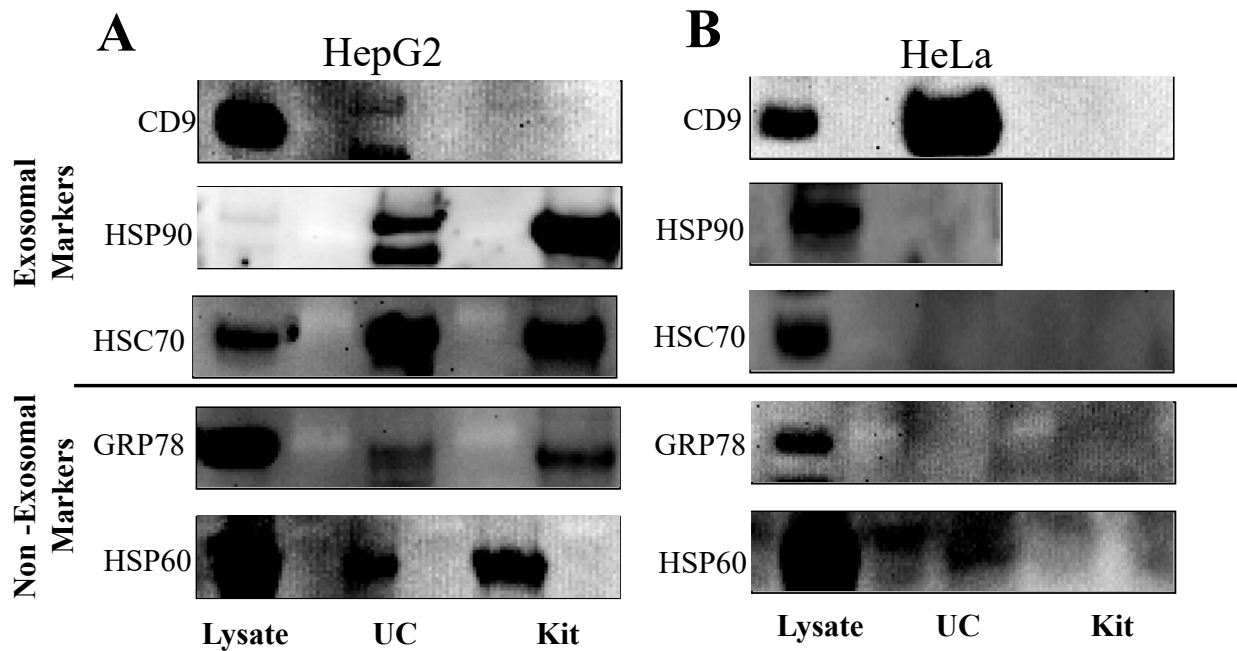


**Figure 4.** Western Blot Analysis of HepG2 and HeLa Exosomes Isolated by Differential Ultracentrifugation and TEIK and Corresponding HepG2 and HeLa Cell Lysate. HepG2 cell lysate and exosomes (A) and HeLa cell lysate and exosomes (B) isolated by differential ultracentrifugation and TIEK were assessed for exosomal marker proteins CD9, HSP90, and HSC70 and non-exosomal marker proteins GRP78 and HSP60.

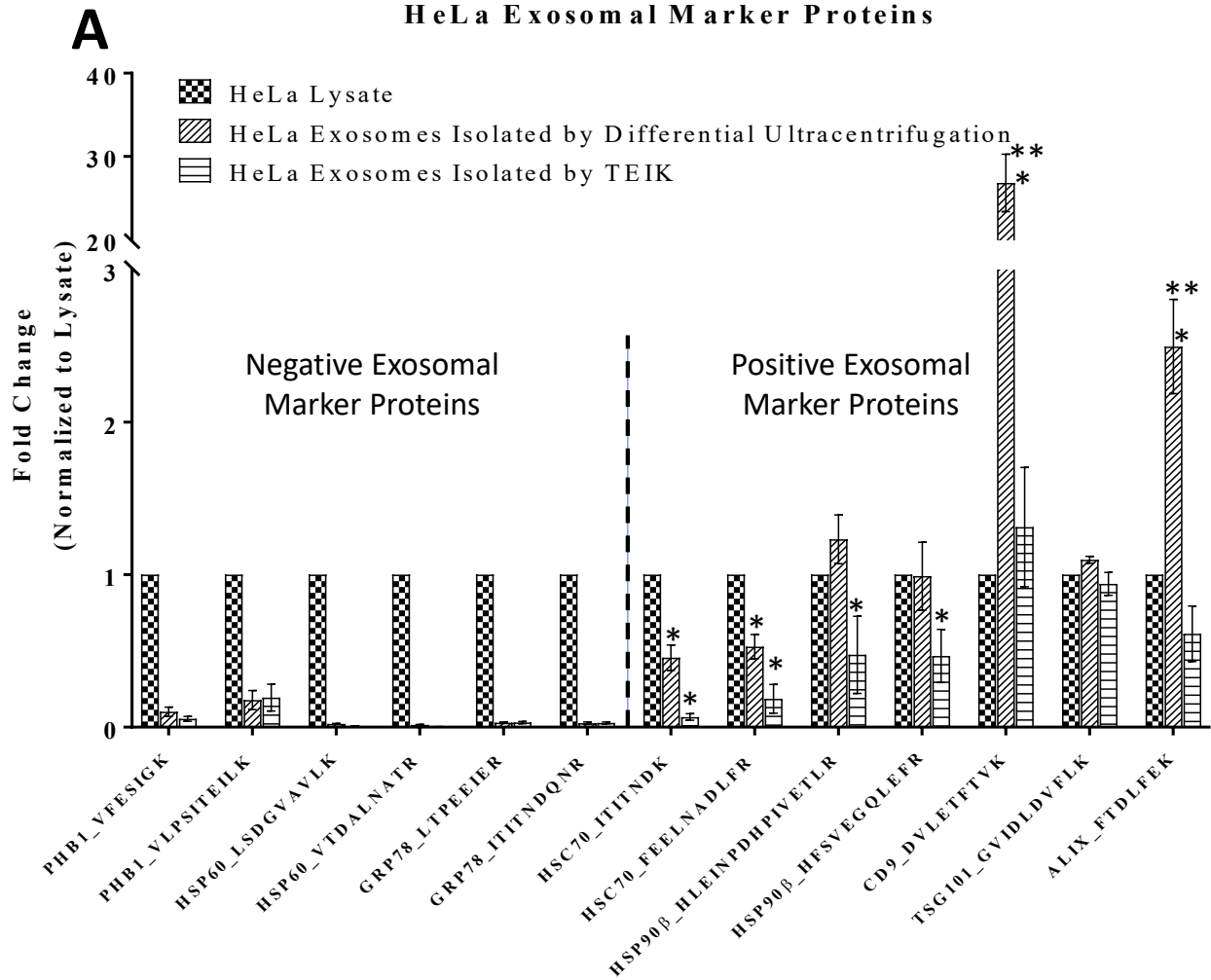
For the HepG2 cell lysate, all proteins were observed, though HSP90 at a very low level. For the HepG2 exosomes isolated by differential ultracentrifugation and TEIK all proteins were observed, except for CD9 after TEIK isolation. Based on the relative intensity of the bands in the blots, it appears both HSP90 and HSC70 proteins are enriched in the exosome preparations compared to the corresponding cell lysate. The HSP60 and GRP78 proteins appear to be more

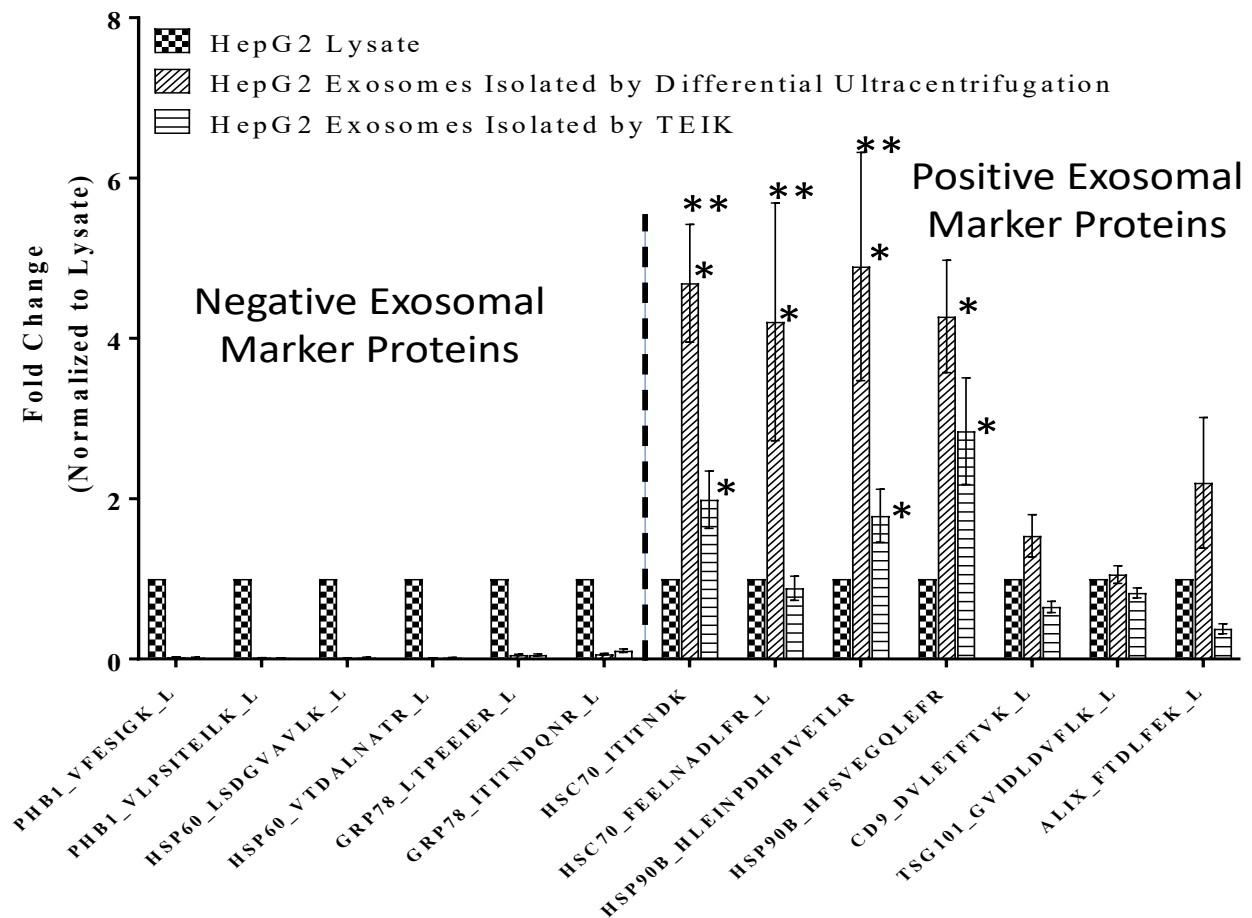
abundant in the HepG2 cell lysate compared to the exosomes isolated by differential ultracentrifugation or the TEIK. The enrichment of HSC70 and HSP90 and decrease in HSP60 and GRP78 in exosomes relative to the HepG2 cell lysate suggests the particles isolated by both differential ultracentrifugation and TEIK are exosomal vesicles. For the HeLa cell lysate, all proteins were detected, however, only the CD9 protein appears to be enriched in the HeLa exosomes after isolation by differential ultracentrifugation. The enrichment of the CD9 protein in the exosomes isolated by differential ultracentrifugation and the lack of non-exosomal marker proteins (HSP60 and GRP78) suggest the particles isolated by differential ultracentrifugation are exosomal vesicles.

### **2.3.5 LC-MRM-MS Analysis of Isolated HepG2 and HeLa Exosomes**

The HeLa and HepG2 total cell lysate and exosomes isolated by differential ultracentrifugation and TEIK were analysed by LC-MRM-MS for the presence and absence of exosomal marker proteins. The data are summarized in **Figure 5A** and **5B**. For HeLa exosomes isolated by differential ultracentrifugation and TEIK, the non-exosomal marker protein levels in the exosomes are lower than then the corresponding cell lysate (left side of **Figure 5A**). This is also the case for the non-exosomal marker proteins in the HepG2 exosomes isolated by both differential ultracentrifugation and TEIK (left side of **Figure 5B**). For the exosomal marker proteins in the HeLa exosomes isolated by TEIK, most were found to be at a similar level, or lower, then the lysate levels (right side of **Figure 5A**). However, when HeLa exosomes were isolated by differential ultracentrifugation, it appeared that both CD9 and ALIX marker proteins were enriched, by approximately 30-fold and 2.5-fold respectively, in the exosomes compared to the lysate (right side of **Figure 5A**). For the HepG2 exosomes isolated by differential ultracentrifugation, all the exosomal marker proteins, except TSG101, appeared to be at higher levels in the exosomes compared to the lysate, with HSC70 and HSP90 $\beta$  being the most heavily

enriched each at ~ 4-fold (right side of **Figure 5B**). For HepG2 exosomes isolated by TEIK, however, only HSP90 $\beta$  was found to be enriched (~ 2-3-fold) in the exosomes compared to the lysate (right side of **Figure 5A**).



**B****HepG2 Marker Proteins**

**Figure 5.** LC-MRM-MS Analysis of HepG2 and HeLa Exosomes Isolated by Differential Ultracentrifugation and TEIK and Corresponding HepG2 and HeLa Cell Lysate. A total of 30  $\mu$ g of cellular and exosomal proteins from HeLa (A) and HepG2 (B) were trypsin digested and assessed for the presence of exosomal marker proteins (HSC70, HSP90 $\beta$ , CD9, TSG101, and ALIX) and non-exosomal marker proteins (PHB1, HSP60, and GRP78) by LC-MRM-MS for 4 biological replicates (n=4). Exosomal marker proteins in exosome preparations whose fold change value was significantly different from the lysate level are marked by (\*). Exosomal marker protein levels which were significantly different between the 2 different isolation methods are marked by (\*\*).

## 2.4 DISCUSSION

The potential use of exosomes in the clinical setting to act as carries of biomarkers, diagnostic tools, and monitor therapeutic responses has been well demonstrated [16-31]. However, a major challenge in the field is the lack of standardized methods for exosome isolation and analysis. Typically, the protein content of the isolated exosomes is investigated by Western blot for the presence of exosomal marker proteins and absence of non-exosomal marker proteins in order to investigate the purity and quality of the exosome preparation [29, 31-34]. Western blot not only relies on the use of antibodies, which are expensive and potentially non-specific, but is also not well multiplexed and therefore requires an abundance of protein for analysis [3]. As demonstrated in **Figure 3** and **Table 3**, exosomal protein yield is quite low, especially for isolation by differential ultracentrifugation. Using a large quantity of exosomal protein to assess the purity and quality of the preparation leaves little protein left for future experiments, hence it would be advantageous to develop a well multiplexed method for exosome analysis.

Here, a LC-MRM-MS-based method for exosome analysis was developed. Unlike Western blot, this assay is well multiplexed and does not require the use of antibodies. The technique for developing these methods has been previously established in this lab [10, 11]. Once the signature peptides for each protein of interest were identified, the LC-MRM-MS method was developed by identifying 3 mass transitions, or fragments, for each peptide of interest. **Table 1** lists the proteins, signature peptides, and mass transitions (precursor and product ions) used to develop the LC-MRM-MS method. As demonstrated in **Figure 1**, 8 exosomal/non-exosomal marker proteins could be monitored, in a 13.5-minute gradient, by 13 different peptides (at 3 mass transitions/peptide) using only 3  $\mu\text{g}$  of a 30  $\mu\text{g}$  total exosomal (or cellular) protein digest, speaking largely to the multiplex-ability of this LC-MRM-MS based assay. In contrast, Western

blot analysis (**Figure 4A** and **4B**) required 15  $\mu\text{g}$  of exosomal protein for each protein (5) that was blotted against, in this case using a total of 75  $\mu\text{g}$  of exosomal protein. If all 8 proteins monitored by LC-MRM-MS were assessed by Western blot at 15  $\mu\text{g}/\text{blot}$ , a total of 120  $\mu\text{g}$  of exosomal protein would be used. Hence, the LC-MRM-MS based assay required 40-fold less protein to get the same, if not more useful information than the tradition Western blot methodology. Specifically, the LC-MRM-MS data could be used to get information regarding the relative abundance of the peptide (and therefore protein) between the cell lysate and different exosome preparations. Such comparison demonstrated that the relative abundance of HSC70 and HSP90 $\beta$  were higher in the HepG2 exosomes isolated by differential ultracentrifugation than in exosomes isolated by TEIK (**Figure 5B**), a comparison that would have been difficult to make based on the Western blot data (**Figure 4A**).

The relative abundance, based on LC-MRM-MS analysis, of exosomal marker proteins (HSC70, HSP90 $\beta$ , CD9, ALIX, and TSG101) appeared at lower levels in exosomes isolated by TEIK than differential ultracentrifugation for both HepG2 (**Figure 5B**) and HeLa (**Figure 5A**) exosome preparations. This supports the previously reported issues with TEIK for exosome isolation leading to a less pure sample preparation [35-38]. Essentially, this method introduces polyethylene glycol (PEG) polymers into the cell culture medium which tie-up the water molecules and cause precipitation of the exosomal vesicles. However, in addition to precipitation of exosomal vesicles, other soluble proteins secreted by the cells are also precipitated. Thus, there appears to be a higher isolation efficiency by TEIK, as demonstrated in **Figure 3** and **Table 3**, however if the protein quantification assay were able to differentiate exosomal protein from soluble protein this would likely not be the case. When samples were prepared for LC-MRM-MS analysis, the digestion was normalized to protein amount (30  $\mu\text{g}$ ) and



the level of soluble proteins contributing to the 30  $\mu$ g is much higher for TEIK preparation than for the ultracentrifuge preparation, resulting in lower levels of exosomal marker proteins relative to differential ultracentrifugation preparations.

In addition to using the LC-MRM-MS method for comparing exosomes isolated by different methods, the method was also used to analyse exosomes from different cell types as well, in this study HepG2 and HeLa cell lines. In this analysis, both the LC-MRM-MS and Western blot methods were consistent with each other in that they revealed different exosomal marker protein expression profiles in HepG2 and HeLa exosomes isolated by differential ultracentrifugation. Specifically, **Figure 4A** and **Figure 5B** suggested that HSC70 and HSP90 $\beta$  are ideal exosomal marker proteins for HepG2 exosomes isolated by differential ultracentrifugation, as these proteins are enriched in the exosomal vesicles compared to the corresponding HepG2 cell lysate. Additionally, **Figure 4B** and **Figure 5A** suggests that CD9 and ALIX are ideal exosomal marker proteins for HeLa exosomes isolated by differential ultracentrifugation, as these proteins are enriched in the exosomal vesicles compared to the corresponding HeLa cell lysate. This data demonstrates the need to develop a set of exosomal marker proteins specific for exosomes from different cell types. Often, the focus is on the development of marker proteins that can be used to identify exosomes from all cell types and that can be used to distinguish exosomal vesicles from other extracellular vesicles (EVs), but such markers are yet to be identified. However, in the same way that different protein biomarkers have been developed for diagnosis of different cancers [39-44], the need to develop different protein biomarkers for exosomes from different cell types was demonstrated; and the utility of LC-MRM-MS-based targeted proteomics for identification of specific exosomal marker proteins was also demonstrated.

## 2.5 CONCLUSION

The use of exosomes in the clinical setting has been of recent interest, however the lack of standardization in exosomal isolation and analysis is a major challenge in the field. Here, a LC-MRM-MS-based method was developed, and the capabilities of LC-MRM-MS-based targeted proteomic techniques to benefit the field of exosomal research were demonstrated. Particularly, the LC-MRM-MS data was generally consistent with the traditional Western blot data, but it required 40-fold less exosomal protein and gave additional information regarding relative abundance of proteins that would be difficult to extract from Western blot data. The LC-MRM-MS method was used to compare exosomes isolated by TEIK and differential ultracentrifugation and was consistent with previous reports of increased contamination of soluble proteins in exosomes isolated by TEIK. Furthermore, the LC-MRM-MS method was used to compare exosomes isolated from different cell lines and suggested a need to change the focus from developing a set of exosomal marker proteins for exosomes secreted by all cell types to developing a unique set of marker proteins for exosomes isolated from different cell types.

## 2.6 REFERENCES

1. Konoshenko, M.Y., et al., *Isolation of Extracellular Vesicles: General Methodologies and Latest Trends*. Biomed Res Int, 2018. **2018**: p. 8545347.
2. Yakimchuk, K., *Exosomes: isolation methods and specific markers*. Materials and Methods, 2015. **5**.
3. Aebersold, R., A.L. Burlingame, and R.A. Bradshaw, *Western blots versus selected reaction monitoring assays: time to turn the tables?* Mol Cell Proteomics, 2013. **12**(9): p. 2381-2.
4. Jayasena, T., et al., *Application of Targeted Mass Spectrometry for the Quantification of Sirtuins in the Central Nervous System*. Sci Rep, 2016. **6**: p. 35391.
5. Parsons, H.T. and J.L. Heazlewood, *Beyond the Western front: targeted proteomics and organelle abundance profiling*. Front Plant Sci, 2015. **6**: p. 301.
6. Picotti, P. and R. Aebersold, *Selected reaction monitoring-based proteomics: workflows, potential, pitfalls and future directions*. Nat Methods, 2012. **9**(6): p. 555-66.
7. Picotti, P., et al., *Full dynamic range proteome analysis of *S. cerevisiae* by targeted proteomics*. Cell, 2009. **138**(4): p. 795-806.
8. Prasad, B., *Targeted MRM Proteomics is a Better Protein Quantification Method Over Western-Blotting*. Journal of Analytical & Bioanalytical Techniques, 2014. **05**(01).
9. Tang, Y.T., et al., *Comparison of isolation methods of exosomes and exosomal RNA from cell culture medium and serum*. Int J Mol Med, 2017. **40**(3): p. 834-844.
10. Michaels, S. and M.Z. Wang, *The revised human liver cytochrome P450 "Pie": absolute protein quantification of CYP4F and CYP3A enzymes using targeted quantitative proteomics*. Drug Metab Dispos, 2014. **42**(8): p. 1241-51.
11. Chen, Y., et al., *Quantification of Flavin-containing Monooxygenases 1, 3, and 5 in Human Liver Microsomes by UPLC-MRM-Based Targeted Quantitative Proteomics and Its Application to the Study of Ontogeny*. Drug Metab Dispos, 2016. **44**(7): p. 975-83.
12. Zaborowski, M.P., et al., *Extracellular Vesicles: Composition, Biological Relevance, and Methods of Study*. BioScience, 2015. **65**(8): p. 783-797.
13. Borges, F.T., L.A. Reis, and N. Schor, *Extracellular vesicles: structure, function, and potential clinical uses in renal diseases*. Braz J Med Biol Res, 2013. **46**(10): p. 824-30.
14. Bebelman, M.P., et al., *Biogenesis and function of extracellular vesicles in cancer*. Pharmacol Ther, 2018. **188**: p. 1-11.

15. Raposo, G. and W. Stoorvogel, *Extracellular vesicles: exosomes, microvesicles, and friends*. J Cell Biol, 2013. **200**(4): p. 373-83.
16. Sonoda, H., et al., *Decreased abundance of urinary exosomal aquaporin-1 in renal ischemia-reperfusion injury*. Am J Physiol Renal Physiol, 2009. **297**(4): p. F1006-16.
17. Hua Zhou, T.P., Angel Aponte, Peter S.T. Yuen, Jason D. Hoffert, Hideo, X.H. Yasuda, Lakhmir Chawla, Rong-Fong Shen, Mark A. Knepper, and Robert, and A. Star, *Exosomal Fetuin-A identified by proteomics: a novel urinary biomarker for detecting acute kidney injury*. Kidney Int, 2006. **70**(10): p. 1847-1857.
18. Miranda, K.C., et al., *Nucleic acids within urinary exosomes/microvesicles are potential biomarkers for renal disease*. Kidney Int, 2010. **78**(2): p. 191-9.
19. Neal, C.S., et al., *Circulating microRNA expression is reduced in chronic kidney disease*. Nephrology Dialysis Transplantation, 2011. **26**(11): p. 3794-3802.
20. Stephanie N. Hurwitz1, M.A.R., Joseph L. Bundy, Xia Liu, Rakesh K. Singh, David G. Meckes, Jr., *Proteomic profiling of NCI-60 extracellular vesicles uncovers common protein cargo and cancer type-specific biomarkers*. Oncotarget, 2016. **7**(52): p. 86999-87015.
21. Hornick, N.I., et al., *Serum Exosome MicroRNA as a Minimally-Invasive Early Biomarker of AML*. Scientific Reports, 2015. **5**(1).
22. Wang, J.L., Yuanyuana; Sun, Wangweia; Zhang, Qinghua; Gu, Taoa; Li, Guangxinb, *Plasma exosomes as novel biomarker for the early diagnosis of gastric cancer*. Cancer Biomarkers, 2018. **21**(4): p. 805-812.
23. Rabinowits, G., et al., *Exosomal microRNA: a diagnostic marker for lung cancer*. Clin Lung Cancer, 2009. **10**(1): p. 42-6.
24. Chen, I.H., et al., *Phosphoproteins in extracellular vesicles as candidate markers for breast cancer*. Proceedings of the National Academy of Sciences, 2017. **114**(12): p. 3175-3180.
25. Akers, J.C., et al., *MiR-21 in the extracellular vesicles (EVs) of cerebrospinal fluid (CSF): a platform for glioblastoma biomarker development*. PLoS One, 2013. **8**(10): p. e78115.
26. Rui Shi, P.-Y.W., Xin-Yi Li, Jian-Xin Chen, Yan Li, Xin-Zhong Zhang, Chen-Guang Zhang, Tao Jiang, Wen-Bin Li1, Wei Ding, Shu-Jun Cheng, *Exosomal levels of miRNA-21 from cerebrospinal fluids associated with poor prognosis and tumor recurrence of glioma patients*. Oncotarget, 2015. **6**(29).
27. Goto, T., et al., *An elevated expression of serum exosomal microRNA-191, -21, -451a of pancreatic neoplasm is considered to be efficient diagnostic marker*. BMC Cancer, 2018. **18**(1): p. 116.

28. Fu, F., et al., *Circulating Exosomal miR-17-5p and miR-92a-3p Predict Pathologic Stage and Grade of Colorectal Cancer*. *Transl Oncol*, 2018. **11**(2): p. 221-232.
29. Qingyun Liu, Z.Y., Shuai Yuan, Weijia Xie, Chengying Li, Zeyao Hu, Ying Xiang, Na Wu, Long Wu, Li Bai, Yafei Li, *Circulating exosomal microRNAs as prognostic biomarkers for non-small-cell lung cancer*. *Oncotarget*, 2017. **8**(8): p. 13048-13058.
30. Whiteside, T.L., *The potential of tumor-derived exosomes for noninvasive cancer monitoring*. *Expert Review of Molecular Diagnostics*, 2015. **15**(10): p. 1293-1310.
31. Melo, S.A., et al., *Glypican-1 identifies cancer exosomes and detects early pancreatic cancer*. *Nature*, 2015. **523**(7559): p. 177-82.
32. Webber, J. and A. Clayton, *How pure are your vesicles?* *J Extracell Vesicles*, 2013. **2**.
33. Joanne L. Welton, S.K., Peter J. Giles, Paul Brennan, Ian A. Brewis, John Staffurth, Malcolm D. Mason, and Aled Clayton, *Proteomics Analysis of Bladder Cancer Exosomes*. *Molecular & Cellular Proteomics*, 2010. **9**: p. 1324-1338.
34. Trairak Pisitkun, R.-F.S., and Mark A. Knepper, *Identification and proteomic profiling of exosomes in human urine*. 2004.
35. Ludwig, A.K., et al., *Precipitation with polyethylene glycol followed by washing and pelleting by ultracentrifugation enriches extracellular vesicles from tissue culture supernatants in small and large scales*. *J Extracell Vesicles*, 2018. **7**(1): p. 1528109.
36. Fan, G.-C., et al., *Exosome isolation from distinct biofluids using precipitation and column-based approaches*. *Plos One*, 2018. **13**(6).
37. Lobb, R.J., et al., *Optimized exosome isolation protocol for cell culture supernatant and human plasma*. *J Extracell Vesicles*, 2015. **4**: p. 27031.
38. Josselin Caradec, G.K., Elham Hosseini-Beheshti, Hans Adomat, Martin Gleave, Emma Guns, *Reproducibility and efficiency of serum-derived exosome extraction methods*. *Clinical Biochemistry*, 2014. **47**: p. 1286-1292.
39. Gam, L.H., *Breast cancer and protein biomarkers*. *World J Exp Med*, 2012. **2**(5): p. 86-91.
40. Zamay, T.N., et al., *Current and Prospective Protein Biomarkers of Lung Cancer*. *Cancers (Basel)*, 2017. **9**(11).
41. Palaniselvam Kuppasamy, N.G., Mashitah M. Yusoffa, Solachuddin J.A. Ichwan, *Proteins are potent biomarkers to detect colon cancer progression*. *Saudi Journal of Biological Sciences*, 2014.
42. Lou, J., et al., *Biomarkers for Hepatocellular Carcinoma*. *Biomarkers in Cancer*, 2017. **9**.

43. Ghosh, D., et al., *A Cell-Surface Membrane Protein Signature for Glioblastoma*. *Cell Syst*, 2017. **4**(5): p. 516-529 e7.
44. Osman, J., et al., *Identification of novel biomarkers in neuroblastoma associated with the risk for bone marrow metastasis: a pilot study*. *Clinical and Translational Oncology*, 2013. **15**(11): p. 953-958.

**Chapter III: Treatment of Hepatoma Cell Line, HepG2, with  $\beta$ -  
naphthoflavone Simultaneously Increased Intracellular and Exosomal  
Expression of CYP1A1**

## TABLE OF CONTENTS

<b>3.1 Introduction.....</b>	<b>81</b>
<b>3.2 Materials and Methods.....</b>	<b>84</b>
3.2.1 Chemicals and Reagents .....	84
3.2.2 HepG2 Cell Culture and Induction of CYP1A1 in HepG2 Cell by $\beta$ -NF .....	85
3.2.3 mRNA Isolation and Quantification from Treated HepG2 Cells .....	85
3.2.4 RT and Real Time-PCR Analysis of mRNA from Treated HepG2 Cells .....	86
3.2.5 CYP1A1 Induction Confirmed in Treated HepG2 Cells by LC-MRM-MS.....	87
3.2.6 EROD Assay for CYP1A1.....	88
3.2.7 LC-MRM-MS Data Analysis.....	88
3.2.8 HepG2 Exosome Collection .....	89
3.2.9 HepG2 Exosome Isolation by Differential Ultracentrifugation.....	89
3.2.10 Exosome Characterization by NTA.....	89
3.2.11 LC-MRM-MS Analysis of the Isolated Exosomes for DME Expression.....	90
<b>3.3 Results .....</b>	<b>91</b>
3.3.1 Confirmation of Intracellular CYP1A1 Induction with Real Time-PCR, Protein Expression, and EROD Assay .....	91
3.3.2 Exosome Characterization by NTA and LC-MRM-MS.....	94
3.3.3 DME Expression in Exosomes Isolated from DMEM Treated HepG2 Cell Culture Medium.....	95
3.3.4 CYP1A1 Induction in Exosomes Isolated from $\beta$ -NF and DMSO Treated HepG2 Cell Culture Medium.....	96
<b>3.4 Discussion .....</b>	<b>99</b>
<b>3.5 Conclusion .....</b>	<b>102</b>
<b>3.6 References.....</b>	<b>103</b>



## LIST OF TABLES

**Table 1.** Sequences of primers used for real time-PCR analysis of mRNA isolated from DMEM, DMSO, AND  $\beta$ -NF treated HepG2 cell cultures..... 86

**Table 2.** Relative quantification of DMEs in DMEM treated HepG2 cell lysate and exosomes isolated by differential ultracentrifugation from DMEM treated HepG2 cell culture medium .... 96

## LIST OF FIGURES

**Figure 1.** Real Time-PCR analysis of mRNA isolated from DMEM, DMSO, and  $\beta$ -NF treated HepG2 cells to demonstrate CYP1A1 induction in  $\beta$ -NF treated HepG2 cells. Error bars represent 3 biological replicates (n=3), asterisks (\*) indicate significant difference in mRNA level from the  $\beta$ -Actin mRNA level. .... 91

**Figure 2:** LC-MRM-MS analysis of treated HepG2 cell lysate to confirm the induction of CYP1A1 intracellularly after treatment with  $\beta$ -NF and to demonstrate the specificity of CYP1A1 induction with HepG2 cells are treated with  $\beta$ -NF. Error bars represent 3 biological replicates (n=3)..... 92

**Figure 3.** 7-EROD Assay to confirm CYP1A1 induction in HepG2 cells after treatment with  $\beta$ -NF in comparison to the vehicle control, DMSO treated HepG2 cells, and the normal growth conditions of DMEM. Error bars represent 3 biological replicates (n=3). .... 93

**Figure 4.** NTA of exosomes isolated from DMEM treated HepG2 cell culture (A), DMSO treated HepG2 cell culture (B), and  $\beta$ -NF treated HepG2 cell culture (C)..... 94

**Figure 5.** Assessing the purity and quality of the exosomes isolated by differential ultracentrifugation from DMEM treated HepG2 cell culture (A, n=4) and DMSO and  $\beta$ -NF treated HepG2 cell culture (B, n=6) by LC-MRM-MS. .... 95

**Figure 6.** Chromatogram demonstrating detection of DMEs in HepG2 exosomes and lysate (A) and relative quantification of DMEs in the HepG2 exosomes and lysate. Error bars represent 4 biological replicates (n=4). .... 96

**Figure 7.** Two (2) peptides, detected by LC-MRM-MR, for CYP1A1 indicate induction of CYP1A1 intracellularly and in the exosomal vesicles after treatment with  $\beta$ -NF (A and C). Both peptides allow for observation of a correlation between lysate levels and exosomal levels after treatment (B and D). Error bars represent 6 biological replicates (n=6). .... 97

**Figure 8.** Monitoring the intracellular and exosomal CYP3A4 (A) and  $\beta$ -actin (B) expression levels after treatment with  $\beta$ -NF by LC-MRM-MS. Error bars represent 6 biological replicates (n=6). .... 98

### 3.1 INTRODUCTION

Metabolic degradation and renal excretion are the primary processes by which the body removes xenobiotics from its system. Unlike renal excretion, metabolic degradation is highly variable among individuals for various intrinsic and extrinsic factors such as age, ethnicity, genetics, diet, smoking, and exercise [1]. This variability poses a challenge in drug development and pharmacotherapy when a drug product has a narrow therapeutic window and is eliminated from the body primarily by metabolic degradation. An example of a drug that falls into this category currently on the market is a blood thinner, warfarin, and is metabolized by Cytochrome P450 (CYP) CYP1A2, CYP2C9 and CYP3A4 [2]. Changes in the activity of these enzymes in an individual on warfarin may significantly alter the pharmacokinetic (PK) exposure leading to adverse effects or a decrease in the therapeutic effect, depending on whether the CYP1A2, CYP2C9 and CYP3A4 activity are inhibited or induced [2]. However, if an individual's metabolic activity can be predicted, the individual can be dosed according to their unique metabolic activity and prevent the adverse effects associated with these drugs.

Currently, an individual's metabolic activity is predicted based on either genotyping or phenotyping procedures. Genotyping is used to determine the DNA sequence that codes for the enzyme of interest, this can be used to determine the polymorphism of the expressed enzyme, and then based on tabulated data, the "typical activity" of the given polymorphism can be used to dose the patient accordingly [3]. This process however fails to account for intrinsic and extrinsic factors that may alter the "typical activity" of an enzyme for an individual. Phenotyping, on the other hand, which is done by administering a cocktail of drugs to a patient, can be used to determine the activity of the expressed enzyme (independent of the polymorphism) and then the patient can be dosed accordingly. While this procedure is used more often in the clinic, it is

costly and inconvenient as it requires monitoring by medical professionals in the hospital [4]. Consequently, there is a need for alternative methods to predict an individual's metabolic activity.

Exosomes are vesicles, typically 30 – 150 nm in diameter, secreted by cells into the extracellular space. They have been found to contain proteins, lipids, and mRNA that reflect the cell from which they were secreted [5]. Since exosomes contain this cellular cargo and are circulating in the extracellular space, they are of recent interest for the development of minimally invasive “liquid biopsies” [6, 7]. Since the liver is the primary location of xenobiotic metabolism, the circulating liver-derived exosomal vesicles may be a source of drug metabolizing enzymes (DMEs) that can be used for development of a “liquid biopsy” procedure for predicating metabolic activity on an individual level. Thereby providing a new basis for personalized medicine.

Unlike genotyping, where populations are grouped into categories, exosomal DME expression may be able to reflect a change in an individual's hepatocyte DME expression level. The expression levels of DMEs in hepatocytes can be altered due to ontogeny, disease, or induction, and in the genotyping process, these altered expression levels are not revealed and therefore not considered in personalized medicine. An individual's liver DME expression profile can potentially be assessed by exosomal DME expression and provide vital information for individualized medicine. Unlike phenotyping, however, where the true activity of the DME is measured, the exosomal DME expression would not be able to predict a change in liver DME activity due to chemical inhibition. That is, if the DME expression profile of the hepatocyte is unchanged, but the activity of the DMEs are altered due to chemical inhibition, this reduced liver

DME activity may not be reflected in the exosomes. In such cases, the phenotyping method may be preferred. However, in the absence of any suspicion of chemical inhibition, the exosomal DME expression may be able to be assessed via a simple blood draw, or “liquid biopsy,” making it more cost efficient and less inconvenient to patients in comparison to phenotyping.

In this study, liquid chromatography – multiple reaction monitoring – mass spectrometry (LC-MRM-MS) was used to examine the exosomal DME expression in exosomes derived from a hepatoma line, HepG2. Further, the ability of exosomal DME expression to be altered to reflect a change occurring within the cells was explored.

## 3.2 MATERIALS AND METHODS

### 3.2.1 Chemicals and Reagents

HepG2 cells were purchased from American Type Culture Collection (Manassas, VA). Dulbecco's modified Eagle's medium (DMEM),  $\beta$ -naphthoflavone ( $\beta$ -NF), dimethyl sulfoxide (DMSO), dithiothreitol (DTT), ammonium bicarbonate (ABC), iodoacetamide (IAM), 7-ethoxyresorufin (7-ER) and resazurin sodium salt were purchased from Sigma-Aldrich Co. (St. Louis). Hepatic fetal bovine serum (FBS), 6-carboxy-X-rhodamine (ROX) reference dye, SYTO 82 orange fluorescent nucleic acid stain, and Guanidinium thiocyanate (TRIzol) were purchased from Life Technologies (Carlsbad, CA). A bicinchoninic acid (BCA) protein assay kit was purchased from Pierce Biotechnology (Rockford IL). Optima grade LC-MS/MS grade acetonitrile, methanol, water, chloroform, formic acid, and isopropanol were ordered through Fisher Chemical (Fair Lawn, NJ). Micron centrifugal filters ultracel regenerated cellulose 10,000 kDa molecular weight cut off (MWCO) columns were purchased from Millipore (Billerica, MA). Protein low bind tubes were purchased from Eppendorf (Westbury, NY). Phosphate buffered saline (PBS; 10x molecular biology grade), was purchased from Cellgro (Manassas, VA). A Beckman Optima™ L-90K preparative ultracentrifuge (Class S), a type 35 rotor, a swinging 28 (SW28) rotor, and ultracentrifuge tubes were purchased from Beckman Coulter (Brea, CA). Sterile 0.22-micron filters and cell culture flasks were purchased from Corning (Corning, NY). High capacity cDNA reverse transcriptase (RT) kit and fast 96-well reaction (0.1 mL) PCR compatible DNA/RNA/RNase free plates were purchased from Applied Biosystems (Foster City, CA). GoTaq hot start colorless master mix, 2x, and sequencing grade modified trypsin were bought from Promega (Madison, WI). Primers were purchased from Invitrogen (Eugene, OR). Thin walled RNase, DNase, and pyrogen free 0.2 mL tubes with dome cap and radioimmunoprecipitation assay (RIPA; 2x) were purchased from Molecular

Bioproducts (San Diego, CA). Protease inhibitor cocktail tablets were purchased from Roche Diagnostics (Indianapolis, IN).

### **3.2.2 HepG2 Cell Culture and Induction of CYP1A1 in HepG2 Cell by $\beta$ -NF**

HepG2 cells were cultured in T-150 flasks at 37 °C and 5 % CO<sub>2</sub> in DMEM containing 10 % v/v FBS prior to treatment with 100  $\mu$ M of  $\beta$ -NF in 0.1 % v/v DMSO, 10 % v/v FBS in DMEM for 48 hours at 37 °C and 5 % CO<sub>2</sub>. An additional HepG2 cell culture was treated with 0.1 % v/v DMSO, 10 % FBS in DMEM to act as a vehicle control.

### **3.2.3 mRNA Isolation and Quantification from Treated HepG2 Cells**

The cellular mRNA was extracted using TRIzol according to the manufacture's protocol for 3 biological replicates (n=3). In short, TRIzol reagent was added to the cells and incubated at room temperature for 5 minutes. Chloroform was added and incubated briefly at room temperature followed by a centrifugation at 12,000 x g for 15 minutes at 4 °C. Approximately 70 % of the top aqueous layer was transferred to a clean RNase/DNase free tube and isopropanol was added and incubated at room temperature for 10 minutes before centrifuged at 12,000 x g for 5 minutes at 4 °C. The supernatant was discarded, and the pellet, containing mRNA, was washed with 70 % ethanol, dried, and resuspended in nuclease free water. The quantity and purity of the isolated mRNA was assessed with a NanoDrop ND1000 Spectrophotometer (NDS, Nanodrop Technologies, Wilmington, DE). Briefly, the NDS was blanked with 2  $\mu$ L of nuclease free water before using the ND1000 version 3.8.1 software to calculate the A260/A280 and A260/A230 ratios as well as the amount of mRNA recovered (ng/ $\mu$ L). A value of two (2) for A260/280 and A260/230 ratios respectively were considered pure RNA.

### 3.2.4 RT and Real Time-Polymerase Chain Reaction (PCR) Analysis of mRNA from Treated HepG2 Cells

Using the High Capacity cDNA RT Kit, 1 µg mRNA was added to a 0.2 mL tube containing 4 mM deoxyribonucleotide triphosphate (dNTP) mixture, 1 x RT buffer, RT random primers and RT enzyme in a total final volume of 20 µL. For each mRNA sample, a non-RT control was also prepared containing all the components listed above except the RT enzyme. The mRNA was converted to single-stranded cDNA using a Bio-Rad C1000 Thermal Cycler (Bio-Rad, Hercules, CA). Specifically, the reaction spent 10 minutes at 25 °C followed by 2 hours at 37 °C and then 5 minutes at 85 °C before being cooled and held at 4 °C. The real time-PCR samples were prepared by combining 12.5 µL of SYTO82/Promega hot start PCR master mix with 10 µM final concentration of forward/reverse (F/R) PCR primers, and 12.5 ng of cDNA (for all samples including the non-RT control), in a total final volume of 25 µL. A list of the primers used can be seen in **Table 1**. The real time-PCR was carried out using an Applied Biosystems® 7500 Fast real time-PCR System (Applied Biosystems, Foster City, CA), spending 5 minutes at 95 °C followed by 40 cycles of 15 seconds at 95 °C and 35 seconds at 60 °C. The cycle threshold (Ct) values generated were used to calculate the fold induction of mRNA relative to β-actin, the housekeeping gene, using double delta Ct analysis method.

**Table 1.** Sequences of primers used for real time-PCR analysis of mRNA isolated from DMEM, DMSO, AND β-NF treated HepG2 cell cultures

Protein	Primer (F/R)	Primer Sequence	PCR Product (# of base pairs)
β-actin	F	AAACTGGAACGGTGAAGGTG	176
β-actin	R	AGAGAAAGTGGGGTGGCTT	
CYP3A4	F	TCAGCCTGGTGCTCCTCTAT	120
CYP3A4	R	GGGATGAGGAATGGAAAGACTGT	
CYP1A1	F	GTTCTACAGCTTCATGACAGAAGATG	127
CYP1A1	R	TTGGCGTTCTCATCCAGCT	
CYP1A2	F	CTGTGGTTCCTGCAGAAAACAG	101



CYP1A2	R	CCCTTCTTGCTGTGCTTGAAC	
--------	---	-----------------------	--

### 3.2.5 CYP1A1 Induction Confirmed in Treated HepG2 Cells by LC-MRM-MS

The treated HepG2 cells for 3 biological replicates (n=3) were pelleted and then lysed with RIPA buffer supplemented with protease inhibitor cocktail for 30 minutes at 4 °C. The lysate was centrifuged at 10,000 x g for 5 minutes at 4 °C, the supernatant was transferred to a clean low protein binding tube and quantified by the BCA assay. A total of 30 µg of total cell lysate was trypsin digested using the quantitative filter-aided sample preparation (qFASP) method. In short, the proteins were reduced with 10 mM DTT in 20 mM ABC and denatured at 95 °C for 3 minutes. The samples were washed on a 10 kDa MWCO column with 50 mM ABC prior to incubation with 10 mM IAM for 20 minutes in the dark at room temperature. The excess IAM was then removed from the column by centrifugation at 14,000 x g for 20 minutes at 20 °C. The proteins were digested with 1 µg of trypsin for 4 hours at 37 °C, the peptides were recovered from the 10 kDa MWCO column by centrifugation into a clean protein low binding tube prior to being spiked with arginine and lysine stable isotope-labelled crude peptides to serve as internal standards (IS) for LC-MRM-MS analysis.

A total of 3 µg of digested protein with IS was separated on an analytical column (ACQUITY UPLC, C18, 1.7 µm, 2.1 x 100 mm) with a gradient consisting of water with 0.1 % v/v formic acid (A) and acetonitrile with 0.1 % v/v formic acid (B) at a rate of 0.4 mL/minute. Specifically, the column was equilibrated in 2 % B for 3 minutes and then increased to 30 % B over the course of 9 minutes. The gradient increased from 30 % B to 95 % B in 1.5 minutes in then back to 2 % B for 2 minutes during each injection. Signature peptides for β-actin, CYP1A1, CYP1A2, and

CYP3A4 were previously identified [8] and monitored using a Waters Xevo TQ-S triple quadrupole MS (Waters, Millford, MA) in electrospray ionization positive (ESI+) mode.

### **3.2.6 7-ethoxyresorufin-O-deethylase (EROD) Assay for CYP1A1**

After treatment, the media was removed, the cells were washed with 1 x PBS, and 2 mL of DMEM without phenol red containing 1  $\mu$ M 7-ER was added to each well. The reactions were quenched with cold methanol immediately after 7-ER addition (zero time point), as well as at 30- and 60-minutes post 7-ER addition. A calibration curve prepared from a 1  $\mu$ M resorufin stock was used to quantify the levels of resorufin, formed by the cells in 3 biological replicates (n=3), which was normalized to the milligram (mg) of cellular protein using a TECAN Infinite M200 PRO (TECAN, Mannedorf, Switzerland) plate reader with an excitation wavelength of 565 nm and emission wavelength of 595 nm.

### **3.2.7 LC-MRM-MS Data Analysis**

Waters MassLynx 4.1 Software was used to was used to operate the Waters Xevo TQ-S triple quadrupole MS. Further, the TargetLynx Application Manager within the MassLynx software was used to analyze the data. Specifically, the chromatographic peaks for each peptide were integrated by the TargetLynx Application to determine the area under the curve (AUC) for each peptide. The normalized peak area was then calculated by dividing the AUC of the light peptide (sample) by the AUC of the heavy peptide (IS). For assessing the CYP1A1 induction in the cell lysate, the “Fold Change” value on the y – axis was calculated by Equation 1 below.

*Equation 1:*

$$\frac{\text{Response Ratio of the Cell Lysate (DMEM, DMSO, or } \beta - \text{NF) Digest}}{\text{Response Ratio of the DMEM Lysate Digest}}$$

### **3.2.8 HepG2 Exosome Collection**

HepG2 cells were cultured in twelve T-150 flasks in DMEM containing 10 % v/v FBS. Cells in four of the T-150 flasks were treated with 0.1 % v/v DMSO in DMEM with 10 % v/v FBS, cells in four T-150 flasks were treated with 100  $\mu$ M  $\beta$ -NF in 0.1 % v/v DMSO in DMEM with 10 % v/v FBS and cells in the remaining four T-150 flasks were maintained in the normal growth conditions (DMEM with 10 % v/v FBS) for 48 hours at 37 °C and 5 % CO<sub>2</sub>. Post treatment, each flask was incubated with 25 mL of its respective treatment media, but with no FBS, for 48 hours at 37 °C and 5 % CO<sub>2</sub>. The media was collected, centrifuged at 500 x g for 10 minutes at 4 °C, filtered with a 0.22-micron filter, and stored at -80 °C until exosome isolation. The 48-hour exosome collection was repeated twice more to collect a total of 300 mL of DMEM, DMSO, and  $\beta$ -NF treated HepG2 media. Upon each collection period, the media was centrifuged, filtered, and stored at -80 °C until exosome isolation.

### **3.2.9 HepG2 Exosome Isolation by Differential Ultracentrifugation**

The collected cell culture medium was thawed on ice and centrifuged at 10,000 x g for 30 minutes at 4 °C to pellet larger vesicles which were discarded, and the supernatant was centrifuged at 100,000 x g for 1 hour at 4 °C. The supernatant was discarded and each pellet, containing the exosomes, was re-suspended in 10 mL of 1 x PBS and centrifuged once more at 100,000 x g for 1 hour at 4 °C. Each pellet was re-suspended in 30  $\mu$ L of 1 x PBS and quantified using the BCA protein assay kit.

### **3.2.10 Exosome Characterization by NTA**

The size and concentration of the isolated exosomal vesicles were assessed using a Malvern NanoSight LM10 Nanoparticle Analysis System equipped with a charge coupled device (CCD) camera and a 638 nm class 3B laser source. Prior to analysis, the chamber was flushed with 1 x

PBS and the optimal imaging location was located using the thumb-print like shape. The exosomes were then introduced to the chamber and 3 x 30 second videos were captured with a fresh volume of sample introduced between each video. The NanoSight 3.2 software was used to process the videos with the auto function selected for the following analysis parameters: detection threshold, blur, minimum tracking length, and minimum particle size.

### **3.2.11 LC-MRM-MS Analysis of the Isolated Exosomes for DME Expression**

Using the qFASP protocol discussed above, 30 µg of exosomal and cellular proteins for 4 biological replicates (n=4) were trypsin digested and prepared for LC-MRM-MS analysis. The analytical conditions (column and gradient) used for the LC-MRM-MS analysis were identical to those discussed above. In the first LC run, signature peptides for exosomal marker proteins heat shock protein 70 kDa (HSC70) and Heat Shock Protein 90 kDa beta (HSP90β) and non-exosomal marker proteins Glucose Regulated Protein 78 kDa (GRP78), Prohibitin 1 (PHB1), and Heat Shock Protein 60 kDa (HSP60) were detected using a Waters Xevo TQ-S triple quadrupole MS. In a second LC run, signature peptides for CYPs (2C9, 2C19, 3A4, 3A5, 3A7, 1A1, 1A2, 4F11, 1B1, 4F3B, 4F2, and 4F12), flavin-containing monooxygenase (FMOs) 1, 3 and 5, and β-actin were detected using specific MRM transitions and a triple-quadrupole MS [8-11] (Waters Xevo TQ-S).

### 3.3 RESULTS

#### 3.3.1 Confirmation of Intracellular CYP1A1 Induction with Real Time-PCR, Protein Expression, and EROD Assay

The isolated mRNA from the treated HepG2 cells was reverse transcribed to cDNA and used for real time-PCR analysis. While heavily debated, an increased level of mRNA can be associated with an increased level of protein, thus the CYP1A1 induction in the treated HepG2 cells can be probed indirectly by real time-PCR analysis [15-17]. The mRNA levels for different DMEs normalized to  $\beta$ -actin, can be seen in **Figure 1**.  $\beta$ -actin was selected as the housekeeping gene as

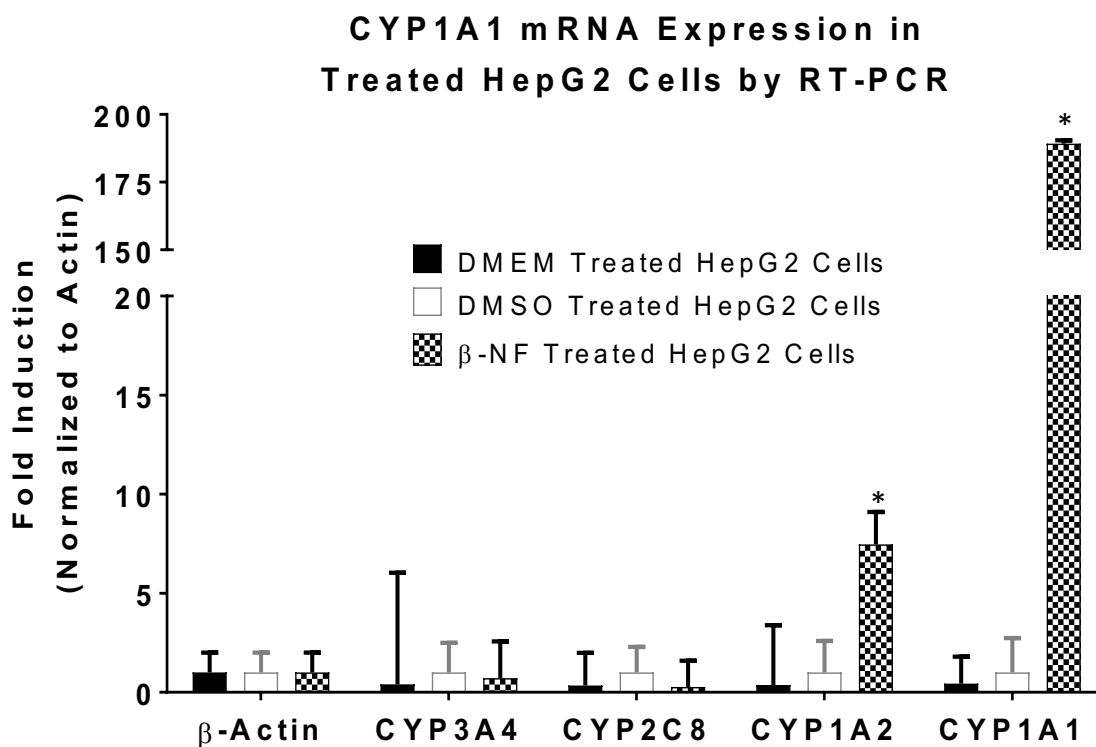


**Figure 1.** Real Time-PCR analysis of mRNA isolated from DMEM, DMSO, and  $\beta$ -NF treated HepG2 cells to demonstrate CYP1A1 induction in  $\beta$ -NF treated HepG2 cells. Error bars represent 3 biological replicates (n=3), asterisks (\*) indicate significant difference in mRNA level from the  $\beta$ -Actin mRNA level.

its expression levels are not expected to change upon treatment with DMEM, DMSO, or  $\beta$ -NF.

The CYP1A1 mRNA level was increased nearly 200-fold in the  $\beta$ -NF treated HepG2 cells,

whereas the CYP1A1 mRNA levels in the DMEM and DMSO treated cells were not.

Additionally, the mRNA for CYP1A2 appeared slightly induced, about 7-fold, in the  $\beta$ -NF treated HepG2 cells compared to the DMEM and DMSO treated HepG2 cells. However, the lack of induction in CYP3A4 and CYP2C8 mRNA levels, and the minimal increase in CYP1A2 mRNA, demonstrates the specificity of the induction.

An LC-MRM-MS method previously developed in the lab [8-11] for DMEs was used to directly probe the DME expression of the treated HepG2 cells. Unlike real time-PCR, the LC-MRM-MS method directly probes the DME expression based on the detection of signature peptides for the DMEs of interest. As seen in **Figure 2**, the CYP1A1 expression in the  $\beta$ -NF treated HepG2 cell

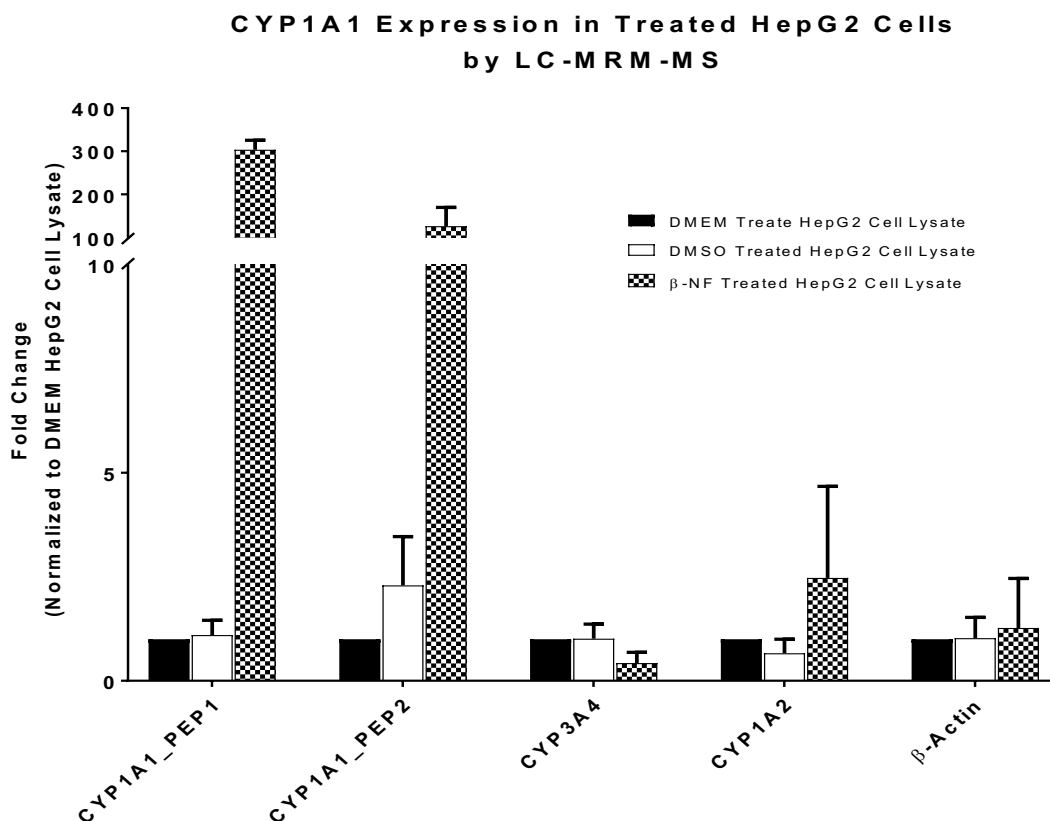


**Figure 2.** LC-MRM-MS analysis of treated HepG2 cell lysate to confirm the induction of CYP1A1 intracellularly after treatment with  $\beta$ -NF and to demonstrate the specificity of CYP1A1 induction with HepG2 cells are treated with  $\beta$ -NF. Error bars represent 3 biological replicates (n=3).

lysate is increased greater than 100-fold from the DMEM culture conditions; and as was demonstrated by real time-PCR, the specificity of the induction for CYP1A1 was further demonstrated based on the lack of increase of other DMEs (CYP1A2 and CYP3A4) expressed in the  $\beta$ -NF treated HepG2 cell lysate versus the DMEM and DMSO treated HepG2 cell lysate. Furthermore, this data suggests the  $\beta$ -actin levels are not changed upon treatment with DMSO, DMEM, or  $\beta$ -NF as expected.

The conversion of 7-ER to resorufin is catalyzed by the CYP1A family. Based on the data in **Figure 1** and **Figure 2**, the primary enzyme of the CYP1A family present in the HepG2 cells is CYP1A1. Therefore, the formation of resorufin, > 80 nM/mg protein after 1 hour, in  $\beta$ -NF treated HepG2 cells, as seen in **Figure 3**, is associated with the CYP1A1 expression.

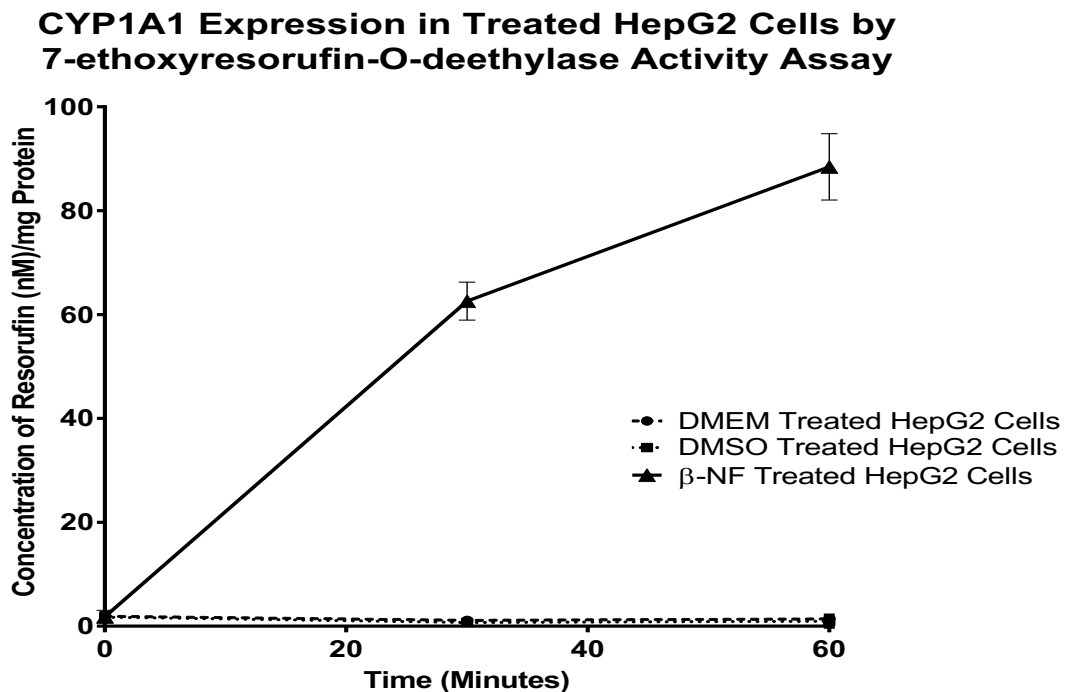


**Figure 3.** 7-EROD Assay to confirm CYP1A1 induction in HepG2 cells after treatment with  $\beta$ -NF in comparison to the vehicle control, DMSO treated HepG2 cells, and the normal growth conditions of DMEM. Error bars represent 3 biological replicates (n=3).

The DMSO and DMEM treated HepG2 cells, acting as the vehicle control and normal growth conditions respectively, do not appear to express in the CYP1A1 enzyme based on the lack of resorufin (0 nM/mg) formed as a function of time compared to the  $\beta$ -NF treated HepG2 cell culture. This data suggests that  $\beta$ -NF induces the CYP1A1 expression intracellularly in HepG2 cells, as expected [12-14].

### 3.3.2 Exosome Characterization by NTA and LC-MRM-MS

Exosomes were isolated from DMEM, DMSO, and  $\beta$ -NF treated HepG2 cell culture medium and characterized by NTA to determine size distribution and concentration. The NTA analysis, which can be seen in **Figure 4**, revealed the particles to have an average (mean  $\pm$  SD) size of 142  $\pm$  3 nm (**4a**), 149  $\pm$  3 nm (**4b**), and 139  $\pm$  4 nm (**4c**), respectively for exosomes from the DMEM, DMSO, and  $\beta$ -NF treated cell cultures, which are all within the expected size range of 30 – 150 nm.

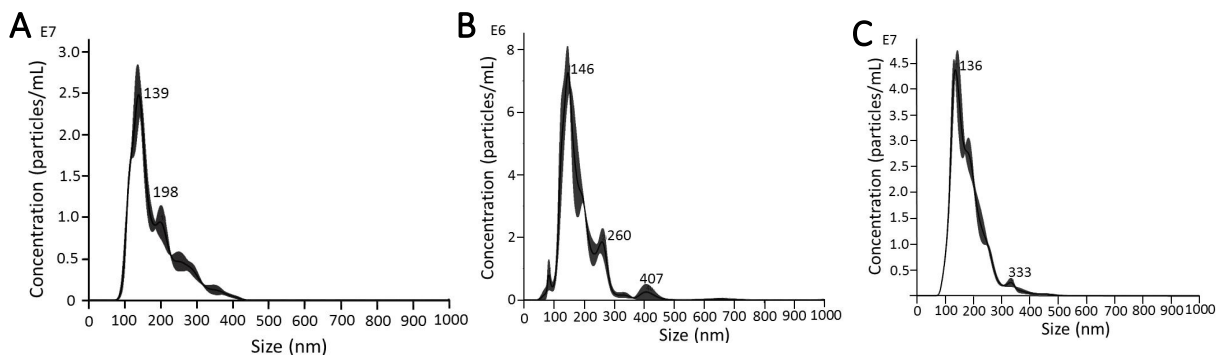


**Figure 4.** NTA of exosomes isolated from DMEM treated HepG2 cell culture (A), DMSO treated HepG2 cell culture (B), and  $\beta$ -NF treated HepG2 cell culture (C)

The purity and quality of the exosome preparation was assessed based on the presence of exosomal marker proteins, HSC70 and HSP90 $\beta$ , and absence of non-exosomal marker proteins, PHB1, HSP60, and GRP78 using a previously developed LC-MRM-MS based method. The data in **Figure 5a** and **5b** demonstrates the levels of exosomal marker proteins are higher in the



exosomes from the DMEM, DMSO, and  $\beta$ -NF treated HepG2 cell cultures compared to their corresponding cell lysate. Additionally, **Figure 5a** and **5b** also suggests the levels of non-exosomal marker proteins are at higher levels in the DMEM, DMSO, and  $\beta$ -NF treated HepG2 cell lysate in comparison to their respective exosome isolations, further confirming that particles observed by NTA are likely exosomal vesicles.

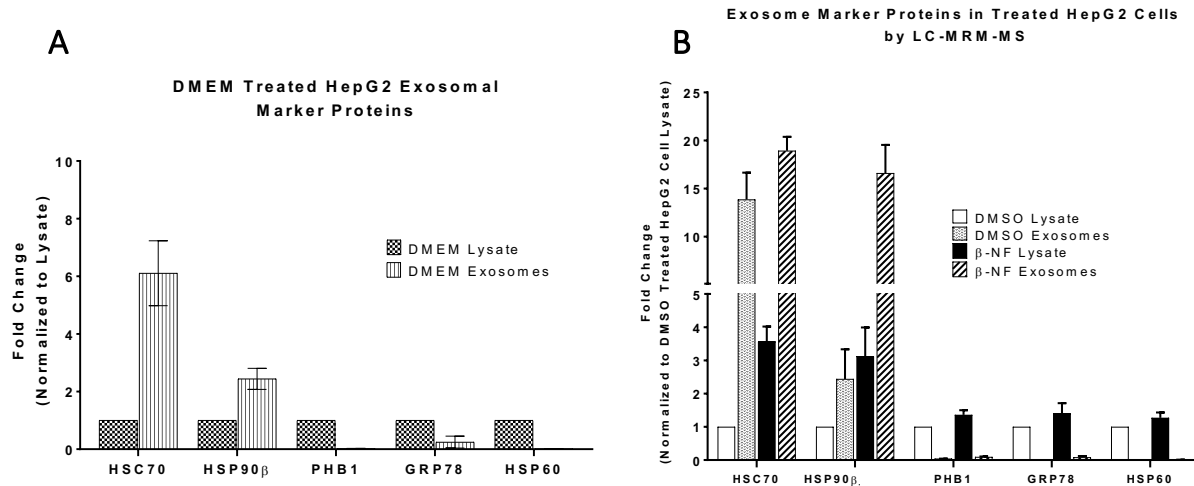


**Figure 5.** Assessing the purity and quality of the exosomes isolated by differential ultracentrifugation from DMEM treated HepG2 cell culture (A, n=4) and DMSO and  $\beta$ -NF treated HepG2 cell culture (B, n=6) by LC-MRM-MS.

### 3.3.3 DME Expression in Exosomes Isolated from DMEM Treated HepG2 Cell Culture Medium

An LC-MRM-MS method for DMEs was previously developed in this laboratory [8-11]. This method was used to probe a 30  $\mu$ g trypsin digest of DMEM treated HepG2 cell lysate and exosomes for DME content. As seen in the chromatogram in **Figure 6a**, CYP4F12, CYP3A4, FMO3, CYP3A7, and CYP4F11 were detected in the HepG2 cell lysate and the exosomes. Relative quantification of the detected DMEs for 4 biological replicates (n=4), in **Figure 6b**, demonstrates that all DMEs, except for CYP4F12, are found at higher levels in the lysate than the exosomes. The fold-increase and amino acid sequence of the signature peptides detected

whose peaks are present in the chromatogram (**Figure 6a**) can be seen in **Table 2**. Overall, this data suggests the presence of DMEs in HepG2 cell lysate and exosomes.

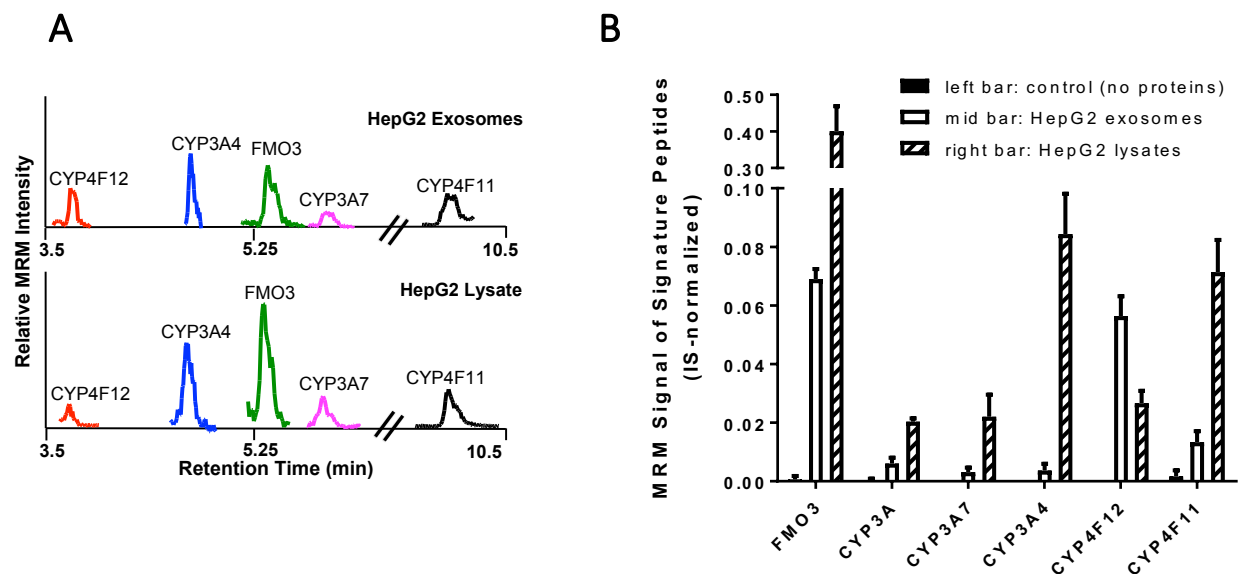


**Figure 6.** Chromatogram demonstrating detection of DMEs in HepG2 exosomes and lysate (A) and relative quantification of DMEs in the HepG2 exosomes and lysate. Error bars represent 4 biological replicates (n=4).

**Table 2.** Relative quantification of DMEs in DMEM treated HepG2 cell lysate and exosomes isolated by differential ultracentrifugation from DMEM treated HepG2 cell culture medium

Enzyme	Fold Difference	Signature Peptide
CYP4F12	2-fold higher in exosomes	SITNASAAIAPK
CYP3A4	20-fold higher in lysate	EVTNFLR
FMO3	5-fold higher in lysate	SNDIGGLWK
CYP3A7	3.5-fold higher in lysate	VISFLTK
CYP4F11	3-fold higher in lysate	VVLALTLLHFR

### 3.3.4 CYP1A1 Induction in Exosomes Isolated from $\beta$ -NF and DMSO Treated HepG2 Cell Culture Medium

By comparing the values in lane 1 (DMSO treated HepG2 cell lysate) and lane 3 ( $\beta$ -NF treated HepG2 cell lysate) of **Figure 7a**, the increase of CYP1A1 intracellularly post  $\beta$ -NF treatment is

clear. Specifically, the CYP1A1 appears to be ~1000 x more abundant in the  $\beta$ -NF treated HepG2 cell lysate in comparison to the DMSO treated HepG2 cell lysate. By comparing the CYP1A1 expression levels in exosomes isolated from the DMSO treated HepG2 cell culture medium (lane 2) and the  $\beta$ -NF treated HepG2 cell culture medium (lane 4), the intracellular induction of CYP1A1 is reflected in the exosomes, though showing only a ~100-fold increase rather than the 1000-fold increase as was seen in the lysate. The data in **Figure 7a** is for a total of 6 biological replicates and the data is plotted slightly differently in **Figure 7b**. Specifically, the correlation between the cellular level and the exosomal level for each experiment can be seen. A second peptide for the CYP1A1 (CYP1A1\_PEP2) protein is plotted in **Figures 7c** and **7d** and overall tells the same story as the other peptide for CYP1A1 (CYP1A1\_PEP1) (**Figures 7a** and **7b**).

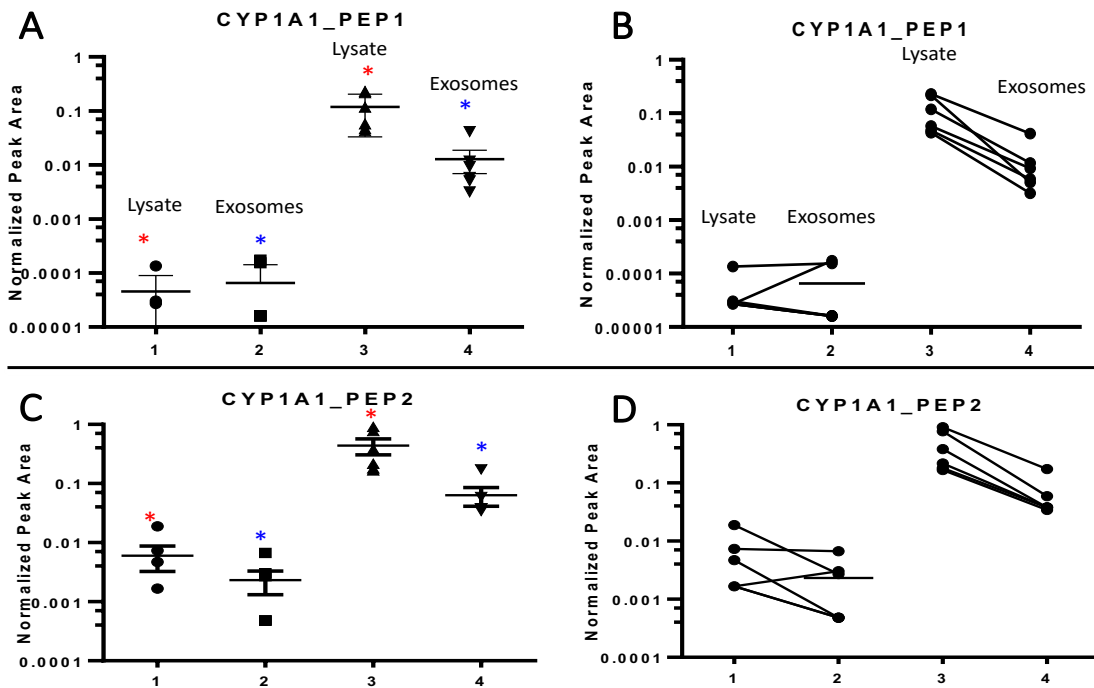


**Figure 7.** Two (2) peptides, detected by LC-MRM-MR, for CYP1A1 indicate induction of CYP1A1 intracellularly and in the exosomal vesicles after treatment with  $\beta$ -NF (A and C). Both peptides allow for observation of a correlation between lysate levels and exosomal levels after treatment (B and D). Error bars represent 6 biological replicates (n=6).

To demonstrate this is a true enrichment of CYP1A1 in the exosomes isolated from the  $\beta$ -NF treated HepG2 cell culture, the levels of CYP3A4 and  $\beta$ -actin were investigated and can be seen in **Figure 8a** and **8b**. By comparing lanes 1 and 3 for both proteins, the intracellular levels of  $\beta$ -actin and CYP3A4 are not changing, as expected [12, 18]. Additionally, the exosomal levels (lanes 2 and 4) are not showing the same type of induction that was observed in **Figure 7** further suggesting the trend seen in **Figure 7** was not an artifact of data analysis, but rather a true induction of CYP1A1 in the exosomal vesicles.

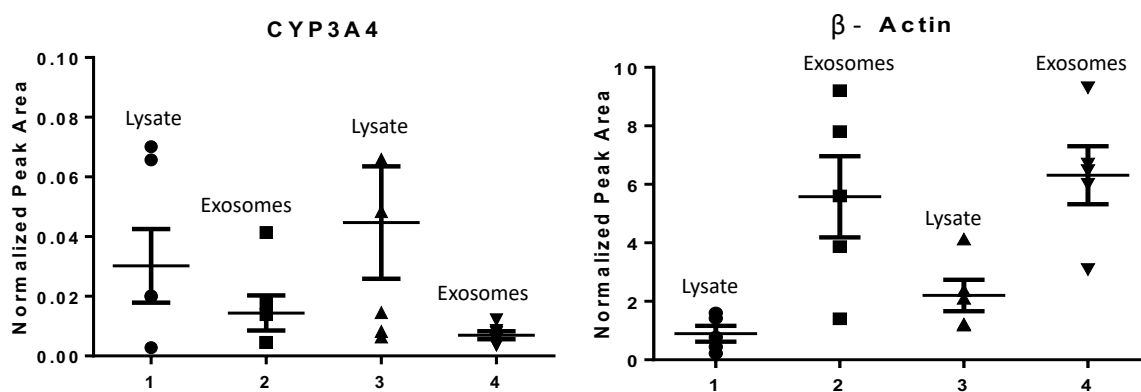


**Figure 8.** Monitoring the intracellular and exosomal CYP3A4 (A) and  $\beta$ -actin (B) expression levels after treatment with  $\beta$ -NF by LC-MRM-MS. Error bars represent 6 biological replicates (n=6).

### 3.4 DISCUSSION

While different methods, such as genotyping and phenotyping, have been developed to predict an individual's metabolic activity, no single method has proven cost efficient and convenient while accounting for different intrinsic and extrinsic factors that can affect DME expression. [3, 4]. Therefore, there is a need for development of alternative methods predict metabolic activity at the individual level, which would allow patients to be dosed certain medications, specifically those eliminated via metabolic degradation and have narrow therapeutic windows, based on their unique metabolic activity. Here, the use of liver-derived exosomes is explored as way to predict metabolic activity at the individual level. Exosomes are membrane bound vesicles secreted by cells into the extracellular matrix and contain proteins, lipids, and other cargo that reflect the cells from which they originate [19]. Therefore, perhaps hepatocyte-derived exosomes circulating in the blood can be used to interrogate the DME content of the liver, thereby allowing for prediction of an individual's metabolic activity via a simple blood draw, or "liquid biopsy".

In order for exosomes to act as surrogates for liver DME activity, the presence of DMEs in exosomal vesicles must first be established. Thus, in the first part of this study, the DME content of an HCC cell line, HepG2, and its exosomes isolated by differential ultracentrifugation was investigated. The isolated exosomes, from DMEM treated HepG2 cell medium, were first interrogated for particle size by NTA; as seen in **Figure 4a** the isolated particles were found to be within the expected size range of exosomes (30 – 150 nm). The purity and quality of the exosome preparation was investigated by LC-MRM-MS analysis for presence of exosomal marker protein HSC70 and HSP90 $\beta$  and non exosomal marker proteins HSP60, PHB1, and GRP78. As demonstrated in **Figure 5a** the exosomal vesicles contain higher levels of the exosomal marker proteins than the corresponding cell lysate and vice versa for the non-exosomal

marker proteins, thus suggesting the particles observed by NTA are exosomal vesicles. The DME content of the HepG2 cell lysate and exosomes was then investigated using LC-MRM-MS analysis, using a method previously developed in the laboratory [9]. As seen in the chromatogram, **Figure 6a**, several CYPs and FMO3 were detected in the HepG2 cell lysate and exosomes, though as demonstrated in **Figure 6b**, the levels were typically higher in the lysate than in the exosomes.

Once the presence of DMEs in exosomal vesicles were established, the ability of the exosomal DME expression to change to reflect a change occurring within the secreting cells was investigated. For this study, a HepG2 cell culture was treated with DMSO, to act as a vehicle control, and another HepG2 cell culture was treated with  $\beta$ -NF.  $\beta$ -NF is an aryl hydrocarbon receptor (AhR) agonist known to induce CYP1A1, but not CYP3A4, expression in HepG2 cells [12-14]. As demonstrated in **Figures 1 – 3** three different assays (7-EROD assay, real time-PCR, and LC-MRM-MS) all indicated a significant increase in the CYP1A1 expression intracellularly after treatment with  $\beta$ -NF, in comparison to HepG2 cells maintained in normal growth conditions (DMEM) and the vehicle control (DMSO). The real time-PCR (**Figure 2**) and LC-MRM-MS analysis (**Figure 3**) also demonstrates the specificity of the CYP1A1 induction intracellularly by  $\beta$ -NF.

Exosomes were isolated by differential ultracentrifugation from the DMSO and  $\beta$ -NF treated HepG2 cell culture medium. The isolated exosomes were analyzed by NTA (**Figure 4b** and **4c**) and LC-MRM-MS (**Figure 5b**) to confirm the particles were within the expected size range of 30 – 150 nm and contained exosomal marker proteins and the non-exosomal marker proteins

were absent. Both NTA and LC-MRM-MS analysis confirmed the particles isolated from the DMSO and  $\beta$ -NF treated HepG2 cell culture medium were exosomes.

Finally, the isolated exosomes could be probed for CYP1A1 by LC-MRM-MS to determine if the CYP1A1 induction intracellularly was reflected in the exosomal vesicles secreted by these cells. As seen in **Figure 7**, two different peptides for the CYP1A1 protein were monitored during the LC-MRM-MS analysis, and both indicated the CYP1A1 expression is increased in the exosomes secreted by the  $\beta$ -NF treated HepG2 cells compared to the vehicle control, DMSO. Furthermore, the trend observed in **Figure 7** was confirmed by also assessing the induction of CYP3A4 and  $\beta$ -actin (**Figure 8**), in which case there was no increase in the levels of these proteins post treatment with  $\beta$ -NF, as expected.

### **3.5 CONCLUSION**

In conclusion, these studies not only established the presence of DMEs in hepatocyte-derived exosomal vesicles, but also suggested the exosomal DME expression can be alerted to reflect a change occurring within the secreting cells. This simultaneous induction supports the proposed idea of using exosomal DMEs as surrogates for liver DME activity, although additional studies including the DME content of exosomes from primary human hepatocytes and their correlation to the DME activity of the secreting hepatocytes and investigating hepatocyte derived exosomes circulating in the plasma are needed to translate the use of exosomal DMEs into the clinics.



### 3.6 REFERENCES

1. Leon Shargel, S.W.P., Andrew Yu, *Applied Biopharmaceutics and Pharmacokinetics*. 6th ed. 2012: The McGraw-Hill Companies.
2. Walker, G., et al., *The pharmacokinetics and pharmacodynamics of warfarin in combination with ambrisentan in healthy volunteers*. Br J Clin Pharmacol, 2009. **67**(5): p. 527-34.
3. Samer, C.F., et al., *Applications of CYP450 testing in the clinical setting*. Mol Diagn Ther, 2013. **17**(3): p. 165-84.
4. Christensen, M., et al., *The Karolinska cocktail for phenotyping of five human cytochrome P450 enzymes*. Clin Pharmacol Ther, 2003. **73**(6): p. 517-28.
5. Raposo, G. and W. Stoorvogel, *Extracellular vesicles: exosomes, microvesicles, and friends*. J Cell Biol, 2013. **200**(4): p. 373-83.
6. Melo, S.A., et al., *Glypican-1 identifies cancer exosomes and detects early pancreatic cancer*. Nature, 2015. **523**(7559): p. 177-82.
7. Zarin Nuzhat, V.K., Shayna Sharma, Gregory E. Rice, Virendra Joshi, Carlos Salomon, *Tumour-derived exosomes as a signature of pancreatic cancer - liquid biopsies as indicators of tumour progression*. Oncotarget, 2017.
8. Wang, Z., et al., *Development of an In Vitro Model to Screen CYP1B1-Targeted Anticancer Prodrugs*. J Biomol Screen, 2016. **21**(10): p. 1090-1099.
9. Chen, Y., et al., *Quantification of Flavin-containing Monooxygenases 1, 3, and 5 in Human Liver Microsomes by UPLC-MRM-Based Targeted Quantitative Proteomics and Its Application to the Study of Ontogeny*. Drug Metab Dispos, 2016. **44**(7): p. 975-83.
10. Michaels, S. and M.Z. Wang, *The revised human liver cytochrome P450 "Pie": absolute protein quantification of CYP4F and CYP3A enzymes using targeted quantitative proteomics*. Drug Metab Dispos, 2014. **42**(8): p. 1241-51.
11. Michael Zhuo Wang, J.Q.W., Jennifer B. Dennison, Arlene S. Bridges, Stephen D. Hall, Sally Kornbluth, Richard R. Tidwell, Philip C. Smith, Robert D. Voyksner, Mary F. Paine and James Edwin Hall, *A gel-free MS-based quantitative proteomic approach accurately measures cytochrome P450 protein concentrations in human liver microsomes*. Proteomics, 2008. **8**: p. 4186-4196.
12. Westerink, W.M.A. and W.G.E.J. Schoonen, *Cytochrome P450 enzyme levels in HepG2 cells and cryopreserved primary human hepatocytes and their induction in HepG2 cells*. Toxicology in Vitro, 2007. **21**(8): p. 1581-1591.

13. Kikuchi, H. and A. Hossain, *Signal transduction-mediated CYP1A1 induction by omeprazole in human HepG2 cells*. *Experimental and Toxicologic Pathology*, 1999. **51**(4-5): p. 342-346.
14. Michael M. Iba, T.N., and Jacqueline Funga, *CYP1A1 induction by pyridine and its metabolites in HepG2 cells*. *Archives of Biochemistry and Biophysics*, 2002.
15. Liu, Y., A. Beyer, and R. Aebersold, *On the Dependency of Cellular Protein Levels on mRNA Abundance*. *Cell*, 2016. **165**(3): p. 535-50.
16. Velez-Bermudez, I.C. and W. Schmidt, *The conundrum of discordant protein and mRNA expression. Are plants special?* *Front Plant Sci*, 2014. **5**: p. 619.
17. Kendrick, N., *A gene's mRNA level does not usually predict its protein level*. 2014.
18. Zhang, R., et al., *Induction of cytochromes P450 1A1 and 1A2 by tanshinones in human HepG2 hepatoma cell line*. *Toxicol Appl Pharmacol*, 2011. **252**(1): p. 18-27.
19. Conde-Vancells, J., et al., *Characterization and comprehensive proteome profiling of exosomes secreted by hepatocytes*. *J Proteome Res*, 2008. **7**(12): p. 5157-66.

**Chapter IV: Isolation and Characterization of Liver-derived Exosomes by  
Liver Marker Protein Asialoglycoprotein-1 (ASGR1) and Proteomic Analysis**

## TABLE OF CONTENTS

<b>4.1 INTRODUCTION .....</b>	<b>109</b>
<b>4.2 MATERIALS AND METHODS .....</b>	<b>111</b>
4.2.1 Chemicals and Reagents .....	111
4.2.2 Cell Culture, Exosome Collection and Isolation by Differential Ultracentrifugation ...	112
4.2.3 NTA for Particle Size and Concentration .....	113
4.2.4 LC-MRM-MS for Exosomal and Non-Exosomal Marker Proteins.....	113
4.2.5 LC-MRM-MS Data Analysis.....	114
4.2.6 Western Blot Analysis .....	115
4.2.7 IP of HLMs, HepG2 Exosomes and HeLa Exosomes by $\alpha$ -ASGR1.....	116
4.2.8 Alexa 488 Conjugation to $\alpha$ -CD9 Antibody.....	117
4.2.9 EPI of HLMs after IP.....	118
<b>4.3 RESULTS AND DISCUSSION .....</b>	<b>119</b>
4.3.1 Expression of ASGR1 in HLMs, HpeG2 and HeLa Cells.....	120
4.3.2 IP of HLMs Based on ASGR1 Expression and Analysis .....	121
4.3.3 Characterization of HepG2 and HeLa Exosomes .....	124
4.3.4 Expression of ASGR1 in HepG2 Exosomes.....	125
4.3.5 IP of HepG2 and HeLa Exosomes Based on ASGR1 Expression and Analysis.....	126
<b>4.4 CONCLUSION .....</b>	<b>129</b>
<b>4.5 REFERENCES.....</b>	<b>130</b>

## LIST OF TABLES

<b>Table 1:</b> Specific MRM transitions monitored in LC-MRM-MS method to analyze HLMs and Exosomes after pull-down with $\alpha$ -ASGR1 modified Dynabeads.....	114
--	-----

## LIST OF FIGURES

<b>Figure 1:</b> Presence of liver-specific marker protein ASGR1 in HLMs (1), HepG2 cell lysate (2), and HeLa cell lysate (3). Normalized to protein loading amount of 15 $\mu$ g. ....	120
---	-----

<b>Figure 2:</b> General workflow for pull-down of HLMs using magnetic beads and the ASGR1 protein – antibody interaction. Immobilization of $\alpha$ -ASGR1 on surface of magnetic beads (A), immobilization of HLMs on magnetic beads (B), pull-down of HLMs on the magnetic beads via a magnet and removal of supernatant and HLMs not attached to the beads (C). ....	122
---	-----

<b>Figure 3:</b> Protein enrichment after HLM pull-down using biotinylated $\alpha$ - ASGR1 antibody immobilized on streptavidin coated beads. The data is showing a fold increase in proteins digested on the beads containing the biotinylated $\alpha$ - ASGR1 antibody versus beads without biotinylated $\alpha$ - ASGR1 antibody for biological triplicate (n=3). Asterisks indicate a statistical difference between amount of protein on the beads with the $\alpha$ - ASGR1 antibody versus the beads without. ....	123
--	-----

<b>Figure 4:</b> NTA analysis of HeLa (A) and HepG2 (B) exosomes isolated by differential ultracentrifugation.....	124
--	-----

**Figure 5:** LC-MRM-MS analysis of HeLa exosomes (A) and HepG2 exosomes (B) after isolation by differential ultracentrifugation of 3 biological replicates (n=3)..... 125

**Figure 6:** Demonstrating the presence of ASGR1 in HepG2 exosomes isolated by differential ultracentrifugation by LC-MRM-MS (A) and Western blot, with 15 µg of exosomal protein in lane 1, and 15 µg of HepG2 cell lysate in lane 2 (B)..... 126

**Figure 7:** Protein enrichment after HepG2 and HeLa pull-down using biotinylated  $\alpha$  - ASGR1 antibody immobilized on streptavidin coated beads. The data is showing a fold increase in proteins digested on the beads containing the biotinylated  $\alpha$  - ASGR1 antibody versus beads without biotinylated  $\alpha$  - ASGR1 antibody for biological triplicate (n=3). Asterisks indicate a statistical difference between amount of protein on the beads with the  $\alpha$  - ASGR1 antibody versus the beads without. .... 127

**Figure 8:** EPI of HLM pulled-down using the ASGR1 antibody-antigen interaction then exposed to an Alexa 488 conjugated  $\alpha$ -CD9 antibody for detection. A sample exposed to beads with biotinylated  $\alpha$ -ASGR1 on its surface (A) is compared to a sample where no biotinylated  $\alpha$ -ASGR1 was exposed to the surface of the beads (B). .... 128

## 4.1 INTRODUCTION

Exosomes are vesicles secreted by cells into the extracellular space. Their formation begins with an inward budding of the plasma membrane to form an early endosome, which then inward buds to form exosomes [1]. Eventually, early endosomes mature into multivesicular endosomes (MVEs) and fuse with the plasma membrane releasing their content, including exosomes into the extracellular space. Exosomes are typically 30 – 150 nm in diameter and contain proteins, RNAs, DNAs, and lipids from the cell they are originating from. In the human body, exosomes are secreted into bodily fluids such as blood, and in the case of cell culture the exosomes are released directly into the cell culture medium [1, 2]. Since exosomes contain cargo from the cell they originate from, they are thought to be a source of biomarkers, and since they are found in plasma, they provide the potential for development of minimally invasive “liquid biopsies” for diagnosis of different diseases, such as cancer [3, 4].

While plasma is 95 % water, it contains an abundance of secreted proteins such as albumin, antibodies, enzymes, clotting factors, and small molecules such as glucose, lipids, and hormones. This results in a complex matrix which the circulating exosomes of interest also reside in. Therefore, in order to probe the exosomal vesicles for biomarkers of interest, it is essential to isolate them from the plasma. This has been done mostly by differential ultracentrifugation and immuno-isolation methods [2, 5]. Differential ultracentrifugation isolates total plasma exosomes, as there is no way for differential ultracentrifugation to separate plasma exosomes based their originating cell or organ. Immuno-isolation methods can also be used to isolate exosomes from different cell types, if a general exosomal marker protein such as Heat Shock Cognate 70 kDa (HSC70), Heat Shock Protein  $\beta$  90 kDa (HSP90 $\beta$ ), Cluster of Differentiation 9 (CD9), or Programmed Cell Death 6-Interacting Protein (ALIX) is used. However, immuno-

isolation methods can be used to isolate a subset of exosomal vesicles, originating from a specific organ, if a specific marker protein for the organ is identified.

The purpose of this study is to establish an immuno-isolation method to isolate liver-derived exosomes, using a liver-specific marker protein Asialoglycoprotein-1 (ASGR1) [6-9]. This liver marker protein was previously identified in exosomes derived from primary rat hepatocytes, thus is expected to also be expressed in exosomes from primary human hepatocytes [10]. By isolating liver-derived exosomes from plasma, the drug metabolizing enzyme (DME) content of the exosomes can be correlated to liver DME activity and provide a new foundation for personalized medicine. Additionally, the liver-derived exosomes can be probed for hepatoma biomarkers and lead to early diagnosis of hepatoma.



## 4.2 MATERIALS AND METHODS

### 4.2.1 Chemicals and Reagents

HepG2 and HeLa cells were purchased from American Type Culture Collection (Manassas, VA). Radioimmunoprecipitation assay (RIPA; 2x) buffer was purchased from Boston BioProducts (Ashland, MA) and protease inhibitor cocktail tablets were purchased from Roche Diagnostics Complete (Indianapolis, IN). Low protein binding microcentrifuge tubes (1.5 mL), Pierce® bicinchoninic acid (BCA) protein assay reagent A and B, bovine serum albumin (BSA) standard, Western blotting filter paper, Slide-A-Lyzer® MINI dialysis units, and Pierce™ antibody biotinylation kit for Immunoprecipitation (IP), were purchased from Thermo Scientific (Rockford, IL). Pooled human liver microsomes (HLMs) were purchased from XenoTech (Kansas City, KS). Laemmli sample buffer, Mini-PROTEAN® TGX™ precast gels, PowerPac™ Basic, Immun-Blot® Polyvinylidene difluoride (PVDF) membranes for protein blotting, Trans-Blot® Turbo™ transfer system, 10x Tris/Glycine,/Sodium Dodecyl Sulfate (SDS) gel running buffer, and Trans-Blot® Turbo™ 5x transfer buffer was purchased from Bio-Rad (Hercules, CA). Non-fat dry milk was purchased from Associated Wholesale Groceries Inc (Kansas City, KS). Anti-ASGR1 ( $\alpha$ -ASGR1) and anti-rabbit ( $\alpha$ -rabbit) horseradish peroxidase (HRP)-labeled antibodies were purchased from Abcam (Cambridge, MA). Tween® 20, sodium chloride, precleaned microscope slides, tris-base (Tris), optima liquid chromatography – MS/MS (LC-MS/MS) grade methanol, acetonitrile, and formic acid were purchased from Fisher Scientific (Fair Lawn, New Jersey). Phosphate buffered saline (PBS; 10x molecular biology grade) was purchased from Cellgro (Manassas, VA). Dynabeads™ M-280 streptavidin, Alexa Fluor™ 488 antibody labeling kit, fetal bovine serum (FBS), and arginine and lysine stable isotope-labelled crude peptides were purchased from Invitrogen by Thermo Fisher Scientific

(Eugene, OR). Micron centrifugal filters ultracel regenerated cellulose 10 kDa molecular weight cut off (MWCO) columns were purchased from Millipore (Billerica, MA). Iodoacetamide (IAM), ammonium bicarbonate (ABC), Dulbecco's modified Eagle's medium – high glucose (DMEM), and DL-Dithiothreitol (DTT) were purchased from Sigma-Aldrich (St. Louis, MO). Sequence grade modified trypsin was purchased from Promega (Madison, WI). Corning® 150cm<sup>2</sup> cell culture flasks, sterile 0.22-micron filters, and cover glass number 1.5 were purchased from Corning (Corning, NY). A Beckman Optima™ L-90K preparative ultracentrifuge (Class S), a Type 35 rotor, a swinging 28 (SW28) rotor, and ultracentrifuge tubes, were purchased from Beckman Coulter (Brea, CA). Purified anti-CD9 ( $\alpha$ -CD9) antibody was purchased from Ancell (Bayport, MN). Eppendorf BioPhotometer Plus and disposable single sealed cuvettes were purchased from Eppendorf (Hauppauge, NY).

#### **4.2.2 Cell Culture, Exosome Collection and Isolation by Differential Ultracentrifugation**

HepG2 and HeLa cells were cultured to confluency in four T150 flasks in DMEM containing 10% v/v FBS. Each flask was incubated with 25 mL of exosome collection media (DMEM without FBS) for 48 hours at 37 °C and 5% CO<sub>2</sub>. This 48-hour incubation was repeated twice more, to collect a total of 300 mL from each cell culture. After each 48-hour incubation, the media was centrifuged at 500 x g, filtered with a 0.22-micron filter and stored at -80 °C until differential ultracentrifugation. Once 300 mL of media from each cell type was collected and filtered, the frozen media was thawed on ice and then centrifuged at 10,000 x g for 30 minutes to pellet larger vesicles. The pellets were discarded, and the supernatant was centrifuged at 100,000 x g for 1 hour. The supernatant was then discarded, and each pellet was resuspended in 10 mL of 1 x PBS and centrifuged once more at 100,000 x g for 1 hour. Each pellet was resuspended in 30  $\mu$ L of 1 x PBS and quantified using the BCA protein assay kit.

#### **4.2.3 Nanoparticle Tracking Analysis (NTA) for Particle Size and Concentration**

NTA measurements were performed on a Malvern NanoSight LM10 Nanoparticle Analysis System equipped with a charge coupled device (CCD) camera and a 638 nm class 3B laser source to determine particle size and concentration. The position of the visual reference (thumb-print-like shape) was checked to ensure the optimal imaging location was in place. The chamber was flushed with 1 x PBS prior to introducing the exosome sample. Once the sample was injected into the chamber, the camera settings were adjusted until the particles appeared as single bright points in the field, and then 3 x 30 second videos were captured with a fresh volume of sample introduced into the chamber between each video. The videos were processed with NanoSight NTA 3.2 software with the auto selection chosen for the following analysis parameters: detection threshold, blur, minimum tracking length, and minimum particle size.

#### **4.2.4 Liquid Chromatography – Multiple Reaction Monitoring – Mass Spectrometry (LC-MRM-MS) for Exosomal and Non-Exosomal Marker Proteins**

The purity of the exosome isolation, for 3 biological replicates (n=3), was assessed based on the presence of exosomal marker proteins HSC70, CD9, ALIX, TSG101, and HSP90 $\beta$  and absence of non-exosomal marker proteins Prohibitin-1 (PHB1), Heat Shock Protein 60 kDa (HSP60), and Glucose Regulated Protein 78 kDa (GRP78). Briefly, 30  $\mu$ g of exosomal protein and total cell lysate was reduced with 10 mM DTT in 20 mM ABC and denatured at 95 °C for 3 minutes. The protein samples were then loaded onto a 500  $\mu$ L 10 kDa MWCO column, washed with 50 mM ABC by centrifugation at 14,000 x g for 20 minutes at 20 °C before adding 10 mM IAM to the samples, still on the 10 kDa MWCO column. The proteins were incubated in the dark at room temperature for 20 minutes and the excess IAM was removed by centrifugation at 14,000 x g for 20 minutes at 20 °C. Finally, the proteins were digested, on the 10 kDa MWCO column, with 1

µg of trypsin for 4 hours at 37 °C. The peptides were recovered from the MWCO column by centrifugation into a clean protein low binding tube and spiked with arginine and lysine stable isotope-labelled crude peptides to serve as internal standards for the peptides in **Table 1**. A total of 3 µg of digested protein with internal standard was separated on an analytical column (ACQUITY UPLC, C18, 1.7 µm, 2.1 x 100 mm) with a gradient of water with 0.1 % (v/v) formic acid (A) and acetonitrile with 0.1 % (v/v) formic acid (B). The gradient increased from 2 % B to 30 % B over the course of 9 minutes at a flow rate of 0.4 mL/minute. The gradient then increased from 30 % B to 95% B in 1.5 minutes, still at 0.4 mL/minute, and then re-equilibrated the column at 2 % B, 98 % A for 2 minutes at 0.4 mL/minute. Signature peptides for exosomal/non-exosomal marker proteins were detected using specific mass transitions, which can be seen in **Table 1**, on a Waters Xevo TQ-S triple-quadrupole MS operating in electrospray ionization positive (ESI+) mode.

**Table 1:** Specific MRM transitions monitored in LC-MRM-MS method to analyze HLMs and Exosomes after pull-down with  $\alpha$ -ASGR1 modified Dynabeads..

Protein	Signature Peptide	Average Mass MH+ (Da)	MRM Precursor Ion (m/z)	MRM Product Ion (m/z)			Retention Time (Minutes)
				1	2	3	
PHB1	VFESIG(K)	780.80	390.22	680.36	533.29	404.25	3.79
	VLPSITTEIL(K)	1214.46	607.37	904.61	817.50	704.42	7.21
HSP60	LSDGVAVL(K)	902.05	451.27	701.42	430.30	260.20	4.37
	VTDALNAT(R)	961.04	480.76	760.39	645.37	461.25	3.34
GRP78	LTPEEIE(R)	987.07	493.76	772.38	675.33	546.29	3.73
	ITITNDQN(R)	1075.14	537.78	860.42	747.34	646.29	3.25
HSC70	ITITND(K)	804.89	402.73	691.40	590.30	477.20	3.24
	FEELNADLF(R)	1254.36	627.30	848.50	735.40	435.30	7.21
CD9	DVLETFTV(K)	1052.19	526.29	724.39	595.35	494.30	6.28
ALIX	FTDLFE(K)	899.99	450.23	752.38	651.33	536.31	5.50
TSG101	GVIDLDVFL(K)	1119.32	559.83	849.47	734.44	506.33	9.82
HSP90B	HFSVEGQLEF(R)	1349.46	450.22	749.39	692.37	564.31	5.28
	HLEINPDHPIVETL(R)	1783.99	594.98	827.50	740.50	617.36	5.20
CYP3A4	EVTNFLR	878.50	440.20	650.40	549.10	435.30	4.66

#### 4.2.5 LC-MRM-MS Data Analysis

The Waters Xevo TQ-S triple quadrupole MS was operated using the Waters MassLynx 4.1 software (Waters, Millford, MA). The data were analyzed with the TargetLynx Application Manager within the MassLynx software. The chromatographic peaks of each peptide and its internal standard were integrated by the TargetLynx software to determine the area under the curve (AUC). The response ratio was then calculated by dividing the AUC of the peptide from the digest (light peptide) by the AUC of the internal standard (heavy peptide). For assessing the purity of exosomes preparations, the “Fold Change” value on the y-axis was calculated by Equation 1. For the IP experiments, the “Fold Increase” value on the y-axis was calculated by Equation 2.

*Equation 1:*

$$\frac{\text{Response Ratio in the Cell Lysate (or Exosome) Digest}}{\text{Response Ratio in the Cell Lysate Digest}}$$

*Equation 2:*

$$\frac{\text{Response Ratio from the Digest Containing the } \alpha - \text{ASGR1 Antibody Dynabeads}}{\text{Response Ratio from the Digest Containing Dynabeads Only (no } \alpha - \text{ASGR1)}}$$

#### **4.2.6 Western Blot Analysis**

HepG2 and HeLa cell pellets were resuspended and lysed with 2x RIPA buffer supplemented with protease inhibitor cocktail for 30 minutes at 4 °C. The lysates were centrifuged at 10,000 x g for 5 minutes at 4 °C. The supernatants were transferred to a clean protein low binding tube and the protein concentration was quantified using the BCA assay. A total of 15 µg of HLMs, HepG2 cell lysate and exosomes, and HeLa cell lysate were mixed with 4x Laemmli Sample Buffer and denatured at 95 °C for 5 minutes before being loaded into separate lanes on a Mini-PROTEAN® TGX™ Precast Gel for electrophoretic separation. The separated proteins were transferred to a PVDF membrane using the Trans-Blot® Turbo™ Transfer System and blocked

with 5 % non-fat milk prior to overnight treatment with  $\alpha$ -ASGR1 antibody (1:500 dilution) at 4 °C. The blot was treated with an  $\alpha$ -rabbit-HRP antibody prior to imaging with a Kodak Image Station 400.

#### **4.2.7 IP of HLMs, HepG2 Exosomes and HeLa Exosomes by $\alpha$ -ASGR1**

A total of 5  $\mu$ g of  $\alpha$ -ASGR1 antibody was dialyzed into 1 x PBS prior to biotinylation using the Pierce™ Antibody Biotinylation Kit for IP. Briefly, the antibody was incubated with 40-fold excess biotin for 30 minutes at room temperature with gentle mixing. The excess biotin was removed with a desalting column, per the protocol in the Biotinylation Kit, and the biotinylated  $\alpha$ -ASGR1 antibody was recovered. The biotinylated  $\alpha$ -ASGR1 antibody was immobilized on 0.5 mg of Dynabeads™ M-280 Streptavidin coated magnetic beads by a 30-minute incubation at room temperature, with gentle mixing, in a protein low binding tube. A control sample was prepared identically, but with no biotinylated  $\alpha$ -ASGR1 antibody. Afterwards, the Dynabeads were washed, resuspended in Tris-buffered saline with 0.05% Tween 20 (TBS-T20 (0.05 %)) and 30  $\mu$ g of HLMs, HepG2 exosomes, and HeLa exosomes (in biological triplicate) were added to vials containing  $\alpha$ -ASGR1 antibody modified Dynabeads and the control Dynabeads (no  $\alpha$ -ASGR1 antibody). The samples were incubated overnight (~16 hours) at 4 °C. MS sample vials were passivated by filling with 200  $\mu$ L of 2 mg/mL BSA and incubating overnight at 4 °C. Post overnight incubation, the samples were removed from the 4 °C, centrifuged briefly, and placed on the magnet for 5 minutes. The supernatant was discarded and the Dynabeads were washed and transferred to a clean protein low binding tube. The Dynabeads were resuspended in 90  $\mu$ L of 50 mM ABC with 4 mM DTT and denatured at 95 °C for 11 minutes. The samples, for biological triplicate IP (n=3), were centrifuged briefly, cooled for 10 minutes at room

temperature, spiked with 10 mM IAM, and incubated in the dark at room temperature for 20 minutes. The samples were digested with 1 µg of trypsin for 4 hours at 37 °C with gentle mixing. The digests were placed on the magnet, and the supernatant was transferred to passivated MS sample vials and spiked with internal standards for LC-MRM-MS analysis as described above.

#### 4.2.8 Alexa 488 Conjugation to α-CD9 Antibody

The Invitrogen Alexa Fluor™ 488 Antibody Labeling Kit was used to label 75 µg of α-CD9 antibody from Ansell. Briefly, 75 µg of α-CD9 antibody was spiked with 0.1 M sodium bicarbonate and transferred to a vial of reactive dye, inverted 10 times to ensure the dye was dissolved, then incubated in the dark for 1 hour at room temperature. The vial was inverted 10 times every 15 minutes throughout the incubation period. Using the gel resin and a spin filter, components E and D respectively of the Labeling Kit, the labeled antibody was recovered by centrifugation at 16,000 x g for 1 minute, and the unreacted Alexa 488 was removed from the solution. The concentration of labeled protein was assessed based on the absorbance at 280 nm (A280), and the degree of labeling (DOL) was calculated based on the moles of dye/moles of protein (see Equations 3 and 4).

*Equation 3:*

$$\text{Protein Concentration (M)} = \frac{[A280 - 0.11(A494)] \times \text{Dilution Factor}}{203,000}$$

A280 is the absorbance of the conjugated α-CD9 antibody at 280 nm  
 A494 is the absorbance of the conjugated α-CD9 antibody at 494nm  
 0.11 is the correction factor accounting for the fluorophore's A280 contribution  
 203,000 molar extinction coefficient cm<sup>-1</sup>M<sup>-1</sup> for typical IgG

*Equation 4:*

$$\text{DOL} = \frac{\text{Moles of Dye}}{\text{Mole of Protein}} = \frac{A494 \times \text{Dilution Factor}}{71,000 \times \text{Protein Concentration (M)}}$$

A494 is the absorbance of the conjugated  $\alpha$ -CD9 antibody at 494nm  
71,000 is the molar extinction coefficient ( $\text{cm}^{-1}\text{M}^{-1}$ )

#### 4.2.9 EPI of HLMs after IP

The initial steps for EPI detection of HLMs after IP on Dynabeads by ASGR1 expression are the same as those described above in the *IP of HLMs, HepG2 Exosomes, and HeLa Exosomes by ASGR1 Expression and LC-MRM-MS Analysis* section. However, after the overnight incubation, the Dynabeads were incubated again, overnight (~16 hours) with 2.25  $\mu\text{g}$  of Alexa 488 conjugated  $\alpha$ -CD9 antibody. After the second overnight incubation, the samples were placed on the magnet for 5 minutes, the supernatant was discarded, and the Dynabeads were washed. Twenty-microliter (20  $\mu\text{L}$ ) of sample was placed on a glass microscope slide with a cover glass and sealed nail polish. The samples were imaged with an Olympus IX81/3I spinning disk confocal inverted microscope, with excitation/emission wavelengths of 495/519 nm.



### 4.3 RESULTS AND DISCUSSION

A liver-specific marker protein, ASGR1, has previously been discovered [6-9]. This protein is a transmembrane lectin protein which makes it an ideal candidate for developing IP methods for liver-derived exosome isolation for two reasons. First, because exosomal formation occurs through an endosomal route, by initial inward budding of the plasma membrane, a majority of exosomal associated proteins are either plasma membrane or cytosolic proteins. Since ASGR1 is a transmembrane protein, this protein it is expected to be found with exosomes [11, 12]. The second advantage of using a transmembrane protein is that it can be used to isolate the intact exosomes. If this protein were enclosed in the exosomal vesicle, the antibody used to capture the exosomes from the plasma would not be able to recognize the protein. Furthermore, a previous proteomic study on exosomes derived from primary rat hepatocytes established the presence of ASGR1 in exosomes, and therefore ASGR1 expected to be present in primary human hepatocyte-derived exosomes as well [10].

In this study we demonstrated, for the first time, the ability to isolate liver-derived exosomes using liver-specific marker protein ASGR1. However, because only 150 – 300 µg of exosomal protein is isolated from 300 mL of cell culture medium, a feasibility study was done using commercially available HLMs. These vesicles are typically 20 - 200 nm in diameter [13], lipid bound, isolated from cell lysate by differential ultracentrifugation. HLMs are vesicles that form by the re-arrangement of the endoplasmic reticulum (ER) upon mechanical cell lysis of human hepatocytes [14]. However, while the HLM content is enriched with proteins and lipids from the ER, it is not a homogenous preparation [15]. Therefore, there are proteins and lipids from other cellular compartments including the plasma membrane, cytosol, mitochondria, and Golgi. A previous proteomics study of HLMs established not only the presence of ASGR1 in HLMs, but

also that is was abundant in these vesicles. Thus, HLMs serve as a viable substitute to exosomes for the purpose of IP method development [15].

#### 4.3.1 Expression of ASGR1 in HLMs, HpeG2 and HeLa Cells

Prior to IP of HLMs by ASGR1, the expression of ASGR1 in HLMs was confirmed along the specificity of the  $\alpha$ -ASGR1 antibody by traditional Western blot methodology. As seen in **Figure 1** there appears to be definite expression of ASGR1 in HLMs based on the band present 37 kDa in lane 1, which is near the expected molecular weight of 33 kDa [6]. In addition to HLMs, HepG2 cell lysate was also examined by Western blot in **Figure 1** for ASGR1 expression. HepG2, a hepatoma cell line, was the cell line of choice to demonstrate the ability of the IP method to capture ASGR1 expressing exosomes [16].

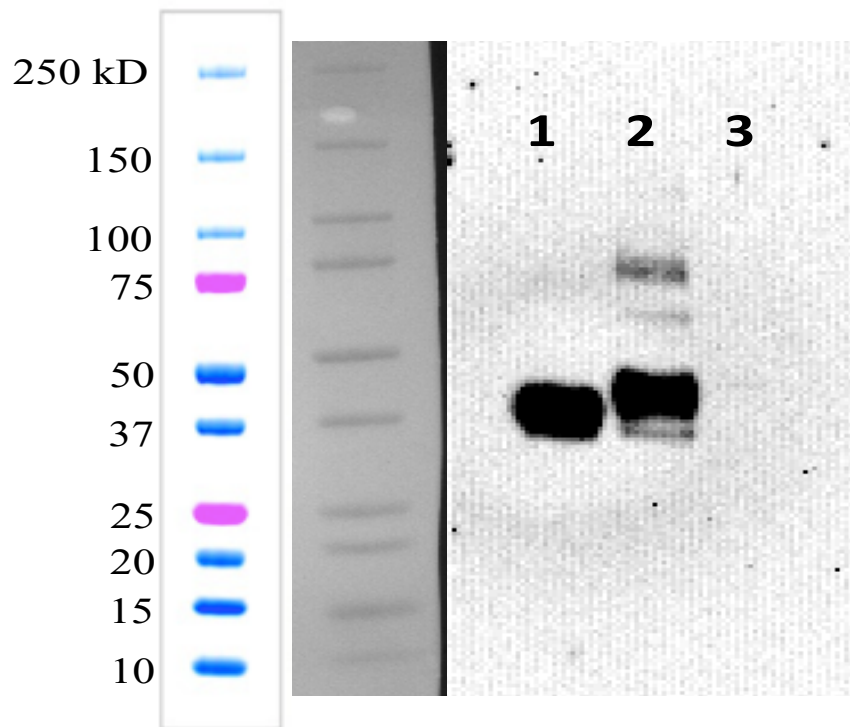


**Figure 1:** Presence of liver-specific marker protein ASGR1 in HLMs (1), HepG2 cell lysate (2), and HeLa cell lysate (3). Normalized to protein loading amount of 15  $\mu$ g.

While ASGR1 is known to be expressed in primary human hepatocytes, the expression of ASGR1 in HepG2 cells had to be confirmed, as protein expression profiles can be altered in disease states, such as cancer [6, 16-19]. If the ASGR1 expression was absent or low in the HepG2 cell line, it would not be a good cell line to use exosomes from for the IP studies. However, based on the presence of a band between 37 and 50 kDa in lane 2 of **Figure 1**, the expression of ASGR1 is confirmed in the HepG2 cell line. The molecular weight of ASGR1 in HepG2 cell lysate is slightly higher than that of HLMs, but this could be due to different glycosylation occurring at one or both of the glycosylation sites of the ASGR1 protein [6]. Additionally, there appears to be higher molecular weight band in the HepG2 cell lysate (lane 2), between 75 and 100 kDa. This could be due to (1) covalent dimerization of the ASGR1 protein that was not reduced in the sample preparation or (2) non-specific binding of the  $\alpha$ -ASGR1 antibody to another protein in the HepG2 cell lysate. However, when looking at the negative control, HeLa cell lysate in lane 3 of **Figure 1**, no bands appeared. HeLa cells are a cervical cancer cell line so the expression of a liver-specific marker protein is not expected [20]. Overall, this data demonstrated the presence of ASGR1 in HLMs, HepG2 cell lysate, and that the  $\alpha$  - ASGR1 antibody to be used for IP method development is active and specific for the ASGR1 protein.

#### **4.3.2 IP of HLMs Based on ASGR1 Expression and Analysis**

After demonstrating the presence of ASGR1 in HLMs as well as the activity and specificity of the  $\alpha$  - ASGR1 antibody, the interaction between the  $\alpha$  - ASGR1 antibody and ASGR1 antigen (protein) was then used to precipitate, or “pull-down”, the HLMs from solution on magnetic beads. The general workflow for this method is summarized in **Figure 2**. Essentially, the  $\alpha$  - ASGR1 antibody is chemically biotinylated by non-specific conjugation of biotin to amine

groups [21]. The biotinylated  $\alpha$  - ASGR1 antibody is exposed to the streptavidin coated magnetic beads (commercially available), which results in  $\alpha$  - ASGR1 antibody coated magnetic beads (**Figure 2a**). The  $\alpha$  - ASGR1 antibody coated beads are then incubated with the HLMs to allow time for capture of the vesicles to the beads, via the antibody-antigen interaction (**Figure 2b**). Finally, the captured vesicles are pulled-down on the magnetic beads when placed on the magnet (**Figure 2c**). The supernatant containing uncaptured vesicles is discarded, resulting in isolation of ASGR1 expressing HLMs which then underwent trypsin digestion and analysis by LC-MRM-MS. A control sample using beads without the  $\alpha$  - ASGR1 antibody, was also digested and analyzed by LC-MRM-MS.

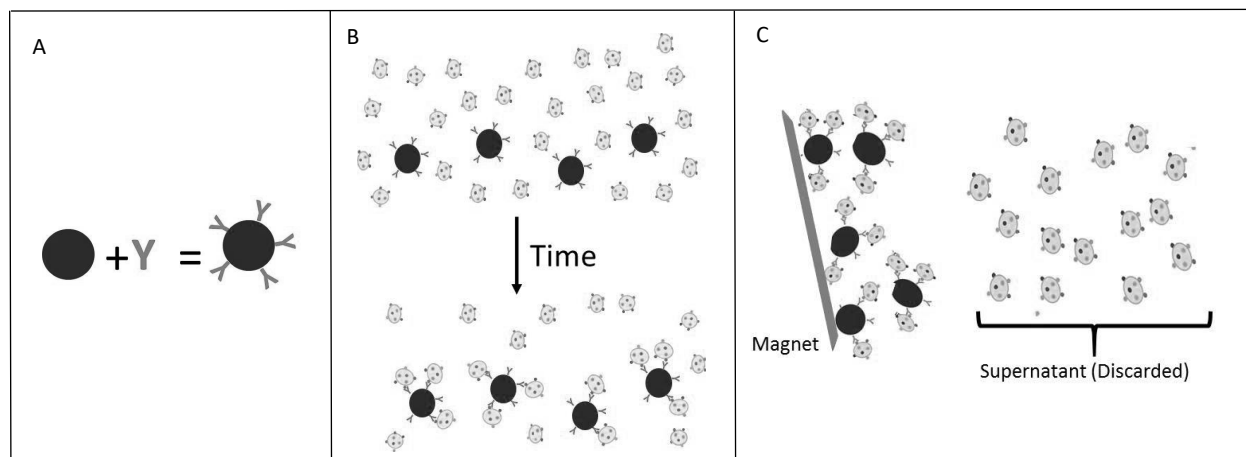


**Figure 2:** General workflow for pull-down of HLMs using magnetic beads and the ASGR1 protein – antibody interaction. Immobilization of  $\alpha$  -ASGR1 on surface of magnetic beads (A), immobilization of HLMs on magnetic beads (B), pull-down of HLMs on the magnetic beads via a magnet and removal of supernatant and HLMs not attached to the beads (C).

In **Figure 3**, the fold increase in protein on beads with biotinylated  $\alpha$  - ASGR1 antibody over beads without the biotinylated  $\alpha$  - ASGR1 antibody can be seen. For ASGR1, there is a (mean +/- SD) 15 +/- 7-fold increase on beads with the  $\alpha$  - ASGR1 antibody compared to beads with no  $\alpha$  - ASGR1 antibody on their surface. The GRP78 protein, which is an ER luminal marker protein, showed a 7.5-fold increase while Cytochrome P450 (CYP) 3A4, which is an ER

anchored protein, showed a 5-fold increase. Other proteins including PHB1, HSC70, and HSP60 are proteins not necessarily associated with the ER, but still show a slight increase of 2-fold.

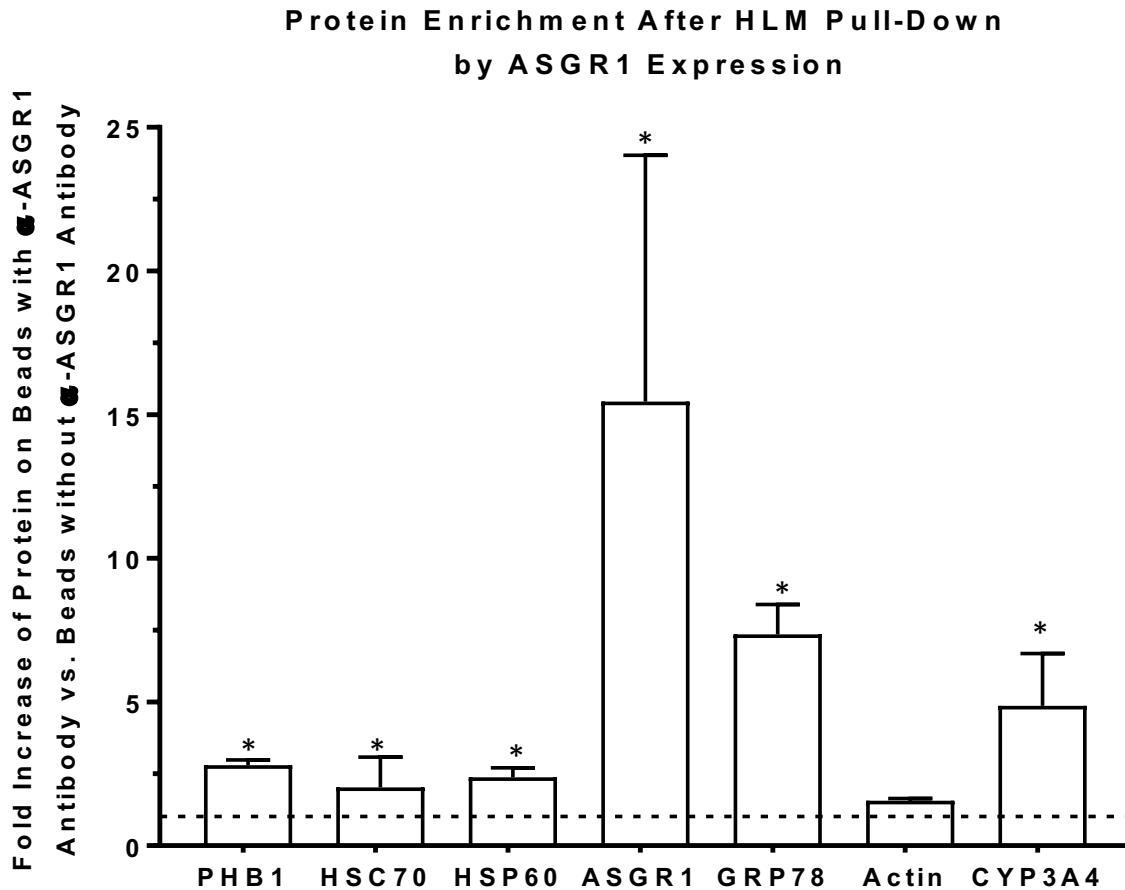


**Figure 3:** Protein enrichment after HLM pull-down using biotinylated  $\alpha$  - ASGR1 antibody immobilized on streptavidin coated beads. The data is showing a fold increase in proteins digested on the beads containing the biotinylated  $\alpha$  - ASGR1 antibody versus beads without biotinylated  $\alpha$  - ASGR1 antibody for biological triplicate (n=3). Asterisks indicate a statistical difference between amount of protein on the beads with the  $\alpha$  - ASGR1 antibody versus the beads without.

Except for ASGR1, the standard deviations were within the 10 % range and statistical analysis revealed a statistical difference in the amount of protein on the beads with the  $\alpha$  - ASGR1 antibody versus the beads without for all proteins except actin. The potential reason for such high variation for ASGR1 is likely due to the intrinsic factors of IP methods [22]. For example, a different aliquot of  $\alpha$ -ASGR1 antibody was thawed and biotinylated, a different aliquot of

beads was used to immobilize the biotinylated  $\alpha$  - ASGR1 antibody, and a different aliquot of HLMs were thawed and captured for each biological replicate. Nevertheless, the purpose of this feasibility study was to demonstrate the ability to isolate ASGR1 expressing vesicles, which based on the enrichment of proteins observed in **Figure 3** was successful.

#### 4.3.3 Characterization of HepG2 and HeLa Exosomes

After successful pull-down of the HLMs by the ASGR1 IP method, the ability to isolate the ASGR1 expressing exosomes by IP could be investigated. In order to have the best chance possible for IP of ASGR1 expressing exosomes, the exosomes were isolated by ultracentrifugation from HepG2 and HeLa cell culture medium prior to IP. The isolated HeLa and HepG2 exosomal vesicles were characterized for particle size by NTA as seen in **Figure 4a** and **4b** respectively. The size of the particles as observed by NTA were 130 +/- 2 nm 139 +/- 3 nm respectively for HeLa and HepG2 exosomes, which falls within the expected size range of exosomes, 30 – 150 nm in diameter [1].

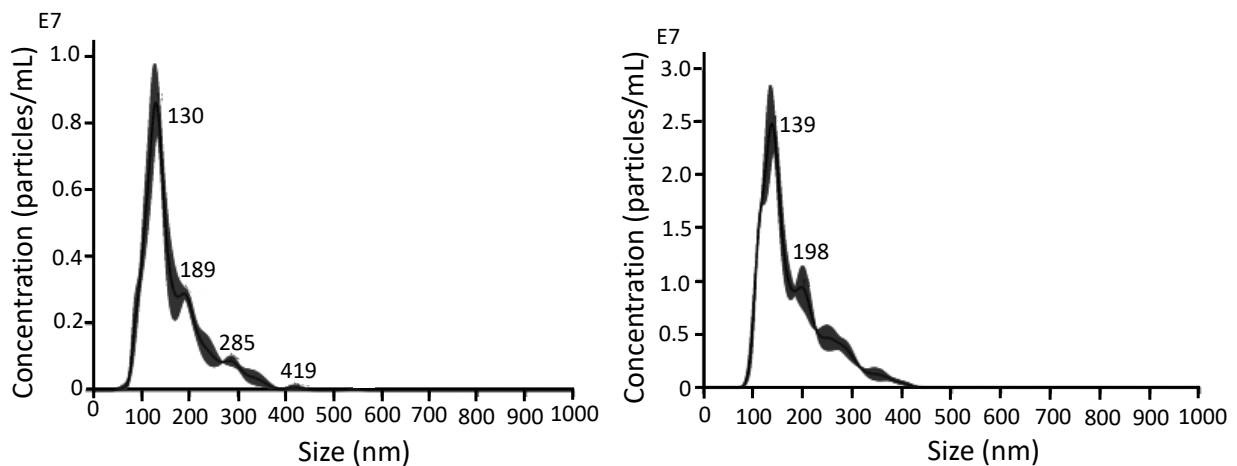


**Figure 4:** NTA analysis of HeLa (A) and HepG2 (B) exosomes isolated by differential ultracentrifugation.

However, NTA does not give any information regarding the content of the extracellular vesicles. Therefore, a 30  $\mu$ g amount of HepG2 and HeLa exosomal protein was trypsin digested and analyzed by LC-MRM-MS analysis, which can be seen in **Figure 5a** and **b**. All proteins in **Figure 5** are normalized to the cell lysate, which is why each protein in the cell lysate shows a 1-fold change (see Equation 1). Both HSC70 and HSP90 $\beta$  are exosomal marker proteins for HepG2 cells while CD9 and ALIX are exosomal marker proteins for HeLa cells; therefore, these proteins are expected to be found at higher levels in the exosomes than in the corresponding cell lysate, which is the trend observed in **Figure 5a** and **b**. At the same time, PHB1, GRP78, and HSP60, are proteins expected to be observed in the cell lysate and at much lower levels in exosomes, which can be easily observed in **Figure 5a** and **b** [12, 23-25]. A combination of NTA and LC-MRM-MS analysis gives confidence that the isolated particles are exosomes.

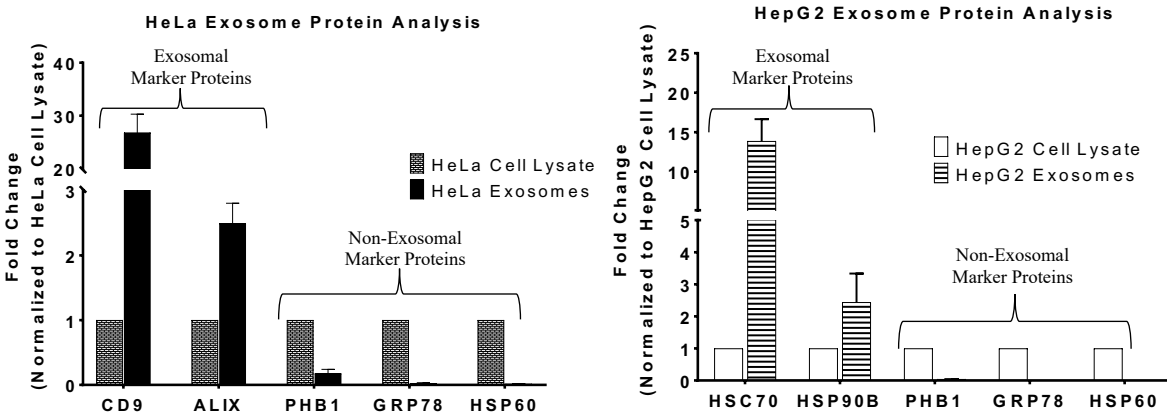


**Figure 5:** LC-MRM-MS analysis of HeLa exosomes (A) and HepG2 exosomes (B) after isolation by differential ultracentrifugation of 3 biological replicates (n=3).

#### 4.3.4 Expression of ASGR1 in HepG2 Exosomes

Previously, the presence of ASGR1 in HepG2 and HeLa cell lysate was investigated (**Figure 1**). Since the HeLa cell lysate lacked ASGR1 expression, as expected, the HeLa exosomal vesicles were not probed for ASGR1 expression in order to conserve the exosomal protein. The ASGR1

expression in HepG2 exosomes was confirmed by both LC-MRM-MS and Western blot as seen in **Figure 6a** and **b** respectively, prior to IP. If ASGR1 is not present in the HepG2 exosomes, the IP of HepG2 exosomes by the ASGR1 antibody-antigen interaction would not be successful. However, both LC-MRM-MS and Western blot suggest HepG2 exosomes contain ASGR1, though at a substantial lower level than the HepG2 cell lysate.

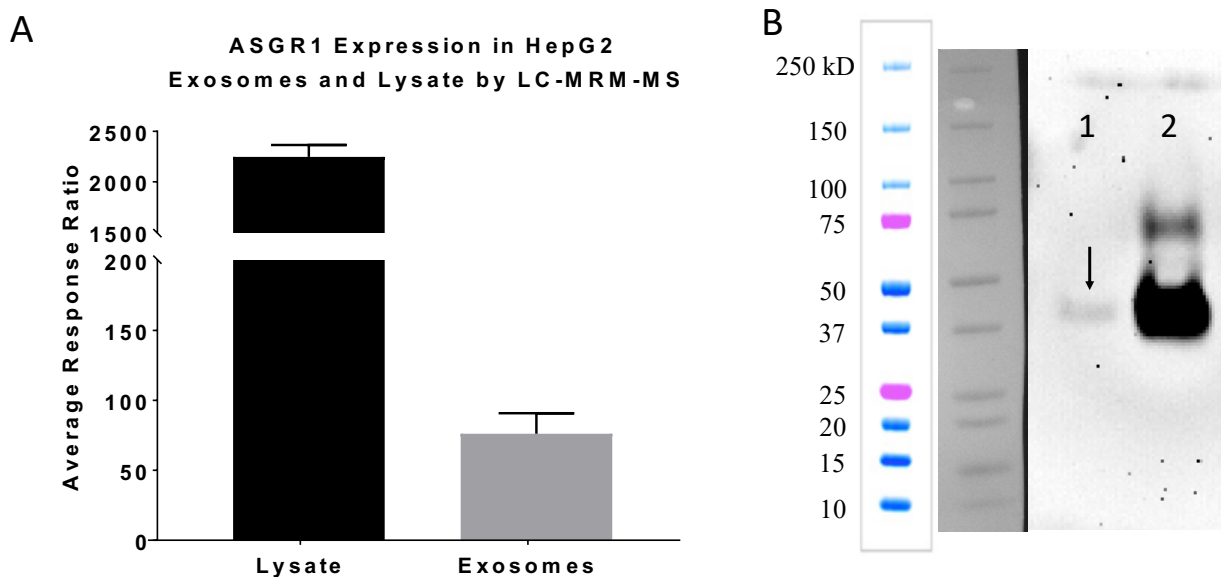


**Figure 6:** Demonstrating the presence of ASGR1 in HepG2 exosomes isolated by differential ultracentrifugation by LC-MRM-MS (A) and Western blot, with 15 µg of exosomal protein in lane 1, and 15 µg of HepG2 cell lysate in lane 2 (B).

#### 4.3.5 IP of HepG2 and HeLa Exosomes Based on ASGR1 Expression and Analysis

Following the exact protocol used for the HLM IP, (**Figure 2a-c**) the HepG2 and HeLa exosomes were exposed to the magnetic beads and pulled-down. The exosomal proteins were trypsin digested and analyzed by LC-MRM-MS in the same way that the HLM samples were treated in the feasibility study. The HepG2 and HeLa exosome pull-downs had a control sample of exosomes exposed to beads that did not have the biotinylated  $\alpha$  - ASGR1 antibody. **Figure 7** shows the fold increase of protein in the sample exposed to the beads with biotinylated  $\alpha$  - ASGR1 antibody versus the sample that did not have the  $\alpha$  - ASGR1 antibody beads. For all



HepG2 proteins, there was a statistically different enrichment, typically between 5 and 7-fold suggesting that exosomes were successfully pulled out of the solution. Not only does this data suggest a successful pull-down of HepG2 exosomes, it also demonstrates the specificity of the pull-down based on the results of the HeLa exosome pull-down (**Figure 7**). Specifically, there was no enrichment of proteins on the beads with the  $\alpha$ -ASGR1 antibody, which is expected as these exosomes do not contain the ASGR1 antigen.

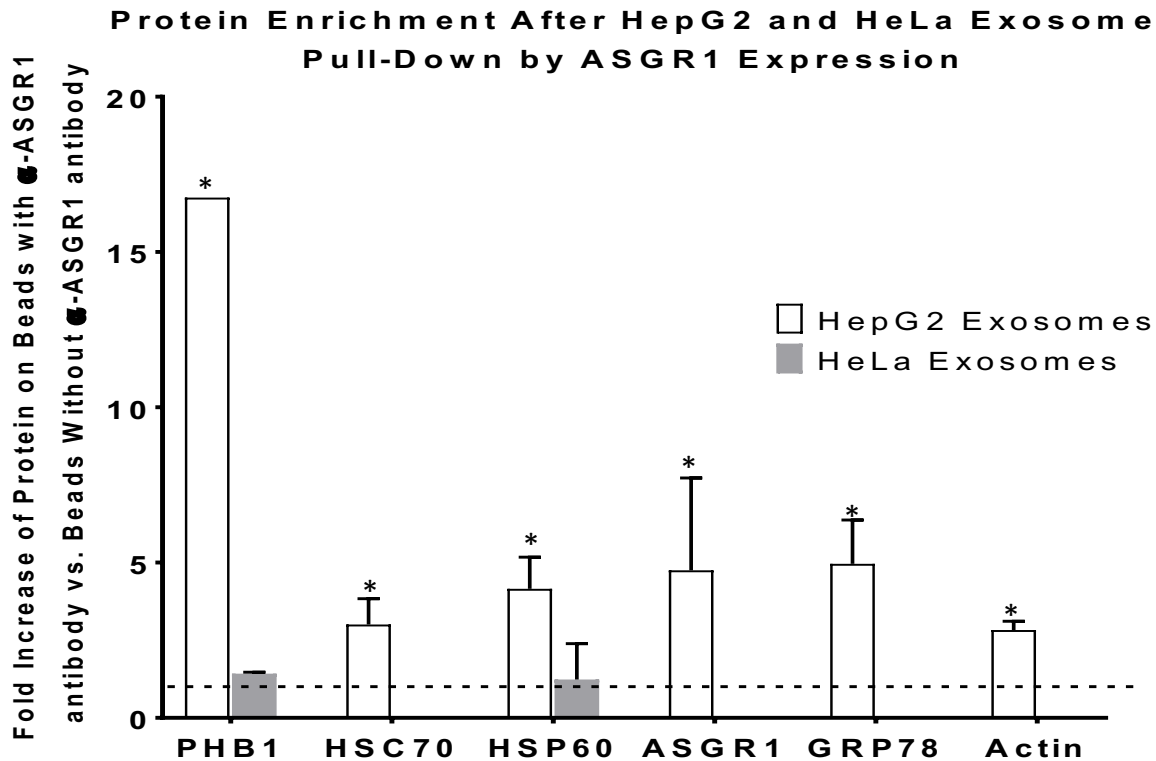


**Figure 7:** Protein enrichment after HepG2 and HeLa pull-down using biotinylated  $\alpha$  - ASGR1 antibody immobilized on streptavidin coated beads. The data is showing a fold increase in proteins digested on the beads containing the biotinylated  $\alpha$  - ASGR1 antibody versus beads without biotinylated  $\alpha$  - ASGR1 antibody for biological triplicate (n=3). Asterisks indicate a statistical difference between amount of protein on the beads with the  $\alpha$  - ASGR1 antibody versus the beads without.

Finally, an alternative method to detect the isolated vesicles on the surface of the magnetic beads was investigated. Using HLMs, since they are readily available and can be obtained without the

time-consuming cell culture and differential ultracentrifugation, the pull-down was repeated, and the particles were detected via EPI. The difference for this experiment was that after the pull-down and sample clean up (step in **Figure 2c**), the sample was incubated with an Alexa 488 conjugated  $\alpha$ -CD9 antibody (DOL = 3.2). The EPI images can be seen in **Figure 8**. In the sample that was exposed to the biotinylated  $\alpha$ -ASGR1 coated beads (**Figure 8a**), there appears to be a higher amount, or larger regions, or fluorescent particles compared to the particles exposed to beads without biotinylated  $\alpha$ -ASGR1 (**Figure 8b**), which is consistent with the LC-MRM-MS data in **Figure 3**. Thus, two different forms of analysis indicate the ASGR1 antibody-antigen interaction can be used to isolated vesicles from a sample.

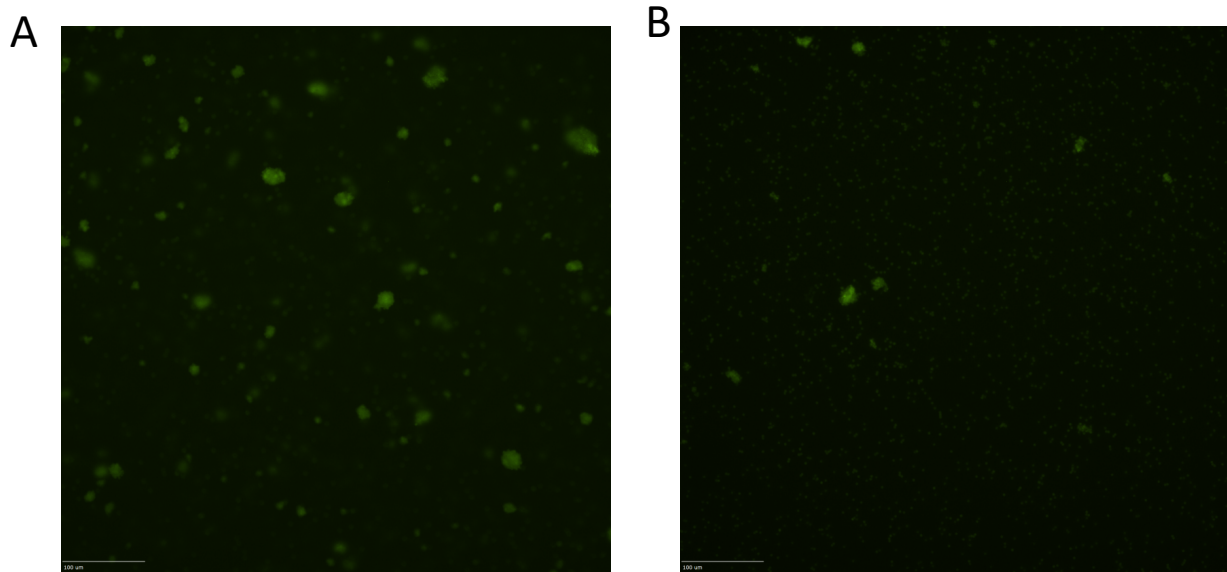


**Figure 8:** EPI of HLM pulled-down using the ASGR1 antibody-antigen interaction then exposed to an Alexa 488 conjugated  $\alpha$ -CD9 antibody for detection. A sample exposed to beads with biotinylated  $\alpha$ -ASGR1 on its surface (A) is compared to a sample where no biotinylated  $\alpha$ -ASGR1 was exposed to the surface of the beads (B).

## **4.4 CONCLUSION**

The potential for exosomes to be used in the clinical setting for many purposes, such as diagnostic tools, has been well demonstrated and is of great interest simply given the vast amounts of literature in the area. The ability to isolate a specific subset of exosomal vesicles based on their cell of origin would be beneficial, as it would potentially increase the ability to detect low levels of biomarkers for diseases, such as cancer, leading to early diagnosis. Here, the ability to isolate liver-derived exosomes based on the expression of liver marker protein ASGR1 is demonstrated.

## 4.5 REFERENCES

1. Raposo, G. and W. Stoorvogel, *Extracellular vesicles: exosomes, microvesicles, and friends*. J Cell Biol, 2013. **200**(4): p. 373-83.
2. Caby, M.P., et al., *Exosomal-like vesicles are present in human blood plasma*. Int Immunol, 2005. **17**(7): p. 879-87.
3. Melo, S.A., et al., *Glypican-1 identifies cancer exosomes and detects early pancreatic cancer*. Nature, 2015. **523**(7559): p. 177-82.
4. Zarin Nuzhat, V.K., Shayna Sharma, Gregory E. Rice, Virendra Joshi, Carlos Salomon, *Tumour-derived exosomes as a signature of pancreatic cancer - liquid biopsies as indicators of tumour progression*. Oncotarget, 2017.
5. Kalra, H., et al., *Comparative proteomics evaluation of plasma exosome isolation techniques and assessment of the stability of exosomes in normal human blood plasma*. Proteomics, 2013. **13**(22): p. 3354-64.
6. UniProt Consortium, T., *UniProt: the universal protein knowledgebase*. Nucleic Acids Res, 2018. **46**(5): p. 2699.
7. Ashwell, G.a.M., A. G. , *The role of surface carbohydrates in the hepatic recognition and transport of circulating glycoproteins*. Advances in Enzymology and Related Areas of Molecular Biology, 1974. **41**(0): p. 99-128.
8. Peters, D.T., et al., *Asialoglycoprotein receptor 1 is a specific cell-surface marker for isolating hepatocytes derived from human pluripotent stem cells*. Development, 2016. **143**(9): p. 1475-81.
9. Schwartz, A.L., Marshak-Rothstein, A., Rup, D. and Lodish, H. F. , *Identification and quantification of the rat hepatocyte asialoglycoprotein receptor*. . Proc Natl Acad Sci U S A, 1981. **78**(6): p. 3348-3352.
10. Javier Conde-Vancells, E.R.-S., Nieves Embade, David Gil, Rune Matthiesen, Mikel Valle, Felix Elortza, Shelly C. Lu, Jose M. Mato, Juan M. Falcon- Perez, *Characterization and Comprehensive Proteome Profiling of Exosomes Secreted by Hepatocytes*. 2008.
11. Bebelman, M.P., et al., *Biogenesis and function of extracellular vesicles in cancer*. Pharmacol Ther, 2018. **188**: p. 1-11.
12. Zaborowski, M.P., et al., *Extracellular Vesicles: Composition, Biological Relevance, and Methods of Study*. BioScience, 2015. **65**(8): p. 783-797.
13. Kawajiri, K., A. Ito, and T. Omura, *Subfractionation of Rat Liver Microsomes by Immunoprecipitation and Immunoabsorption Methods*. J. Biochem, 1976. **81**: p. 779-789.

14. Asha, S. and M. Vidyavathi, *Role of Human Liver Microsomes in In Vitro Metabolism of Drugs—A Review*. Applied Biochemistry and Biotechnology, 2009. **160**(6): p. 1699-1722.
15. Achour, B., et al., *Global Proteomic Analysis of Human Liver Microsomes: Rapid Characterization and Quantification of Hepatic Drug-Metabolizing Enzymes*. Drug Metabolism and Disposition, 2017. **45**(6): p. 666-675.
16. *Hep G2 [HEPG2] (ATCC® HB-8065™)*.
17. Roberti, M.P., et al., *Protein expression changes during human triple negative breast cancer cell line progression to lymph node metastasis in a xenografted model in nude mice*. Cancer Biol Ther, 2012. **13**(11): p. 1123-40.
18. Waldemarson, S., et al., *Protein expression changes in ovarian cancer during the transition from benign to malignant*. J Proteome Res, 2012. **11**(5): p. 2876-89.
19. Viviana Salvatore, G.T., Silvia Bolzani, Stefano Focaroli, Sandra Durante, Maria Carla Mazzotti and Mirella Falconi, *Simulating tumor microenvironment: changes in protein expression in an in vitro co-culture system*. 2014.
20. *HeLa (ATCC® CCL-2™)*.
21. FisherScientific, *Pierce Antibody Biotinylation Kit for IP*.
22. Administration, U.S.D.o.H.a.H.S.F.a.D., *Bioanalytical Method Validation Guidance for Industry*. 2018.
23. Yáñez-Mó, M., et al., *Biological properties of extracellular vesicles and their physiological functions*. Journal of Extracellular Vesicles, 2015. **4**(1).
24. Borges, F.T., L.A. Reis, and N. Schor, *Extracellular vesicles: structure, function, and potential clinical uses in renal diseases*. Braz J Med Biol Res, 2013. **46**(10): p. 824-30.
25. Tauro, B.J., et al., *Comparison of ultracentrifugation, density gradient separation, and immunoaffinity capture methods for isolating human colon cancer cell line LIM1863-derived exosomes*. Methods, 2012. **56**(2): p. 293-304.

## **Chapter V: Major Conclusions and Future Directions**

## TABLE OF CONTENTS

<b>5.1 Major Conclusions</b> .....	<b>135</b>
<b>5.2 Future Directions</b> .....	<b>138</b>
5.2.1 Use Liver-Derived Exosomes to Diagnose Early Stage Hepatoma.....	138
5.2.2 Develop LC-MRM-MS Methods for Lipid Analysis of Exosomes.....	139
5.2.3 Develop LC-MRM-MS Methods for RNA Analysis of Exosomes.....	141
<b>5.3 References</b> .....	<b>143</b>

## LIST OF TABLES

<b>Table 1.</b> Phospholipid species associated with the different peaks in the chromatogram of Figure 2.....	140
---	-----

## LIST OF FIGURES

<b>Figure 1.</b> Presence of AFP in HeLa, Huh7, and HepG2 cell lysate and exosomes isolated by differential ultracentrifugation. AFP protein expression was assessed by LC-MRM-MS analysis after trypsin digestion and sample preparation by qFASP.....	138
<b>Figure 2.</b> Detection of phospholipids by LC-MRM-MS isolated from 100 $\mu$ L of healthy human plasma by addition of acetonitrile at a 2:1 ratio (acetonitrile: plasma) followed by brief centrifugation. The species associated with each peak is listed in Table 2. ....	140



## 5.1 MAJOR CONCLUSIONS

The utility of exosomes in the clinical setting has been well demonstrated. Specifically, it has been demonstrated that exosomes can act as carriers of biomarkers for different diseases, used as drug delivery systems, as antigen presentation vesicles, monitor patient response to treatment, and in vaccine development [1-14]. An additional advantage of these vesicles is that, since they are located in the extracellular space (i.e. blood, urine, saliva, etc..) they can be collected by minimally to non-invasive procedures.

As reviewed in Chapter 1, there are a number of different types extracellular vesicles secreted by cells into the extracellular space and the vesicles are differentiated by size, biogenesis, and biological purpose [15-17]. While the study of exosomal vesicles are of highest interest, due to their endosomal route of formation, no isolation technique has been developed to isolate exosomal vesicles from all other extracellular vesicles secreted by the cells. That is, different isolation methods result in a different mixture of extracellular vesicles with the exosomal vesicles being enriched in the given mixture [15, 16]. Additionally, there are numerous ways in which isolated exosomes can be assessed for purity and quality. Due to various isolation and analysis methods and the lack of standardization in exosome isolation and analysis, benefits of exosomes in the clinical setting are yet to be realized.

In Chapter 2, the lack of standardization and challenges associated with developing standard methods was addressed. Specifically, the gold standard for exosome isolation, differential ultracentrifugation, was compared to a more clinically friendly method of exosome isolation, a commercially available exosomes precipitation kit. The protein content of the isolated exosomal vesicles, for two different cell lines, were assessed by traditional Western blot and a newly developed liquid chromatography – multiple reaction monitoring – mass spectrometry (LC-MRM-MS) based method. Not only is the LC-MRM-MS based methodology more selective

and specific than traditional Western blotting, it is inherently better multiplexed requiring 30-fold less exosomal protein to monitor the presence/absence of the same proteins in any given sample. The advantages of LC-MRM-MS analysis in exosomal research were demonstrated.

In Chapter 3, the new LC-MRM-MS method was employed to study the presence of drug metabolizing enzymes (DMEs) in isolated exosomal vesicles. The idea is that the DME content of exosomes can correlate to the DME activity of the liver, thus providing a minimally-invasive blood based biopsy for an individual's liver DME activity and providing a new bases for personalized medicine. For the first time, we demonstrated the presence of DMEs in HepG2 exosomes and the ability of the exosomal DMEs to reflect a change in DME content occurring within the cells.

In Chapter 4, methods for isolating liver-derived exosomes were investigated in order to try to make the idea of using liver-derived exosomes in the clinical setting more realistic. The presence of liver specific marker protein, Asialoglycoprotein -1 (ASGR1), was identified in exosomes derived from primary rat hepatocytes, thus is expected to also be found in exosomes derived from primary human hepatocytes [18]. Due to the expense of human liver tissue for culture and exosome collection, HepG2 cells were used as a model system. The presence of ASGR1 in HepG2 cell lysate and exosomes was confirmed by both Western blot and LC-MRM-MS based techniques. The ability to capture HepG2 exosomes based on the ASGR1 expression was then established using immunomagnetic precipitation.

Overall, the purpose this dissertation was to develop LC-MRM-MS based methods to aid in the development of standardization of exosomal analysis methods. Further, the developed method was then used to study the DME content of HepG2 exosomes and the ability of exosomal DME content to be altered to reflect a change occurring within the cell from which they are being secreted. Finally, methods for isolating liver-derived vesicles was investigated in order to

establish a clinical friendly protocol that can be used to isolate a patient's liver-derived exosomes from a single blood draw.

## 5.2 FUTURE DIRECTIONS

### 5.2.1 Use Liver-Derived Exosomes to Diagnose Early Stage Hepatoma

Currently, the biomarker used to diagnose patients with hepatoma in the clinical setting is  $\alpha$ -fetoprotein, or AFP [19, 20]. However, due to lack of sensitivity, once this biomarker is identified in a patient's bloodwork, the cancer is late stage and gives the patient a grim prognosis [19]. Preliminary data, in **Figure 1** suggests AFP is present in HepG2 and Huh7 cell lysate and exosomes, which is expected as these are hepatoma cell lines. If immunomagnetic precipitation methods are developed to isolate liver-derived exosomes from plasma, the presence of AFP in exosomes can be probed and potentially allow for earlier diagnosis of hepatoma due to increased sensitivity, ultimately giving patients a better prognosis.

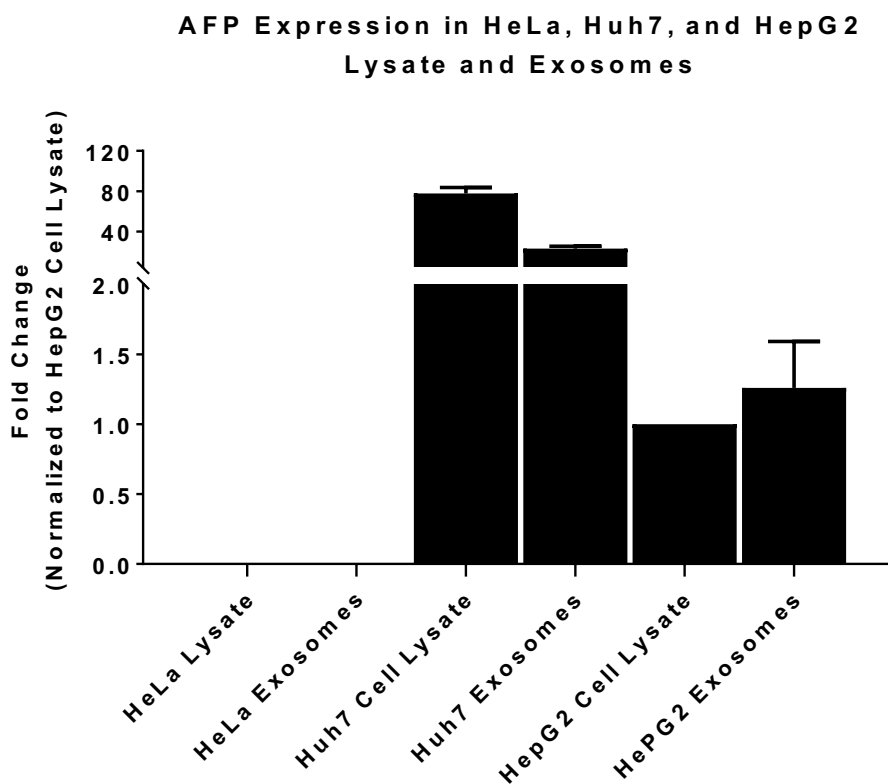


**Figure 1.** Presence of AFP in HeLa, Huh7, and HepG2 cell lysate and exosomes isolated by differential ultracentrifugation. AFP protein expression was assessed by LC-MRM-MS analysis after trypsin digestion and sample preparation by qFASP.

Interestingly, AFP is a protein found abundant in fetal livers and another hepatoma biomarker of interest, midkine (MDK), is also found in fetal livers but associated with cancer or precancerous lesions in adults [20]. Thus, two biomarkers for hepatoma are fetal liver associated proteins, suggesting that maybe the liver becomes more fetal like when hepatoma develops. Much like AFP and MDK, Cytochrome P450 3A7 (CYP3A7) is a fetal liver associated protein, if the liver becomes more fetal like in hepatoma, perhaps the expression of CYP3A7 increases in hepatoma, and therefore is also a potential biomarker for hepatoma. By looking at AFP in liver-derived exosomes, hepatoma maybe able to be diagnosed at earlier stage and the potential for MDK and CYP3A7 to act as additional biomarkers for hepatoma and their presence in exosomes is a potential future direction to this project, and that could have significant impact on hepatoma diagnosis and prognosis in the clinical setting. Further, the presence of glypican – 1 in exosomes has been identified as a specific marker for cancer exosomes, by further investigating the presence or absence of glypican – 1 in addition to AFP, MDK, and CYP3A7 the confidence in a true hepatoma diagnosis can be increased [21].

### **5.2.2 Develop LC-MRM-MS Methods for Lipid Analysis of Exosomes**

The primary focus of this dissertation was on the proteomic analysis of exosomes and developing methods to assess the protein profiles of exosome isolations. However, as was the case with proteins, the lipid profiles of exosomes are expected to be different than that of the originating cell [15, 22]. Specifically, the abundance of sphingomyelin (SM) and phosphatidylserine (PS) are expected to be enriched in exosomes compared to the cell however phosphatidylcholine (PC) and phosphatidylethanolamine (PE) are expected to be less abundant in exosomes than in the secreting cell [23, 24]. As was done for proteins in Chapter 2, an LC-MRM-MS method was developed for exosomal phospholipid analysis. The chromatogram in **Figure 2** demonstrates the ability to detect

several phospholipids extracted from healthy human plasma. The phospholipids associated with each peak in the chromatogram are defined in **Table 1**, with arachidonic acid serving as the internal standard (IS). Future studies can focus on validating this method, using it to assess exosomal and lysate phospholipids, and be expanded to include other lipids such as cholesterol.

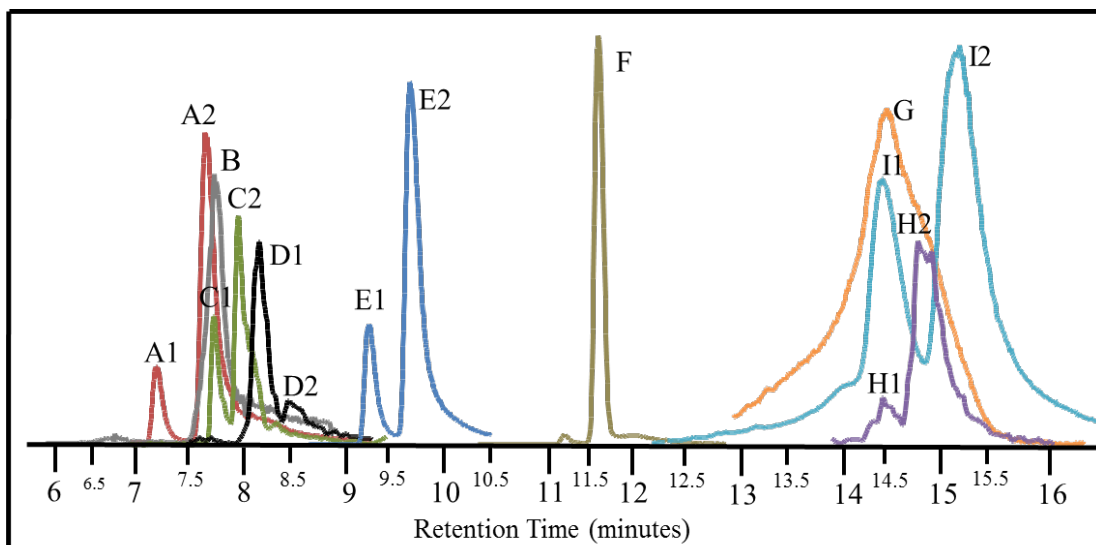


**Figure 2.** Detection of phospholipids by LC-MRM-MS isolated from 100  $\mu$ L of healthy human plasma by addition of acetonitrile at a 2:1 ratio (acetonitrile: plasma) followed by brief centrifugation. The species associated with each peak is listed in Table 2.

**Table 1.** Phospholipid species associated with the different peaks in the chromatogram of Figure 2.

Peak	Phospholipid	Intensity
A1	2-acyl LysoPC (C16:0)	6.08E+06
A2	1-acyl LysoPC (C16:)	
B	LysoPE (C16:0)	2.08E+05
C1	2-acyl LysoPA (C16:0)	8.60E+04
C2	1-acyl LysoPA (C16:0)	
D1	2-acyl LysoPS (C18:1)	4.22E+04
D2	1-acyl LysoPS (C18:1)	
E1	2-acyl-LysoPC (C18:0)	7.68E+06
E2	1-acyl LysoPC (C18:0)	
F	Aracaidonic Acid (C20:4)	1.88E+07

G	PC (C16:0/C18:1)	8.07E+06
H1	PS (C18:0/C22:6)	1.56E+04
H2		
I1	PC (C16:0/C18:2)	1.99E+07
I2		

### 5.2.3 Develop LC-MRM-MS Methods for RNA Analysis of Exosomes

Most commonly, mRNA analysis is done by sequence based indirect methods, such as real time polymerase chain reaction (RT-PCR), and requires preamplification and/or chemical or enzymatic modification of the mRNA of interest [26, 27]. While these methods have proven to be highly sensitive (down to 100 fM), they are expensive and labor intensive [26]. Mass spectrometry (MS) based techniques to study biomolecules, such as proteins, lipids, and RNAs are appealing since they are highly sensitive, selective, and have wide dynamic ranges [27]. Thus, it would be ideal to develop an LC-MRM-MS based method for investigating exosomal RNA, which would build further on the proteomic and lipidomic methods. Due to the fact RNA is composed of four different nucleotides, different RNA sequences result in similar MS patterns, making MS analysis of RNA complicated [27]. However, methods have been developed to change an RNA signal into a peptide signal for MS detection [27]. Briefly, exosomal RNA can be extracted and incubated with a biotinylated DNA-peptide probe. When the DNA (which is specific for an RNA of interest) hybridizes to the RNA, the DNA is cleaved by duplex specific nuclease (DSN) separating the 3' end with the peptide probe and the biotinylated 5' end. The exosomal RNA is now available for additional hybridization with the DNA-peptide probe, allowing for amplification of the exosomal RNA signal. Eventually, the unreacted biotinylated DNA-peptide probe and cleaved 5' end of the DNA (which is biotinylated) is removed using streptavidin coated beads. By using different peptide probes for different DNA sequences, specific to different RNAs of interest, the method can be multiplexed as it would allow for

identification of different RNAs of interest based on the presence/absence of different peptides. By implementing this method, or a similar method, the primary cargo of exosomes (proteins, lipids, and RNA) can be investigated using LC-MRM-MS based methods in this laboratory.



### 5.3 REFERENCES

1. Alvarez-Llamas, G., et al., *Recent advances in atherosclerosis-based proteomics: new biomarkers and a future perspective*. Expert Rev Proteomics, 2008. **5**(5): p. 679-91.
2. Al-Nedawi, K., B. Meehan, and J. Rak, *Microvesicles: messengers and mediators of tumor progression*. Cell Cycle, 2009. **8**(13): p. 2014-8.
3. Simpson, R.J., et al., *Exosomes: proteomic insights and diagnostic potential*. Expert Rev Proteomics, 2009. **6**(3): p. 267-83.
4. Zhou, H., et al., *Exosomal Fetuin-A identified by proteomics: a novel urinary biomarker for detecting acute kidney injury*. Kidney Int, 2006. **70**(10): p. 1847-57.
5. Sonoda, H., et al., *Decreased abundance of urinary exosomal aquaporin-1 in renal ischemia-reperfusion injury*. American Journal of Physiology-Renal Physiology, 2009. **297**(4): p. F1006-F1016.
6. Nathalie Chaput, C.T., *Exosomes: immune properties and potential clinical implementations*. 2011.
7. Bobrie, A., et al., *Exosome secretion: molecular mechanisms and roles in immune responses*. Traffic, 2011. **12**(12): p. 1659-68.
8. Lai, R.C., et al., *Exosomes for drug delivery - a novel application for the mesenchymal stem cell*. Biotechnol Adv, 2013. **31**(5): p. 543-51.
9. Lydia Alvarez-Erviti, et al., *Delivery of siRNA to the mouse brain by systemic injection of targeted exosomes*. 2011.
10. Gatti, S., et al., *Microvesicles derived from human adult mesenchymal stem cells protect against ischaemia-reperfusion-induced acute and chronic kidney injury*. Nephrol Dial Transplant, 2011. **26**(5): p. 1474-83.
11. Reis, L.A., et al., *Bone Marrow-Derived Mesenchymal Stem Cells Repaired but Did Not Prevent Gentamicin-Induced Acute Kidney Injury through Paracrine Effects in Rats*. PLoS ONE, 2012. **7**(9).
12. Bruno, S., et al., *Microvesicles Derived from Mesenchymal Stem Cells Enhance Survival in a Lethal Model of Acute Kidney Injury*. PLoS ONE, 2012. **7**(3).
13. Akao, Y., et al., *Microvesicle-mediated RNA molecule delivery system using monocytes/macrophages*. Mol Ther, 2011. **19**(2): p. 395-9.
14. Bruno, S., et al., *Mesenchymal stem cell-derived microvesicles protect against acute tubular injury*. J Am Soc Nephrol, 2009. **20**(5): p. 1053-67.

15. Zaborowski, M.P., et al., *Extracellular Vesicles: Composition, Biological Relevance, and Methods of Study*. BioScience, 2015. **65**(8): p. 783-797.
16. Yáñez-Mó, M., et al., *Biological properties of extracellular vesicles and their physiological functions*. Journal of Extracellular Vesicles, 2015. **4**(1).
17. Borges, F.T., L.A. Reis, and N. Schor, *Extracellular vesicles: structure, function, and potential clinical uses in renal diseases*. Braz J Med Biol Res, 2013. **46**(10): p. 824-30.
18. Javier Conde-Vancells, E.R.-S., Nieves Embade, David Gil, Rune Matthiesen, Mikel Valle, Felix Elortza, Shelly C. Lu, Jose M. Mato, Juan M. Falcon- Perez, *Characterization and Comprehensive Proteome Profiling of Exosomes Secreted by Hepatocytes*. 2008.
19. Jiatao Lou<sup>1</sup>, L.Z., Shaogang Lv, Chenzi Zhang and Shuai Jiang, *Biomarkers for Hepatocellular Carcinoma*. 2017.
20. UniProt Consortium, T., *UniProt: the universal protein knowledgebase*. Nucleic Acids Res, 2018. **46**(5): p. 2699.
21. Melo, S.A., et al., *Glypican-1 identifies cancer exosomes and detects early pancreatic cancer*. Nature, 2015. **523**(7559): p. 177-82.
22. Raposo, G. and W. Stoorvogel, *Extracellular vesicles: exosomes, microvesicles, and friends*. J Cell Biol, 2013. **200**(4): p. 373-83.
23. E´.BIRO´, J.W.N.A., F. J. HOEK, G. GORTER, L. M. PRONK, A. STURK\* and R. NIEUWLAND, *The phospholipid composition and cholesterol content of platelet-derived microparticles: a comparison with platelet membrane fractions*. 2005.
24. Brzozowski, J.S., et al., *Lipidomic profiling of extracellular vesicles derived from prostate and prostate cancer cell lines*. Lipids Health Dis, 2018. **17**(1): p. 211.
25. Xia, Y.Q. and M. Jemal, *Phospholipids in liquid chromatography/mass spectrometry bioanalysis: comparison of three tandem mass spectrometric techniques for monitoring plasma phospholipids, the effect of mobile phase composition on phospholipids elution and the association of phospholipids with matrix effects*. Rapid Commun Mass Spectrom, 2009. **23**(14): p. 2125-38.
26. Yin, B.C., Y.Q. Liu, and B.C. Ye, *One-step, multiplexed fluorescence detection of microRNAs based on duplex-specific nuclease signal amplification*. J Am Chem Soc, 2012. **134**(11): p. 5064-7.
27. Xu, F., T. Yang, and Y. Chen, *Quantification of microRNA by DNA-Peptide Probe and Liquid Chromatography-Tandem Mass Spectrometry-Based Quasi-Targeted Proteomics*. Anal Chem, 2016. **88**(1): p. 754-63.

## **APPENDICIES**

**Appendix 1: A Mechanistic Understanding of Polysorbate 80 Oxidation in  
Histidine and Citrate Buffer Systems**

## Abstract

In our previous published work, we reported rapid PS80 oxidation in histidine buffer after brief stainless steel exposure and the ability of citrate and EDTA to prevent this oxidation. The focus of our current study was to mechanistically understand PS80 oxidation by studying the impact of temperature, light, stainless steel and the role of citrate and EDTA. Additionally, PS80 oxidation was studied in three different buffer systems: histidine, citrate, and phosphate. When the PS80 containing buffers were exposed to elevated temperature of 50 °C in glass containers, no PS80 oxidation was observed in either histidine and citrate buffer systems after 30 days; however, PS80 oxidation was observed in phosphate buffer within 14 days. This study demonstrated that temperature does not initiate PS80 oxidation in histidine or citrate buffer systems but may be a factor in phosphate buffer. When the 3 buffer systems containing PS80 were exposed to 20, 50, and 100 % ICH light conditions and subsequently incubated at 50°C, the PS80 in phosphate buffer underwent oxidation within 7 days, whereas the PS80 in histidine and citrate buffer systems showed oxidation products only after 14 and 35 days, respectively. While PS80 in phosphate buffer seemed to be most vulnerable to light, PS80 in both histidine and citrate buffers underwent oxidation at a much slower rate, with the rate higher in histidine buffer compared to citrate buffer. Finally, the ability of citrate and EDTA to act not only as chelators, but also as a radical quencher/scavenger was demonstrated when metal ions such as Fe (2+) were spiked into histidine buffer containing PS80. While no radicals were detected by NMR or EPR, the observation of PS80 oxidation products indicate the presence of free radicals at concentrations below the limit of detection of these techniques.

For complete publication see:

Doyle, L. M., Sharma, A. N., Gopalrathnam, G., Huang, L., & Bradley, S. (2019). A Mechanistic Understanding of Polysorbate 80 Oxidation in Histidine and Citrate Buffer Systems – Part 2. PDA Journal of Pharmaceutical Science and Technology. DOI:10.5731/pdajpst.2018.009639

**Appendix II: Development of an In Vitro Model to Screen CYP1B1-Targeted  
Anticancer Prodrugs**

## Abstract

Cytochrome P450 1B1 (CYP1B1) is an anticancer therapeutic target due to its overexpression in a number of steroid hormone-related cancers. One anticancer drug discovery strategy is to develop prodrugs specifically activated by CYP1B1 in malignant tissues to cytotoxic metabolites. Here, we aimed to develop an in vitro screening model for CYP1B1-targeted anticancer prodrugs using the KLE human endometrial carcinoma cell line. KLE cells demonstrated superior stability of CYP1B1 expression relative to transiently transfected cells and did not express any appreciable amount of cognate CYP1A1 or CYP1A2, which would have compromised the specificity of the screening assay. The effect of two CYP1B1-targeted probe prodrugs on KLE cells was evaluated in the absence and presence of a CYP1B1 inhibitor to chemically "knock out" CYP1B1 activity (CYP1B1 inhibited). Both probe prodrugs were more toxic to KLE cells than to CYP1B1-inhibited KLE cells and significantly induced G0/G1 arrest and decreased the S phase in KLE cells. They also exhibited pro-apoptotic effects in KLE cells, which were attenuated in CYP1B1-inhibited KLE cells. In summary, a KLE cell-based model has been characterized to be suitable for identifying CYP1B1-targeted anticancer prodrugs and should be further developed and employed for screening chemical libraries.

For complete publication see:

Wang, Z., Chen, Y., Drbohlav, L. M., Wu, J. Q., & Wang, M. Z. (2016). Development of an In Vitro Model to Screen CYP1B1-Targeted Anticancer Prodrugs. *Journal of Biomolecular Screening*. DOI:10.1177/1087057116675315



**Appendix III: Quantification of Human Hepatic Drug-metabolizing Enzymes  
by Quantitative Filter-aided Sample Preparation (qFASP)**

## Abstract

Quantification of drug metabolizing enzymes (DMEs) is essential for the characterization of developmental expression patterns and determination of environmental and regulatory influences. Absolute DME expression levels also are important inputs for mechanistic physiologically-based pharmacokinetic models aimed at predicting drug exposure and drug response in diverse populations (e.g., pediatric, geriatric and ethnic groups). Liquid chromatography-multiple reaction monitoring mass spectrometry (LC-MRM MS)-based targeted proteomics has provided specific and multiplexed quantification of DMEs in human liver microsomes (HLM) but required synthesis of stable isotope-labeled peptide standards and/or recombinant protein standards to achieve absolute quantification. Here we report the development of LCMS<sup>E</sup> global proteomics and quantitative filter-aided sample preparation (qFASP) protocol to achieve robust, proteome-scale, label-free absolute quantification of DMEs in HLM. The qFASP protocol reduced sample-to-sample variability and improved recovery of hydrophilic and hydrophobic peptides, while maintaining efficient removal of phospholipids from protein digests and wide dynamic range for quantification. A total of 48 DMEs were identified and quantified from a pooled HLM, including 19 cytochrome P450s (CYPs), 2 flavin-containing monooxygenases (FMOs), 16 UDP-glucuronyltransferases (UGTs) and 11 other enzymes. Furthermore, using a panel of 8 individual donor HLMs, inter-individual variability in the DME expression was demonstrated using LCMS<sup>E</sup> global proteomics and quantification results strongly correlated with those determined by LC-MRM targeted proteomics, although concentration values could differ significantly. Hence, label-free LCMS<sup>E</sup> global proteomics coupled with robust sample preparation protocols (e.g., qFASP) may help expand our understanding of developmental expression patterns and environmental/regulatory influences on clinically important, as well as under-recognized, human hepatic DMEs.

For complete publication see:

Chen, Y., Doyle, L. M., Qiu, I. X., & Wang, M. Z. Quantification of Human Hepatic Drug-metabolizing Enzymes by Quantitative Filter-aided Sample Preparation (qFASP). Submitted to *Journal of Drug Metabolism and Deposition*, under review.

**Appendix IV: Lack of Efficacy of Miltefosine for Amebic Encephalitis Despite  
Higher-Than-Recommended Dosing**

We present a patient with Acquired Immunodeficiency Syndrome (AIDS) and *Acanthamoeba* encephalitis treated with miltefosine. Despite high dosing and therapeutic plasma levels, concentration of the drug in the cerebrospinal fluid was negligible. Further research is needed to assess miltefosine brain parenchyma penetration, and its role in the treatment of amebic encephalitis.

For complete publication see:

Monogue, M. L., Watson, D., Alexander, J. S., Doyle, L. M., Wang, M. Z., Prokesch, B.C. Standard and High-Dose Miltefosine is Sub-Optimal for Treatment of Late Stage Amebic Encephalitis. Submitted to Journal of Clinical Infectious Disease, under review.

**Appendix V: Development of Liquid Chromatography – Multiple Reaction  
Monitoring – Mass Spectrometry (LC-MRM-MS)-Based Targeted Proteomics  
Method for Analysis of Exosome Marker Proteins and Its Application in  
Evaluating Different Exosome Preparations**

## Abstract

The ability of exosomes to act as carriers of biomarkers has been demonstrated and shown potential for clinical applications. A major challenge, however, is the lack of standardized methods for exosome isolation and analysis. Traditionally, immunoassays are used for assessing exosome preparations, however these assays are not well multiplexed and require the use of antibodies. Here, a liquid chromatography – multiple reaction monitoring – mass spectrometry (LC-MRM-MS) method is developed and used to assess exosome preparations from HeLa and HepG2 cell lines isolated by differential ultracentrifugation and a Total Exosome Isolation Kit (TEIK). LC-MRM-MS analysis indicated the abundance of exosomal marker proteins in exosomes isolated by the TEIK were generally lower than in the exosomes isolated by differential ultracentrifugation, indicating a higher purity exosome preparation by differential ultracentrifugation. LC-MRM-MS analysis was consistent with traditional Western blot methods, with lower levels of non-exosomal marker proteins in the exosome preparations compared to the corresponding cell lysate, and higher levels of exosomal marker proteins in the exosome preparations relative to the lysate. The LC-MRM-MS method is consistent with traditional Western blot assay, but requires 40-fold less protein, is quantitative, inherently specific and multiplexed, and does not require the use of antibodies.

Manuscript in preparation